Boron-Based Design of Active Ligands of Vitamin D Nuclear Receptor

Hélio Martins Gil
Mestrado em Bioquímica
Departamento de Química e Bioquímica
2018

Orientadores
Rita Sigüeiro Ponte, Facultad de Química, USC
Jose Enrique Rodriguez Borges, FCUP

Coorientadores
Antonio Mouriño Mosquera, Facultad de Química, USC
Julián Loureiro, Facultad de Química, USC

Todas as correções determinadas pelo júri, e só essas, foram efetuadas.

O Presidente do Júri,

Porto, _____/_____/_____

Acknowledgments

Firstly, I would like to express my gratitude to my advisors Professor Dr. Antonio Mouriño, Professor Dr. Enrique Borges and Professor Dra. Rita Sigüeiro for their support and guidance during this year. The opportunity to integrate this research group widened my knowledge in the field of Organic Chemistry and provided me with an invaluable experience.

I would like to thank my mentor and friend Xiao for his teachings and immense patience during this course. His counselling, insightful comments and encouragement were important assets for my learning.

I would also like to thank Professor Dr. Miguel Maestro and all my laboratory colleagues for the support and good environment that was provided. Special thanks to Patri for always being there for us in the most stressful moments and for all the good moments that we shared.

I want to thank University of Porto for the opportunity to study abroad under the Erasmus+ program, without which none of this would be possible. I would also like to thank to the University of Santiago de Compostela for hosting me during this year.

I could not forget all the friendships that grew during these 5 years. To my friends from RUCA, specially Romeu and Diogo, thank you for being part of the person that I am today and for all the laughs, conversations and fun we had together. And to Beatriz, for always being there for me and for being the angular stone in the wonderful and most atrocious moments.

Last but not least, I am grateful to my parents and sister for being my shelter and always supporting me while writing this thesis and all my life.

Resumo

Os boronatos e ácidos borónicos são historicamente conhecidos pela sua importante aplicação em reações de acoplamento de Suzuki. Para além da sua importância em síntese orgânica, os ácidos borónicos também são encontrados em aplicações no campo do design de fármacos, substituindo grupos funcionais como ácidos carboxílicos de modo a alterar as propriedades físico-químicas de candidatos a composto líder. Contudo, poucos derivados de ácidos borónicos foram sintetizados para estudos biológicos devido a dificuldades associadas à sua preparação. Recentemente, também se descobriu que o calcitriol (a forma ativa da vitamina D_3) ativa pelo menos 229 genes associados a diversas doenças, incluindo artrite, diabetes e cancro, sugerindo que o calcitriol pode possuir uma gama mais alargada de funções biológicas do que inicialmente pensado. Estudos sobre a relação estrutura-função de numerosos análogos do calcitriol demonstraram que os seus efeitos calcémicos podem ser significativamente reduzidos durante atividades de diferenciação celular, não tendo sido desvendado o mecanismo exato. Neste projeto levou-se a cabo a síntese de um análogo de Vitamina D contendo um éster borónico na cadeia lateral, de modo a melhorar a sua interação com o recetor da vitamina D (VDR) e tendo em vista futuros ensaios pré-clínicos.

Palavras-chave: Vitamina D, Ácidos borónicos, Ésteres borónicos, Acoplamento de Suzuki, Cross metathesis, Síntese, Calcitriol, VDR, LBD, Docking

Abstract

Boronates and boronic acids have an important application in Suzuki coupling reactions. Apart from their role (significance) in organic synthesis, boronic acids find applications in the drug discovery field, replacing structural motifs such as carboxylic acids or hydroxyl moieties to alter the physicochemical properties of lead candidates. However, relatively few alkyl boronic acid derivatives have been synthesized or biologically evaluated, due to problems associated with their preparation. Recently, it was also found that 1α,25-dihydroxyvitamin D_3 (1,25D or calcitriol, the active form of vitamin D_3) activates at least 229 genes associated with several diseases, including arthritis, diabetes and cancer, suggesting that 1,25D might be involved in a broader range of biological functions than originally thought. In an attempt to combine the biological properties of 1,25D with the advantages of boron chemistry, several vitamin D analogs containing borononic groups have been designed and docked in the ligand binding domain of the vitamin D receptor. Hence, it was carried out the synthesis of a theoretically highly active boronic ligand of the vitamin D receptor (VDR), with a view on preclinical studies.

Key words: Vitamin D, Synthesis, Boronic acid, Boronic ester, Suzuki coupling, Cross metathesis, , Calcitriol, Vitamin D receptor, Ligand binding domain, Vitamin D analogs, Docking.

Index

List of Figures

List of Schemes

List of Abreviations

1,25D	1α,25-Dihydroxyvitamin D_3
^{13}C-NMR	Carbon-13 nuclear magnetic ressonance
^{1}H-NMR	Proton nuclear magnetic ressonance
AF-2	Activation function 2
Arg	Arginine
B_2pin_2	Bis(pinacolato)diboron
BAX	Bcl-2-associated X protein
Bcl-2	B-cell lymphoma 2
BNCT	Boron neutron capture therapy
C/EBPβ	Interleukin 6-Dependent DNA-Binding Protein
CoA	Coactivators
CYP24A1	Cytochrome P450 family 24 subfamily A member 1
CYP27B1	Cytochrome P450 family 27 subfamily B member 1
CYP2R1	Cytochrome P450 family 2 subfamily R member 1
d	Doublet
DBD	DNA binding domain
DBP	Vitamin D-binding protein
dd	Doublet of doublets
ddd	Doublet of doublet of doublets
DIBAL-H	Diisobutylaluminum hydride
DMAP	4-(Dimethylamino)pyridine
DMF	*N,N*-Dimethylformamide
DMP	Dess-Martin periodinane
DMSO	Dimethyl sulfoxide
DNA	Deoxyribonucleic acid
dppf	Diphenylphosphinoferrocene

dt	Doublet of triplets
EGRF	Epidermal growth factor receptor
eq	Equivalents
ESI	Electrospray ionization
EtOAc	Ethyl acetate
FGF23	Fibroblast growth factor 23
GA	Genetic Algorithm
His	Histidine
HPLC	High-performance liquid chromatography
HRMS	High-resolution mass spectrometry
Hz	Hertz
Im	Imidazole
IR	Infrared
J	Coupling constant
LBD	Ligand binding domain
LDA	Lithium diisopropylamide
Leu	Leucine
m	multiplet
M^+	Molecular Ion
MARRS	Membrane-associated rapid response steroid
MHz	Megahertz
min	Minutes
MS	Mass Spectrometry
MTBE	Methyl *tert*-butyl ether
^{n}BuLi	*n*-Butyllithium
NCX1	Sodium-calcium exchanger
OPG	Osteoprotegerin
PCy_3	Tricyclohexylphosphine

PDB	Protein data bank
Ph	Phenyl
Phe	Phenylalanine
PMCA1b	Plasma membrane calcium ATPase
ppm	Parts per million
PTH	Parathyroid hormone
PTH1R	Parathyroid hormone receptor
RANK	Receptor activator of nuclear Factor κB
RANKL	Receptor activator of nuclear Factor κB ligand
R_f	Retention factor
rt	Room temperature
RXR	Retinoid X receptor
s	singlet
Ser	Serine
t	triplet
TBAF	Tetrabutylammonium fluoride hydrate
TBS	*terc*-Butyldimethylsilyl
Tf	Trifluoromethanesulfonate
THF	Tetrahydrofuran
TLC	Thin Layer-Chromatography
TOF	Time-of-flight
TRPV	Transient receptor potential vanilloid
Tyr	Tyrosine
UV	Ultraviolet
Val	Valine
VDR	Vitamin D nuclear receptor
VDREs	Vitamin D response elements

Introduction

Introduction

1. Vitamin D Discovery

In 1919, Sir Edward Mellanby was the first to confirm that rickets was a dietary deficiency disease. To do so, he fed dogs a typical Scottish diet (Scottish people had the highest incidence of rickets), and the dogs developed rickets identical to the human disease. He therefore postulated that the disease was developed after "a diminished intake of an anti-rachitic factor, which is either [McCollum's] fat-soluble factor A, or has a similar distribution to it".[1]

McCollum, in 1922, decided to test whether vitamin A was responsible for the healing of rickets,[2] and this test is acclaimed to be the key experiment in the discovery of vitamin D.[3] The observation that oxidized cod-liver oil could not prevent xerophthalmia but could prevent rickets in rats, showed that "oxidation destroys fat-soluble factor A without destroying another substance which plays an important role in bone growth".[3] The resulting conclusion was that fat-soluble factor A was composed of two substances, one termed later "vitamin A" and the newly discovered antirachitic factor, which was named vitamin D_2.[4]

Years later, it was discovered[3] that the natural form of vitamin D in the human organism was vitamin D_3 (Figure 1).

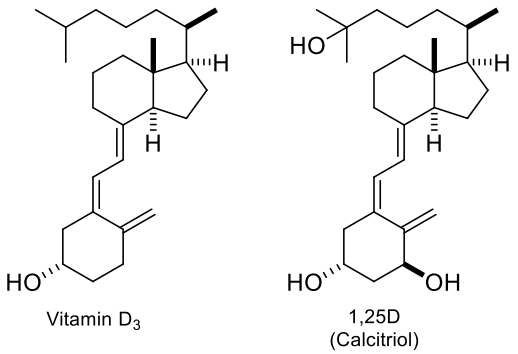

Figure 1. Structure of Vitamin D_3 and its active metabolite 1,25D (calcitriol).

Vitamin D_3, through is active form 1,25D ($1\alpha,25(OH)_2D_3$; calcitriol), is responsible for the calcium and phosphorous homeostasis. Besides these classical functions, this hormone also plays a role in the control of cellular proliferation and differentiation, cellular apoptosis and immune system. These characteristics led to the application of 1,25D in the treatment of diseases such as osteoporosis, psoriasis and different types of cancer.[5, 6]

2. Structure and Nomenclature

The natural form of vitamin D in biological systems was discovered by Windaus and named vitamin D_3. It is produced in the skin by UV irradiation of 7-dehydrocholesterol (7-DHC)[7] and biologically transformed to an active hormone, calcitriol, through enzymatic transformations.

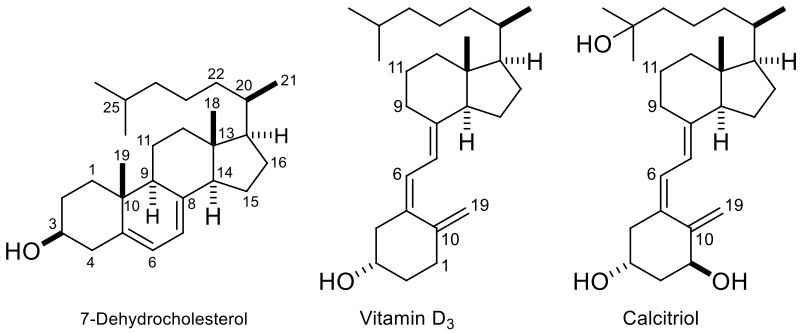

Figure 2. Structure and nomenclature of 7-dehydrocholesterol, vitamin D_3 and calcitriol.

Vitamin D is classified as a steroid hormone, being included in the same category of other classical hormones, such as testosterone, estradiol, cortisol or aldosterone. Steroids are natural compounds that present a common basic structure of four fused rings (**A** to **D**).[8]

Vitamin D and its derivatives are part of a subtype of steroids called secosteroids, and they display a triene system as a result of a photochemical rupture of C9-C10 bond from ring **B** of the steroid precursor (7-DHC).

In comparison to other steroidal hormones, vitamin D_3 and its metabolites have high conformational flexibility, mainly due to the presence of a triene system and a side chain (Figure 3).

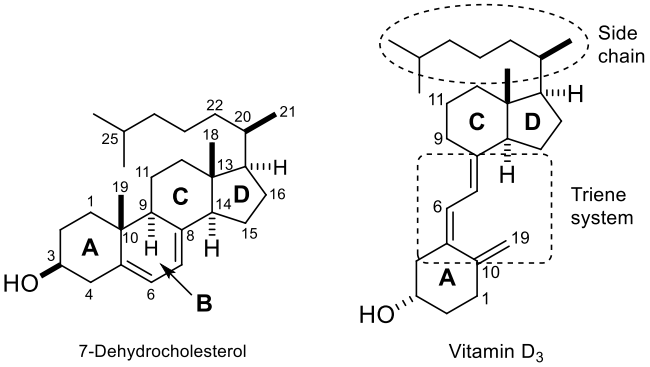

Figure 3. Structure and nomenclature of vitamin D_3 and its steroidal precursor.

3. Vitamin D Metabolism

Vitamins are defined as heterogeneous compounds without energetic value that can only be obtained through diet and cannot be synthesised by the organism. Though vitamin D_3 is classified as a vitamin due to historical factors, it can be obtained through diet or via UV light mediated endogenous transformation in the epidermis.

In terms of diet, vitamin D_3 is obtained in significant quantities through the ingestion of fish oils, mushrooms, egg yolk or even liver. Nowadays, some milks, cereals or juices are enriched with vitamin D_3, to ensure the ingestion of the dietary reference intake of vitamin D.[9]

Despite the referred dietary sources of vitamin D_3, its endogenous transformation in the skin is still the most important and accountable source of this vitamin.[10]

Vitamin D is produced in the skin as a result of solar exposure in a process that involves the photolysis of epidermal 7-DHC (provitamin D) and consequent conversion in previtamin D_3 (Scheme 1). This previtamin, through a process of antarafacial sigmatropic shifting of hydrogens is converted into vitamin D.[11] Lumisterol and taquisterol are also produced from previtamin as by-products.

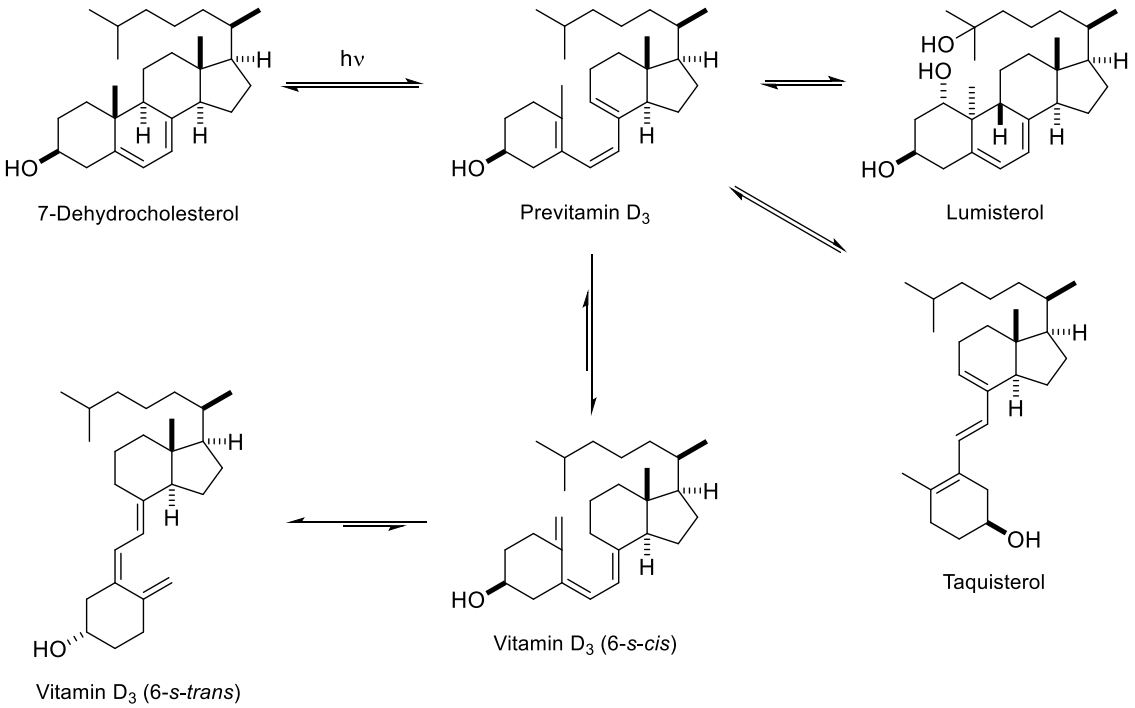

Scheme 1. Metabolic route of vitamin D formation in the skin.

However, this metabolite is not active in this form and must be activated downstream to portray its biological functions. Therefore, the vitamin undergoes a hydroxylation in the liver, catalysed by *CYP2R1*, a 25-hydroxylase, member of the cytochrome P450 superfamily of enzymes to afford 25(OH)D_3.[12] This enzyme is reported to be one of the most important 25-OHases, since its deletion in genetic studies leads to a vitamin D dysfunction phenotype.[13] The metabolite 25(OH)D_3 is transported in the blood mainly by association with the vitamin D binding protein (DBP).

The second hydroxylation occurs in the distal tubules of the kidney, under the action of the mitochondrial *CYP27B1*, giving place to the final and active hormone, 1α,25(OH)$_2D_3$ (1,25D; calcitriol).[14]

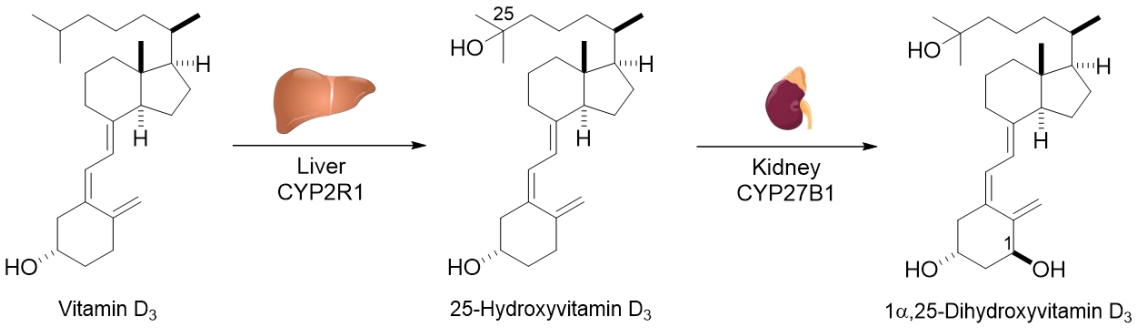

Vitamin D_3 — 25-Hydroxyvitamin D_3 — 1α,25-Dihydroxyvitamin D_3

Scheme 2. Biological activation of vitamin D_3

This hormone has widespread biological effects and, as such, its action is rigorously controlled by different enzymes. The degradation pathway is accomplished *via* the CYP27A1, a microsomal enzyme that is constitutionally expressed in the kidney and stimulated by 1α,25(OH)$_2D_3$.[15] This pathway leads to the oxidative rupture of the side chain, via hydroxylation of 1α,25(OH)$_2D_3$ at carbon 23 or 24 to give 1,24,25-trihydroxyvitamin D_3 [1,24,25(OH)$_3D_3$] or 1,25-hydroxyvitamin D_3-26,23-lactone, respectively.[16] Each oxidation leads to distinct metabolites that lack the biological activity of the hormone. One of the final products of this route is calcitroic acid, which is biologically inert and hydrosoluble, easing its excretion in the urine. Deletion studies on the gene *CYP27A1* show a hypercalcemic and hypercalciuric phenotype,[17] that were later attributed to the toxicity induced by high amounts of circulating 1α,25(OH)$_2D_3$.

Calcitriol is also tightly controlled by endocrine factors parathyroid hormone (PTH) and the fibroblast growth factor 23 (FGF23).

The important endocrine feedback circuit involves the 1α,25$(OH)_2D_3$ high levels acting to suppress the *CYP27B1* gene, to downregulate PTH secretion and to increase the expression of FGF23 in bone tissues.

Understanding the molecular foundations for the regulation of CYP27B1 and CYP27A1 by their primary regulators, PTH, 1α,25$(OH)_2D_3$ and FGF23 is of utmost importance, since it allows the better comprehension of diseases that implicate the production and degradation of vitamin D.

4. Mode of Action of 1α,25$(OH)_2D_3$

The steroid hormone 1α,25$(OH)_2D_3$, as other steroid hormones, exerts its biological functions through the regulation of gene transcription, called the classical genomic responses, or through the activation of a series of rapid transduction signal pathways at the plasma membrane, called the rapid or nongenomic responses.

4.1. Genomic actions and Vitamin D Receptor

The genomic actions of vitamin D are a result of the interaction of the active hormone, 1,25D, with the nuclear vitamin D receptor (VDR) in a very stereospecific way, binding 1α,25$(OH)_2D_3$ with high affinity (Kd ≈ 0.5 nmol/L).[18] 1,25D enters the cells through passive diffusion, after being transported from the kidneys associated with the vitamin D binding protein (DBP). Binding of the 1,25D with VDR leads to a conformational shift of VDR at the *C*-terminal and induces heterodimerization between VDR and the retinoid X receptor (RXR). This alteration also enables the region termed AF-2 on the VDR to interact with other proteins like transcription factors, including coactivator proteins such as SRC-1.[19] The 1,25D-VDR-RXR-CoA complex then binds to certain DNA sequences named response elements (VDREs) at the promoter sites of the targeted genes, leading to gene transcription (Figure 4).[20]

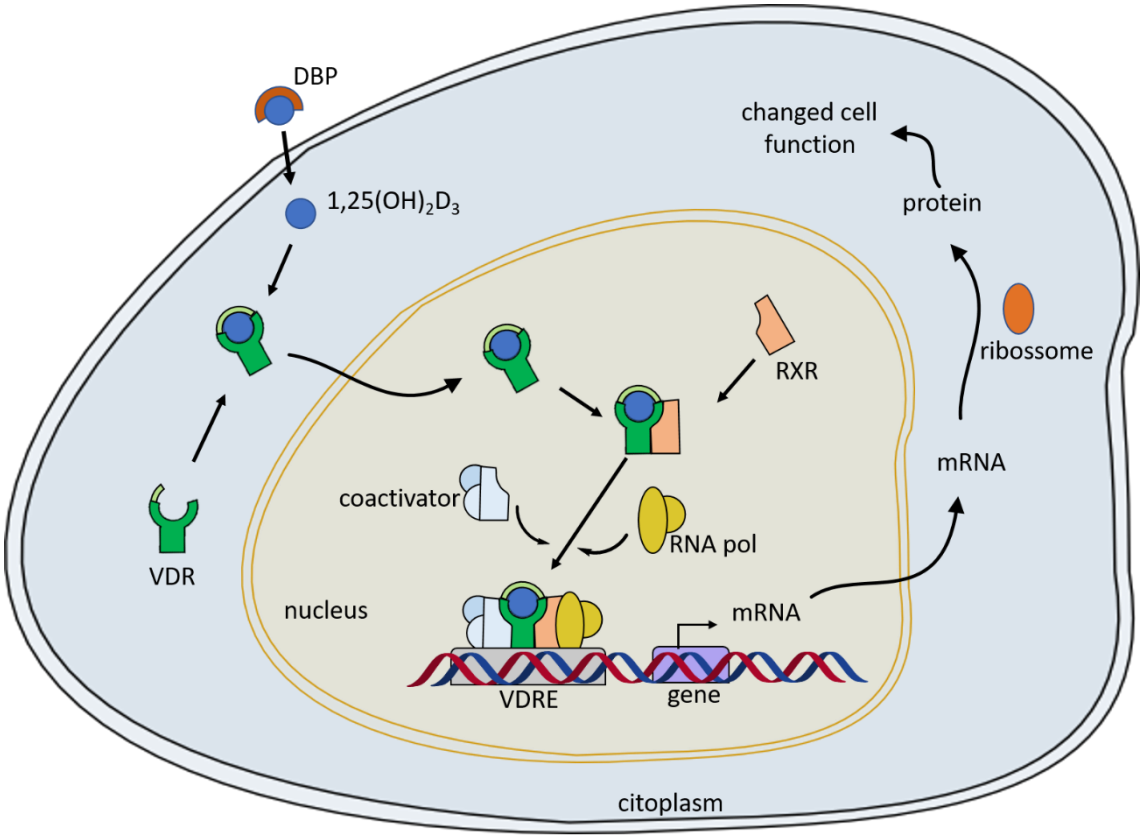

Figure 4. Mode of action of 1α,25(OH)$_2$D$_3$

A vast amount of work on VDR coactivators has unveiled that these proteins may possess intrinsic histone acetylase activity, being essential for gene transcription.

4.1.1. The vitamin D receptor

The VDR was first found in the chicken intestine[21], with the human and rat VDR being found shortly after. Its biochemical properties, including its ability to bind DNA were only unveiled later and showed similarities to other steroid hormones receptors.

The VDR is phylogenetically conserved, with the human VDR having only 4 more amino acids at the *N*-terminal chain when compared to the rat analogous. it has two different domains: the DNA-binding domain (DBD) and the ligand-binding domain (LBD, Figure 5). At the *N*-terminus is a truncated A/B domain of 22 aminoacids with few described activities. The DNA-binding domain, also called the C region, contains two zinc fingers. A small D region, or hinge domain, provides flexibility to the protein and links the DBD to the LBD. The LBD is a complex region accountable for the high-affinity binding of the ligand, for the dimerization with RXR and for the binding to transcription factors.

Although the crystalline structure of the entire VDR has not yet been unravelled, the structures of the separate domains are known and enable us to study different interactions within the protein.

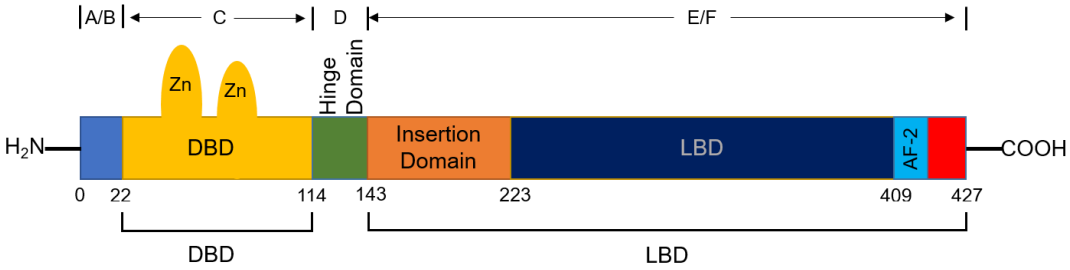

Figure 5. Schematic view of amino acid sequences of the human Vitamin D Receptor (VDR).

4.1.1.1 DNA binding domain

As previously mentioned, the VDR possesses a conserved DNA binding domain (DBD) that consists of two zinc atoms coordinated by 8 histidine residues in a geometry that resembles a tetrahedron.[22] The zinc finger closer to the *N*-terminus is responsible for the binding to the DNA VDREs, while the other zinc finger helps stabilize the dimerization with RXR

The DBD contains two α helixes (H1 and H2) that are packed together in a perpendicular angle, with the hydrophobic residues facing the DNA. Helix H1 is responsible for the binding to DNA, as it binds to repeats of 5'-AGAACA-3' palindromic sites and thus inserts itself in the DNA major groove.[23]

Water molecules also play a role in the interaction between the VDR and the DNA by bridging the gap between protein side chains and DNA functional groups.[24]

4.1.1.2 Ligand Binding Domain

This highly variable *C*-terminus domain is responsible for the high affinity between the protein and the $1\alpha,25(OH)_2D_3$ hormone.

In the human VDR, the LBD has an insertion domain between residues 143 and 223 (connecting helices H1 and H3). This insertion domain is highly variable between species and does not have any recognized biological function. Structurally, this insertion domain has few short β strands and high percentage of negatively charged residues, which may explain the weak VDR stability and high nonspecific contacts that interfere with crystallization procedures.[25] Indeed, Moras and colleagues, hypothesized that the presence of this segment in the VDR was the reason the first

attempts to obtain the crystal structure of the LBD failed. They successfully managed to create a mutated VDR that lacked the flexible insertion domain. Since the mutated region is far from the aminoacids that interact with the ligand or with corepressors and coactivators, it should not interfere with the biological functions of the receptor.[26] The structure of the mutated VDR complexed with 1,25D and other synthetic agonists was obtained (Figure 6).[25]

The global construction of the VDR LBD is similar to other nuclear receptors LBDs, presenting 13 α helices in a 3-layer sandwich structure, as well as 3 stranded β sheet. It is suitable to note that the structure of the helix H1 and its relative position in the LBD allows the stabilization of its global structure by intramolecular contacts. Localized in C-terminus, the H12 helix is a crucial component of the LBD, as its interactions with different ligands provide a critical control of the agonists/antagonists actions on the nuclear receptor. Furthermore, H12 contains a seven aminoacids region, the ligand dependent activation function (AF-2) that acts as a molecular switcher in response to the ligands.[27]

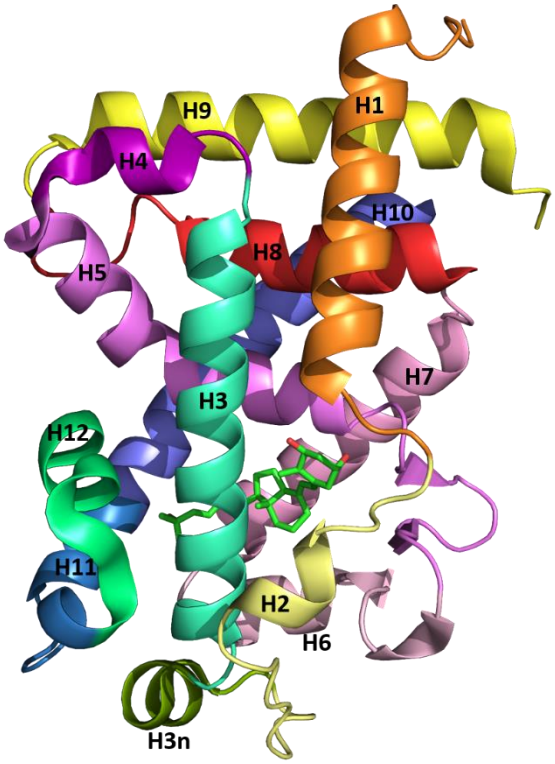

Figure 6. Crystallographic structure of LBD bound to calcitriol (PDB: 1DB1).

4.1.1.3 VDR ligand stabilization network

Understanding the key molecular interactions between calcitriol and its receptor is essential to interpret how changes in the ligand can modulate the biological responses. Detailed analysis on the crystal structure of the VDR's LBD complexed with its natural ligand has provided comprehensive insights on the most important ligand-receptor interactions.[28]

The 1α,25(OH)$_2$D$_3$ adopts a β-chair conformation in the VDR pocket, with the C1α-OH and C3β-OH in equatorial and axial orientation, respectively.

The conjugated triene system connecting the **A** ring to the **CD** bicycle, shows an almost *trans* conformation with a torsion angle on the C6-C7 bond of -149º, inside the receptor. This torsion makes the ligand adopt an overall curved geometry, unlike the ligand in an unbound state, which presents a planar geometry. A hydrophobic channel surrounds the triene system, stabilizing its conformation, through van der Waals interactions with aminoacids Ser-275 (H5), Trp-286 and Leu-233 (H3).

The **C** ring also interacts with Trp-286 (on the α face), whereas the methyl on C18 reaches out to the Val-234 on the H3 helix.

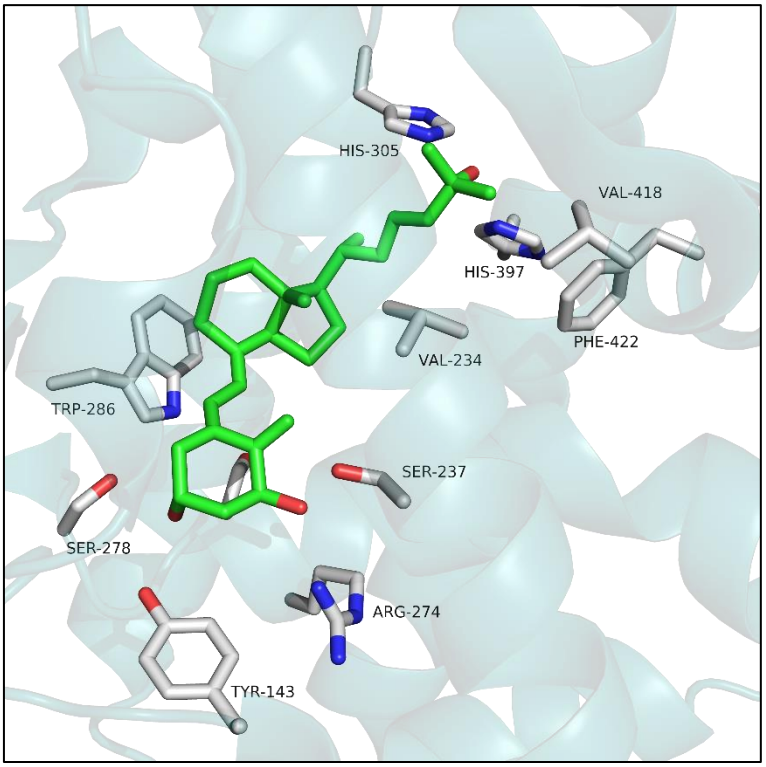

Figure 7. General view of calcitriol in the binding pocket.

Regarding the **A ring**, the C1α-OH group forms hydrogen bonds with Ser-237 (H3) and Arg-274 (H5), while the C3-OH group makes hydrogen bonds with residues Ser-278 (H5) and Tyr-143 (loop H1-H2).

The side chain at C17 adopts an extended conformation parallel to the C13-C18 bond and is surrounded by hydrophobic residues. These interactions are thought to keep the active conformation of the ligand while bound to the LBD.[29]

At the end of the side chain, C25-OH interacts with His305 and His397, through hydrogen bonds. In addition, the H12 helix in its active configuration also establishes van der Waals interactions with the methyl C27, through Val-418 and Phe-422.

It is also important to point out the fact that the ligand binding cavity of the *h*VDR is large, with the ligand only occupying 56% of the total available volume. Additional space is observed near the **A** ring, as well as in the side chain, which could allocate several types of modified new ligands.

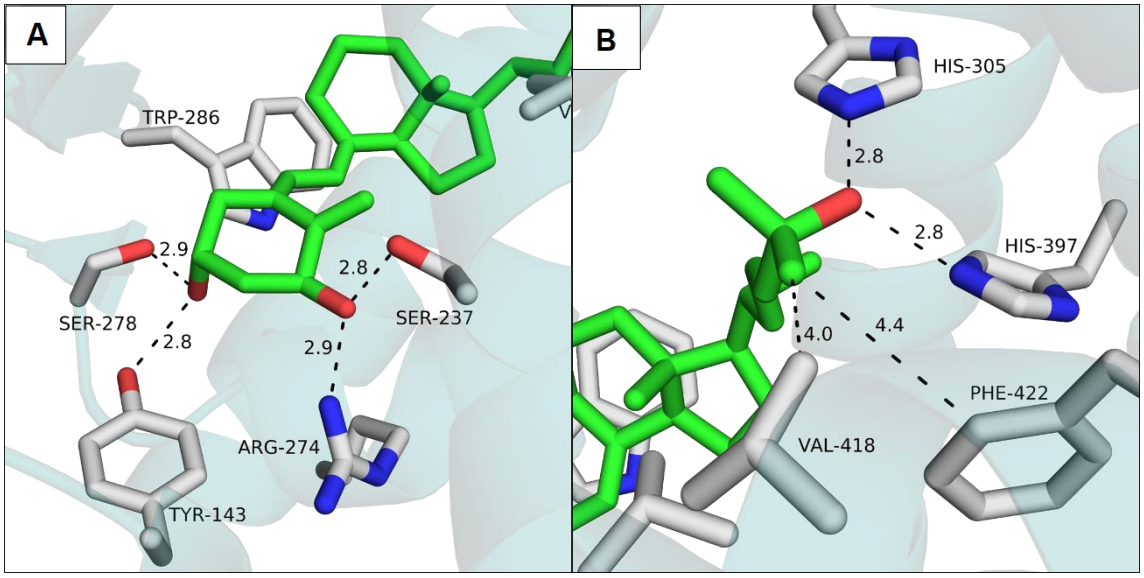

Figure 8. Key molecular interactions of calcitriol in the binding pocket.

4.2. Non-genomic actions

Vitamin D was initially thought to only act on genomic level, as discussed above, and it was not until later that some actions were considered too rapid to be accounted as changes at a genomic level.

It is presently recognized that 1α,25$(OH)_2D_3$ has non-genomic actions that essentially manifest as the activation of signaling molecules (PLC, PLA2, PI3K, p21ras) and rapidly generated second messengers, such as Ca^{2+}, cAMP or fatty acids. These effects can be accompanied by the activation of protein kinases, protein kinase A, MAP kinases, PKC or Ca^{2+}-calmodulin kinase II, for example.

In terms of large scale effects, the non-genomic actions of 1,25D are responsible for:[30]

- Opening of Ca^{2+} and Cl^- channels;
- Rapid increase in the absorption of calcium at the intestinal level;
- Insulin secretion by β pancreatic cells;
- Quick migration of endothelial cells;
- Decreasing of PTH secretion;
- Stimulation of osteoclastic bone resorption;
- Decreasing production of collagen type I.

Further research led to the characterization of a new receptor[31] besides VDR that may mediate rapid responses, named membrane-associated rapid response steroid (MARRS). This receptor is located on the cell membrane or in the perinuclear area, within lipid rafts, but not on the nucleus.

In conclusion, the non-genomic actions of vitamin D are yet superficially studied in comparison to the genomic actions. Future research on this field will help to elucidate the mechanisms by which these actions are accomplished.

5. Biological Activity of Vitamin D

The hormone $1\alpha,25(OH)_2D_3$ is implied in a wide variety of biologic processes that can be classified as classical and non-classical functions. The classical functions are responsible for the calcium and phosphate homeostasis. The non-classical functions encompass cell differentiation and proliferation processes, modulation of immune responses and control of tissue malignancy progression.

- Calcium Homeostasis

Through its interaction with many proteins, calcium is involved in different aspects of the organism, such as neuronal transmission, enzymatic regulation, muscle contraction or cell differentiation. Such diverse functions are controlled through a tight regulation of cellular compartments and extracellular fluids, by the activity of several calcium ATPases, channels and exchangers located in plasmatic membranes and endoplasmic reticulum membrane.

This homeostasis involves the cooperation between the kidneys, the intestine, the liver, the parathyroid gland and the skeleton, in which the 1α,25$(OH)_2D_3$ hormone plays a major role (Figure 9).

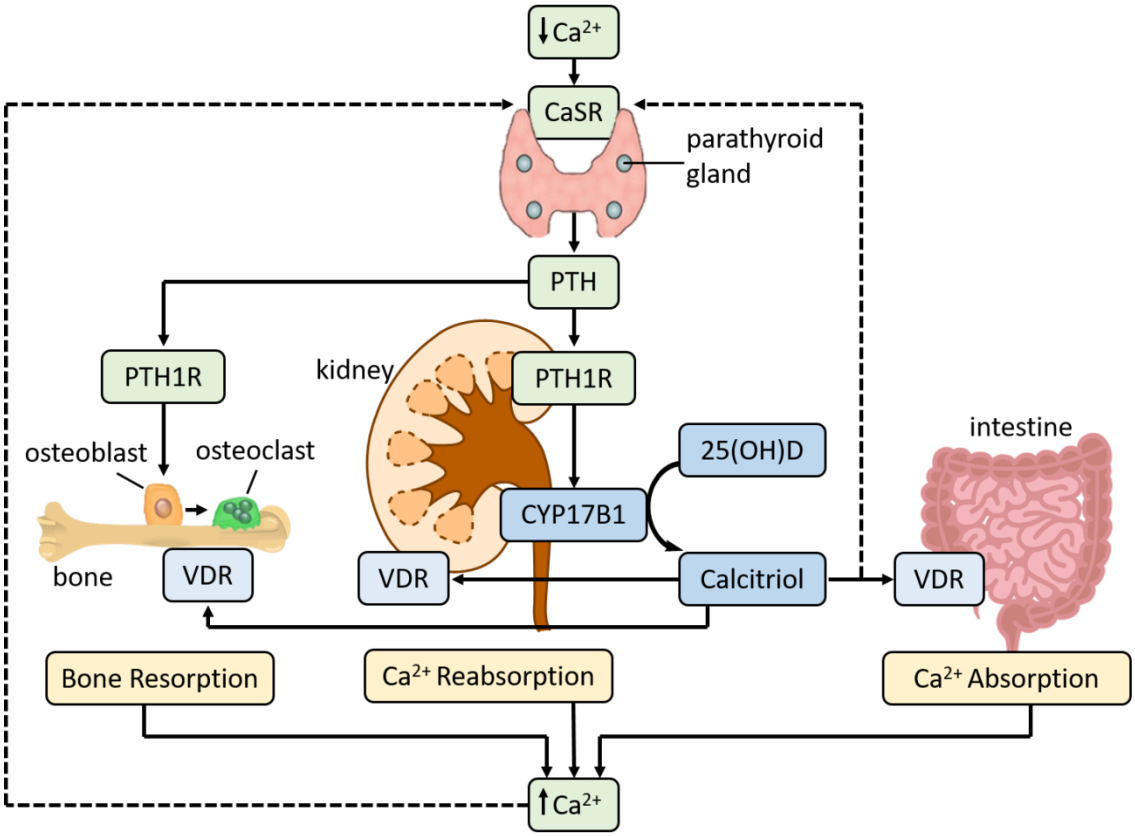

Figure 9. Overview of the calcium homeostasis.

- PTH Regulation

Parathyroid hormone, PTH is produced in the parathyroid gland. PTH in the blood will induce 1α-hydroxylase in the kidney, inducing 1α,25$(OH)_2D_3$ production.

In a negative feedback loop, the newly synthesized calcitriol will act on the parathyroid gland in two ways. First, it interacts with VDR that is expressed in this gland, acting on a negative VDRE here located, exerting suppression of PTH production[32]. It also increases parathyroid sensitivity to Ca^{2+} inhibition by increasing the expression of calcium sensing receptor (CaSR), further regulating PTH levels.[33] This enables the regulation of PTH production and the proliferation of the gland

These actions of 1α,25$(OH)_2D_3$ are manipulated in the clinical practice as a method of treating secondary hyperparathyroidism in renal failure.[34]

- Intestinal Calcium Absorption

Vitamin D is reported to be essential in enhancing the absorption of intestinal ions, calcium and phosphate, mainly in the duodenum portion.[35] Experiments with mice lacking VDR, 1α-hydroxylase or both, have evidenced that these mice express the same phenotype visible in patients with vitamin D-dependent rickets.[36] This shows that 1α,25$(OH)_2D_3$ and VDR are both needed for an efficient intestinal calcium absorption.

Calcium uptake in the intestinal cells is accomplished in a transcellular fashion, mediated by active transport trough the interior of the cells and also by paracellular transport, which does not require energy and can be found throughout the intestine.

- Renal Calcium Reabsorption

In the kidney, the most important endocrine effect of 1α,25$(OH)_2D_3$ is its own regulation, as there is an increase of the levels of 24-hydroxylase and a suppression of 1α-hydroxylase. Calcitriol is also involved in the reabsorption of calcium in the nephron, mainly in the proximal tubules.[37]

Similarly to intestinal absorption, renal reabsorption is accomplished via paracellular and transepithelial transport, the latter occurring in three steps.

VDR and 1α,25$(OH)_2D_3$ play an important role in modulating calcium renal reabsorption through the upregulation of proteins such as D28k, NCX1 and TRPV5.[21]

- Bone Calcium Regulation

Vitamin D is also essential to the development and maintenance of the skeleton, by regulating the calcium uptake and release in osteoblasts and osteoclasts.

Osteoblasts are responsible for the promotion of bone formation, while osteoclasts break bone tissue and release calcium. Osteoblasts express a surface ligand, RANKL, which can bind protein RANK, which is expressed in osteoclast cells, or osteoprotegerin (OPG), a soluble ligand osteoblast-derived. When RANKL binds RANK on the osteoclast surface, it triggers a signaling cascade that leads to differentiation and maturation of osteoclasts. OPG acts as a decoy for RANK, disrupting RANKL-RANK interactions and binding RANKL in a competitive way, inhibiting osteoclast development.[38]

Calcitriol and PTH are modulators of bone resorption, as they enhance the expression of RANKL and inhibit OPG formation. Both 1α,25$(OH)_2D_3$ and VDR conjoined actions

are needed to ensure optimal osteoblastic bone formation and osteoclastic bone resorption.[39]

- Suppression of cell growth

There has been evidence that 1α,25$(OH)_2D_3$ inhibits clonal proliferation in several cancerigenous cell lines and promotes its differentiation towards less aggressive phenotypes.

The mechanisms known to date suggest that 1,25D can arrest the malign cell cycle in the G_0/G_1 phases. It also induces the expression of cyclin-dependent kinase inhibitors p21 and p27, promotes the sequestering of activated EGRF into endosomes or even enhances the expression of C/EBPβ, leading to diminished cellular proliferation.

- Apoptosis Regulation

Calcitriol induced apoptosis enables the control of hiperproliferative disorders.

In breast and prostate cancer cells, 1,25D induces apoptosis through the modulation of pro-apoptotic proteins, such as Bax and increases the intracellular Ca^{2+} concentration that leads to the activation of several caspases. Further studies in MCF7 cell lines elicited that calcitriol increases the effects of ionizing radiation in these cells.

In contrast to the pro-apoptotic effect in malign cells, calcitriol exerts protective effects in normal cells, as it protects against UV-radiation or chemotherapy induced apoptosis.

- Modulation of immune responses

1α,25$(OH)_2D_3$ is effective in controlling infections, autoimmune diseases and tolerance to transplants, mainly by inducing differentiation of macrophages, antigen-presenting cells, dendritic cells and lymphocytes.

Several infectious diseases are known to be related to vitamin D deficiency, such as tuberculosis. 1α,25$(OH)_2D_3$ is also known to potentiate the destruction of microbes. Furthermore, lack of vitamin D is associated with some autoimmune diseases, for instance, Crohn's disease, multiple sclerosis or type 1 diabetes.

6. Vitamin D_3 Analogs

In order to induce the aforementioned physiological effects in the clinic, supraphysiological doses of 1,25D would have to be administered. This, however, would result in *in vivo* calcemic side effects, like hypercalcemia and hypercalciuria.

In this sense, several calcitriol analogs were developed to minimize these negative calcemic side-effects, while preserving or even enhancing the beneficial effects of the hormone. Some of the synthesized compounds are tissue-specific, have low calcemic properties and can be administrated in higher doses when compared with the native hormone.[40]

Nowadays there are more than 3000 published analogs that were synthesized by pharmaceutic industries and academic institutions. Most of the existing analogs are agonists of the VDR receptor, although some antagonists and inverse agonists can be found.[41, 42]

All of the analogs interact with the VDR-LBD region and their adopted conformation inside the receptor characterizes their functional profile. The interactions between these analogs and the VDR are best analysed by crystal structures, which provide detailed information about the molecular strucutres of the analogs inside the receptor.[25]

6.1. Clinically Approved Analogs

On the present day, almost all positions of the vitamin D structure have been modified in order to create new analogs. Most of the modifications are produced in the side chain since it is directly related to the biologic response and selectivity of the compounds. The integrity of the triene system is essential for the biological activity of the vitamin and therefore few analogs have alterations at this site. The **CD** bicycle is also usually left untouched, due to lack of information on the structure-activity correlation and to the difficulty in synthesizing such compounds.

The main goal of developing analogs is their therapeutic application in proliferative diseases (such as psoriasis), in bone disorders (such as osteoporosis) and in different types of cancer.[6]

Paricalcitol and doxercalciferol are two clinically approved analogs used to treat secondary hyperparathyroidism. Falecalcitriol and maxacalcitol are also used with the same goal but are exclusively used in Japan. All these compounds have the ability to decrease the elevated levels of circulating PTH by supressing it.[43]

Tocalcitol, calcipotriol and, more recently, maxacalcitol are used to treat psoriasis. They can be administrated as monotherapy or used in combination with topic steroids. They have pro-differentiation and anti-proliferative effects on keratinocytes.

In the case of osteoporosis, the existing analogs in clinical trials, alfacalcidol and eldecalcitol, are only tested in Japan. Their use increases bone mineral density and reduces the risk of new vertebral fractures.[44, 45]

Figure 10 shows some calcitriol analogs that have clinical application.

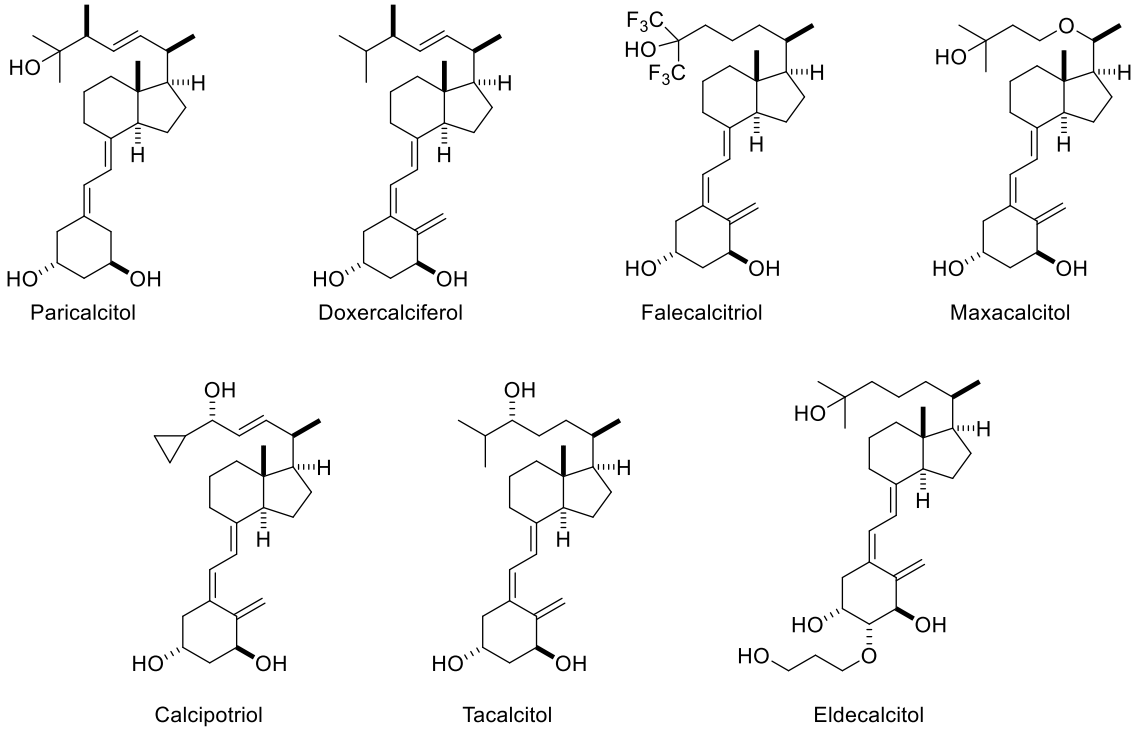

Figure 10. Overview of clinically approved vitamin D analogs.

6.2. Boron in Drug Design

It was only recently that the carbon neighbour, boron, began to catch the attention of researchers and pharmaceutical industries. Nowadays, boron is being investigated as an alternative to carbon in drug design.[46]

There are interesting differences between carbon and boron. The latter possesses both metallic and non-metallic characteristics since it can form oxides and salts [B_2O_3, $B_2(SO_4)_3$] as well as acids (H_3BO_3).

Boron is a trivalent metal but, unlike a metal, it has great electron affinity that results from its vacant *p*-orbital. The charge distribution allows the formation of non-covalent bonds, needed to form transient connections with active sites that are important in several biochemical reactions.

Given this structural and electronic aspects, boron compounds can give rise to a new generation of drugs, capable of binding to target molecules not accessible to carbon-based compounds.

In this endeavour, the first boron-based drug, Velcade® (bortezomib; Millennium Pharmaceuticals, Boston, MA, USA, Figure.11), was designed and clinically tested as a proteasome inhibitor for the treatment of multiple myeloma. The drug successfully passed phase III trials and received several regulatory approvals from FDA (US Food and Drug Administration) and by the EMEA (European Medicines Agency)[47]. Initially, Velcade® was used in confined cases but was later extended to treat newly diagnosed myeloma patients.

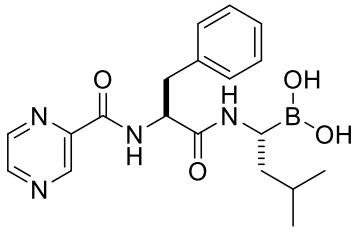

Figure 11. Bortezomib, marketed as Velcade® by Millennium Pharmaceuticals.

6.3. Boron in BNCT

Aside from drug design, boron also plays an important role in Boron Neutron Capture Therapy (BNCT).[48, 49] This therapy takes advantage of the nuclear reaction that occurs when the stable boron isotope, boron-10 (^{10}B) is irradiated with low-energy neutrons.

Boron and the neutrons are, on their own, usually inoffensive to the cells. However, when boron atoms are irradiated with a stream of neutrons, the B-10 atoms fissure and produce (^{4}He) α particles that have a high cytotoxic effect,. Furthermore, this reaction only exerts its effects in cells that accumulated boron and therefore it is harmless to the surrounding tissue. The main challenge is to develop boron compounds that can be taken up by cancer cells selectively.

The instruments used to produce the low-energy neutron beams are also a challenge to overcome, since it requires special nuclear reactors that are not affordable or accessible to most hospital centres.[50]

6.4. Boronic Acids

The utility of boronic acids is intimately connected to their unique electronic and physicochemical properties. In organic synthesis there are many boron-based reagents, which reflects its usefulness in the world of organic chemistry.[51]

One of the properties of boronic acids is their strong Lewis acid character, due to the boron open shell. Most phenylboronic acids present a pKa in the 4.5-8.8 range. Upon different substitutions, boronic acids can readily convert from a trigonal planar neutral sp^2 boron to a tetrahedral anionic sp^3 boron, under physiological conditions. This conversion makes these compounds good transition state analogs for inhibitors of hydrolytic enzymes.[52] Indeed, nowadays, there are boronic analogs used as enzymatic inhibitors of several enzymes, such as peptidases, proteases, transpeptidases as well as nitric oxide synthase (NOS).

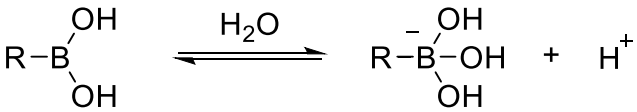

Figure 12. Conversion of boronic acids under physiological conditions. Adapted from Yang, et al. 2003.[53]

Another application of boronic acids is the already mentioned BNCT, where the unique properties of the boron-10 isotope are exploited. The intent is to establish a targeted delivery of boron-carrying compounds, in high concentration, to cancer cells. By doing so, these compounds would be ideal for localized radiation therapy.

One more potential use for boronic acid compounds is the creation of feedback-controlled delivery systems for insulin. The idea comes from the fact that boronic acids can interact with dihydroxylated compounds, for instance, sugars. The ideal controlling signal for this application would be glucose concentration changes. The goal would be to create boronic acid polymers that could store insulin in their interior and upon a change in glucose concentration, detected by the interaction between glucose and boronic acids on the polymer surface, the polymer would change its permeability and release insulin into the blood stream.

Given the biological applications of boronic acids, and the many potential compounds that can be designed, this field of investigation has yet to be fully exploited.

Objectives

Objectives

Given the growing number of applications for boron ligands in the drug discovery field, this work focuses on the development of boronic acid and boronic ester analogs of 1α,25(OH)$_2$D$_3$, with a view on biological studies.

For this purpose, the main objectives of this thesis are:

1. Docking of new boronic 1,25D analogs into the crystallographic structure of the VDR(LBD) complex to explore their *in silico* affinity for the VDR;
2. Synthesis of the analogs that showed higher theoretical affinity towards the receptor. Figure 13 shows the chosen analogs to be synthesized (**A4** and **E4**).

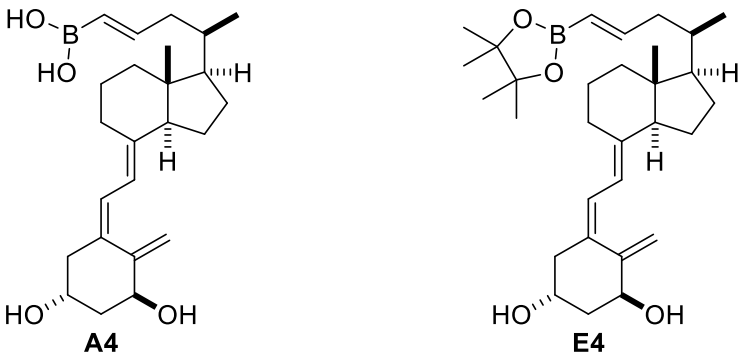

Figure 13. Target analogs of this work.

Results and Discussion

Results and Discussion

1. Docking Studies

The analogs were docked into the VDR(LBD), following a protocol developed in this research group, to predict their affinity for the vitamin D receptor.

The structures of the docked analogues (**A1**-**A4, E1**-**E4**) are shown in Figure 14.

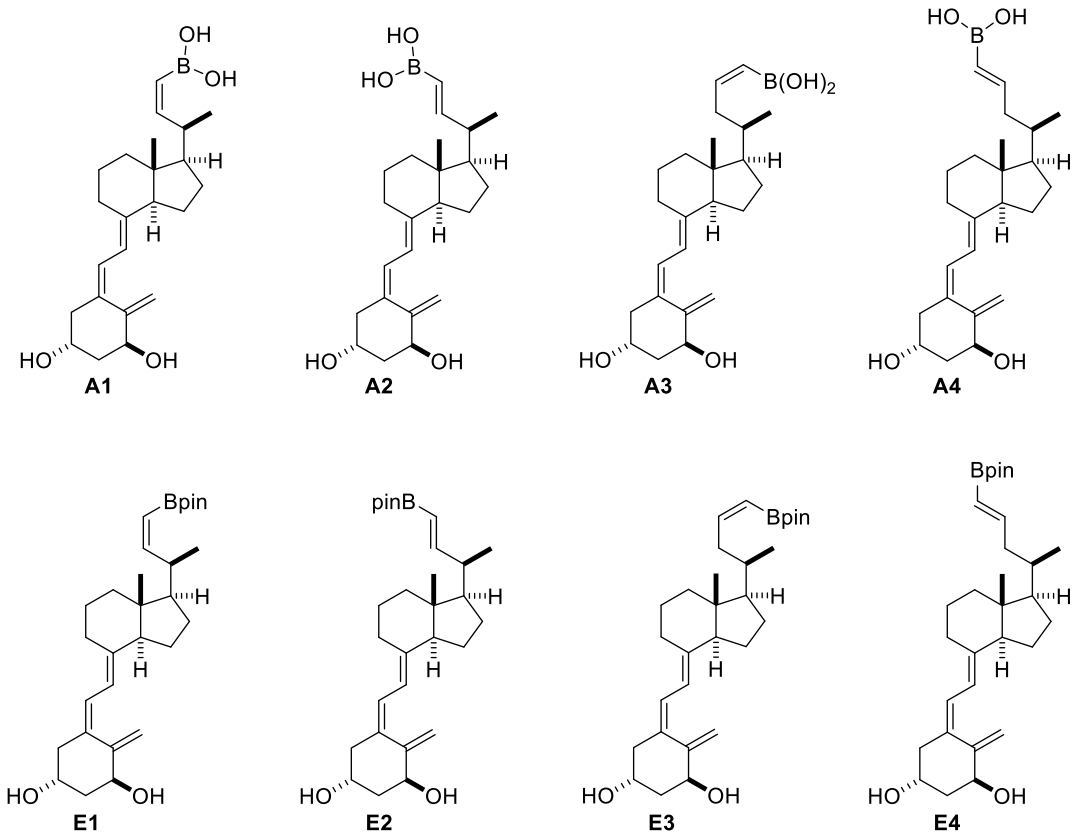

Figure 14. Structure of the docked vitamin D analogs.

The proposed analogs differ from one another by: the length of their side chain, the functional group at the end of the side chain and the configuration of the double bond.

Firstly, the proposed analogs were built, using the three-dimensional structure of 1,25D, obtained from the crystal calcitriol-VDR(LBD) complex (PDB code: 1DB1). Modifications to the analogs were carried out with the builder mode of *Pymol* and the editing tool provided by *Chem3D* software.

Docking studies to predict the affinity of each analog for the VDR(LBD) were made using the *Gold* software (version Suite 5.2). A modified structure of VDR(LBD), with inclusion of hydrogens and missing gap regions, was used as the protein. The binding site of the protein was set automatically with a 10 Å radius.

Docking was performed in 25 independent genetic algorithm (GA) runs. In each run, a maximum of 125000 GA operations were performed in a single population of 100 individuals. Default parameters were employed for hydrogen bonds (4.0 Å) and Van der Waals interactions (2.5 Å). ChemPLP was used as the scoring function and GoldScore was used as the re-scoring function.

For each ligand, the three best solutions were normalized using the score of 1,25D as the reference value (100%). Figure 15 and Figure 16 represent the main interactions between the docked analogs and the amino acids of VDR. The relative score for each analog with respect to the natural hormone are shown in brackets.

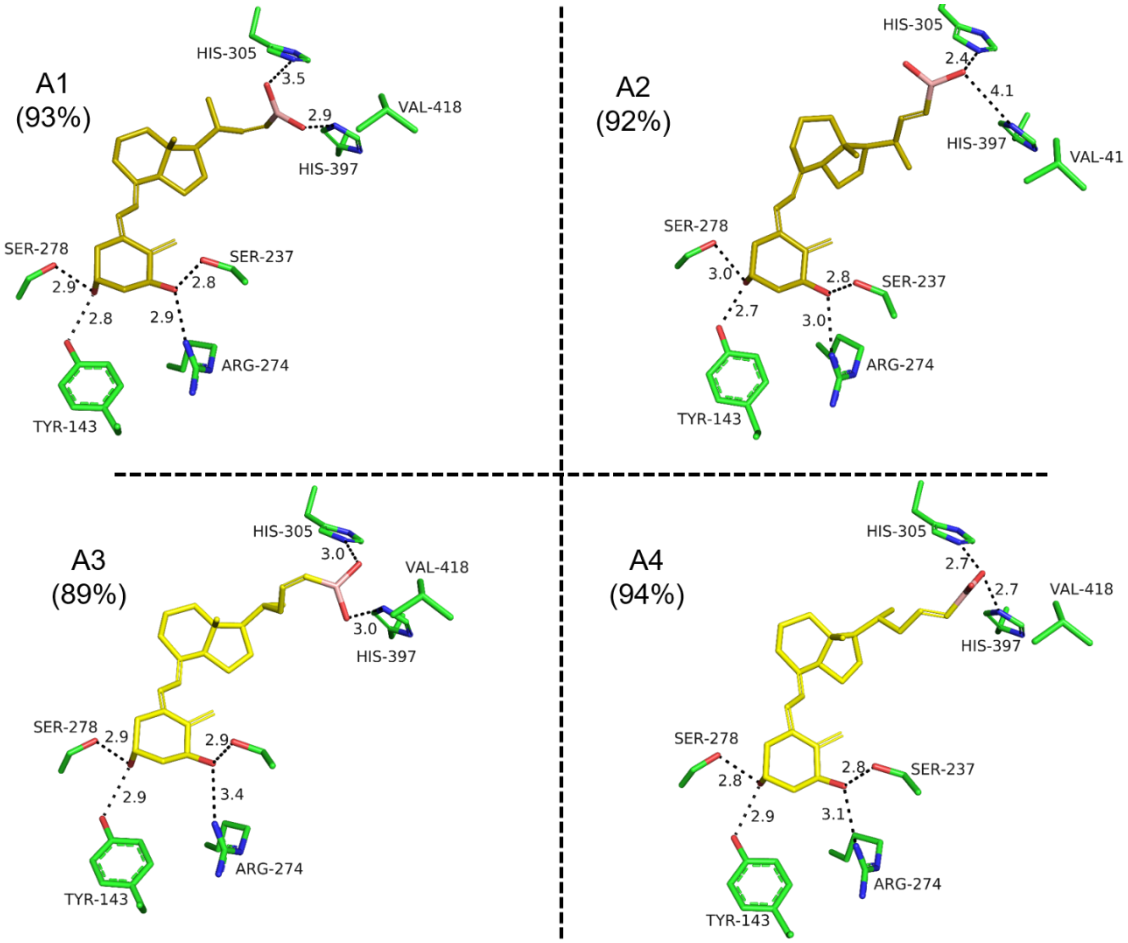

Figure 15. Ligand-VDR(LBD) interactions and relative scores for boronic acids analogs (A1-A4).

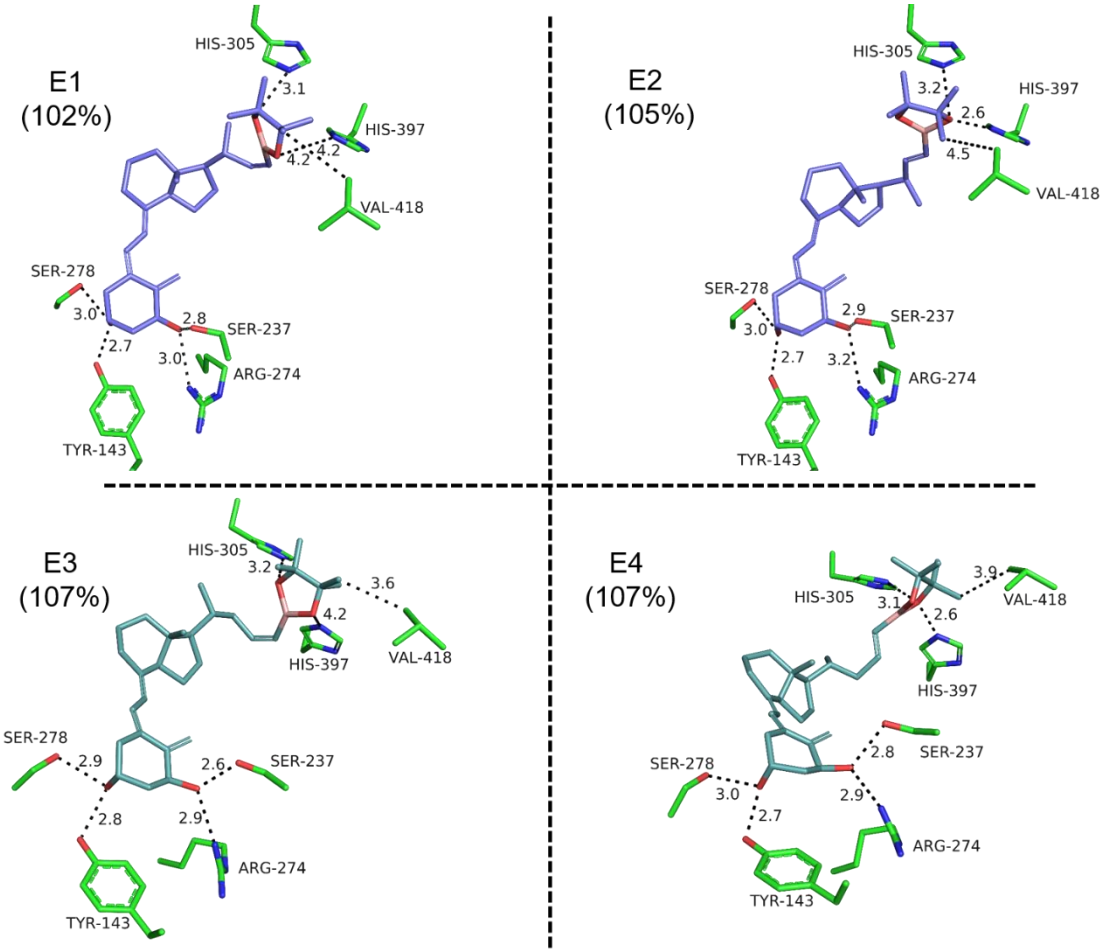

Figure 16. Ligand-VDR(LBD) interactions and relative scores for boronic esters analogs (E1-E4).

Overall, the adopted conformations of the ligands vary little from that of calcitriol, as seen by the maintenance of the C3-OH and C1-OH hydrogen bonds with VDR for all analogs. Analogs with a boronic ester group at the side chain (Figure 16) present better scores when compared with the corresponding compounds with terminal boronic acid groups (Figure 15).

Ligands **A1** and **A2** show lower score in comparison with the natural ligand (93% and 92%, respectively). Ligand **A1**, despite the low score, shows stable hydrogen bonds through the OH groups with the amino acid residues in the binding pocket. Ligand **A2** appears to bind effectively with VDR(LBD), but the *trans* configuration seems to move the hydroxyl groups of the boronic acid apart from His-397.

The side chains of both analogs **A1** and **A2** are far away from Val-418 (which is thought to be important to grant the transcriptional activity to the ligands that bind the receptor). We do not expect transcriptional activity for the analogs **A1** and **A2** because no interactions of the corresponding side chains with Val-418 are observed.

The side chains of **A3** and **A4** bind effectively with the His-305 and His-397 residues through the corresponding BOH groups. The verified lower scores for these analogs can be explained by different van der Walls interactions maintained between the analogs and the protein.

In compound **E1**, one oxygen of Bpin interacts with His-305 by hydrogen bonds while no interactions of the same nature are observed with His-397. One methyl from Bpin also interacts with the amino acid Val-418. Therefore, based on these observations, this compound should induce transcription.

Regarding compound **E2,** it binds effectively with both His-305 and His-397, by hydrogen bonding. Although the distance between the methyl group on the Bpin and Val-418 is slightly larger, this analog should bind well to the VDR receptor *in vivo* and induce transcription.

Even though analog **E3** does not interact with His-397 by hydrogen bonding, the methyl of its Bpin group is close to Val-418. Therefore, this compound might be an agonist.

Analog **E4** binds strongly by hydrogen bonds with both His-305 and His-397. In addition, the methyl of Bpin is close to Val-418. Therefore, this compound should behave as a superagonist.

After analysing all the docked ligands in terms of score and interactions with the receptor amino acids, it is possible to designate the analogs **A1**, **A4**, **E2** and **E4** as the ones that should induce a stronger activity of VDR.

In order to assess the validity of the *in silico* predictions, analog E4 was chosen to be synthesized, due to its score (107%) and interactions with the most relevant residues in the active centre of the VDR. Moreover, analog **E4** would be a precursor of analog **A4** (94%) by removal of the pinacol ester in the side chain. The final goal is to characterize their biological profile *in vivo.*

Figure 17 illustrates the superimposition of the structures obtained by docking for analogs **A4** and **E4** with the natural hormone in the active site of the VDR.

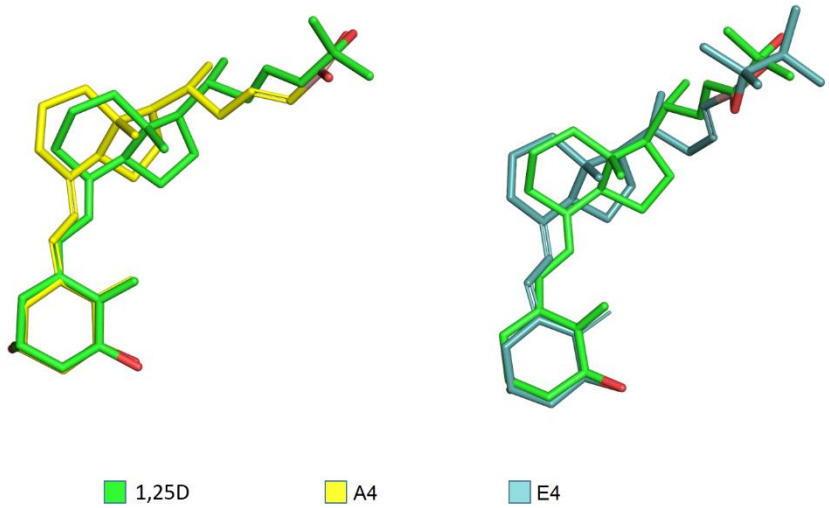

Figure 17. Superimposition of 1,25D with analogs **A4** (left) and **E4** (right) in the VDR active site.

2. General retrosynthetic route

The synthetic plan for the proposed compounds is depicted in the Scheme 3.

The boronic acid **A4** would be obtained by deprotection of its boronic ester precursor **E4**. The triene system arises by a Pd-catalyzed ring closure on enol-triflate **2** and subsequent Suzuki−Miyaura coupling with boronate **1**. Boronate **1** would derive from the known Inhoffen-Lythgoe diol **3**, readily obtained by reductive ozonolysis of commercial vitamin D_2.[54] Enol-triflate **2** would be prepared from epoxide **4**.

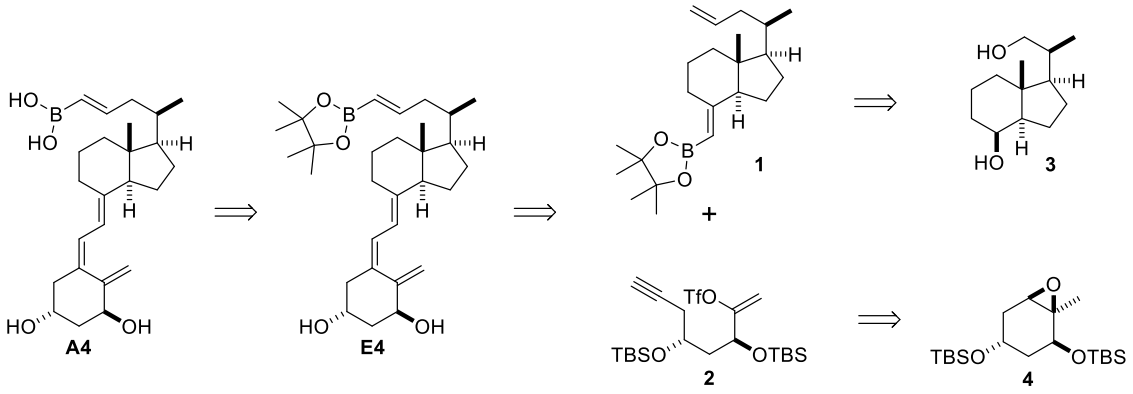

Scheme 3. Retrosynthetic analysis of analogs **A4** and **E4**.

3. Synthesis of boronate **1** (upper fragment)

The synthesis of boronate 1 is depicted in Scheme 4

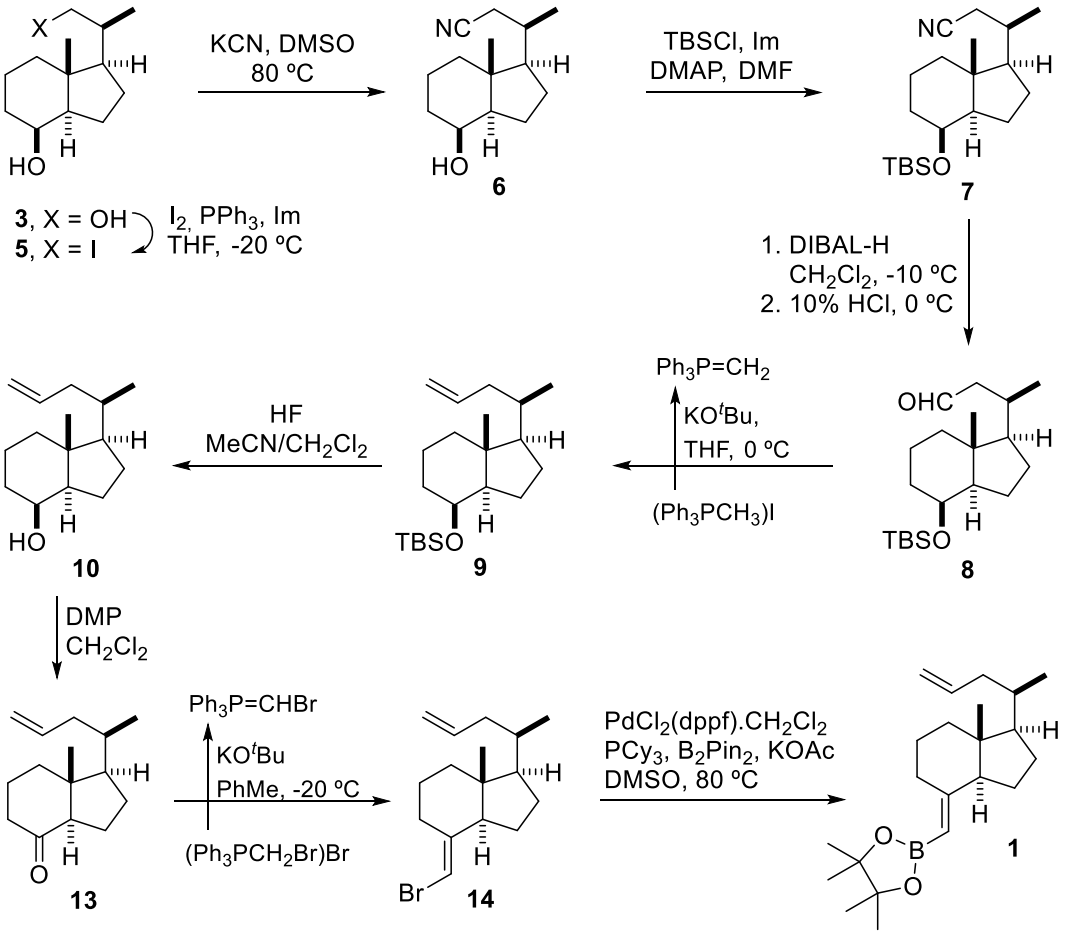

Scheme 4. Synthesis of boronate **1** from Inhoffen-Lythgoe diol.

3.1. Synthesis of alkene **10**

Starting from the Inhoffen-Lythgoe diol **3**, the first step in the synthesis of boronic ester **1** was the formation of alkene **10** (Scheme 4), following procedures previously developed in this research laboratory.

Alcohol **3** was treated with iodine in the presence of triphenylphosphine and imidazole and provided iodide **5** in 90% yield. Treatment of **5** with potassium cyanide gave nitrile **6** in 97% yield. Compound **6** was then protected with *tert*-butyldimethylsilyl chloride in the presence of 4-dimethylaminopyridine to give **7** in good yield.

Reduction of the nitrile functionality with diisobutylaluminium hydride in dichlroromethane, followed by treatment of the resulting mixture with a solution of chloridric acid provided aldehyde **8** in 82% yield.

The resulting aldehyde **8** was then submitted to a Wittig reaction. In this reaction, treatment of compound **8** with the ylide $Ph_3P=CH2$, generated by reaction of the phosphonium salt $(Ph_3PCH_3)I$ with potassium *tert*-butoxide, originated olefin **9** in 90% yield.

Scheme 5 shows the proposed mechanism for this Wittig-type reaction.

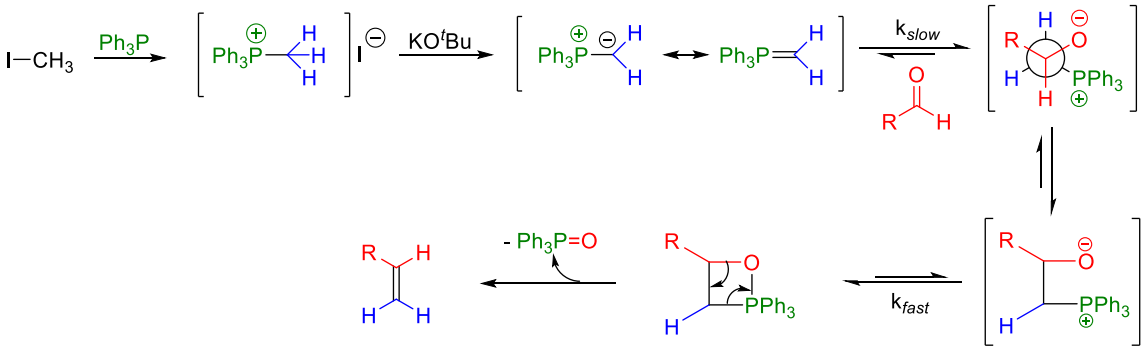

Scheme 5. Proposed mechanism of the Wittig reaction for olefin **9**.

In this case, since the ylide possesses two hydrogens, there is no stereoselectivity and the final product is the olefin **9** in 90% yield.

Figure 18 shows the most significant signals of the NMR spectra for compound **9**.

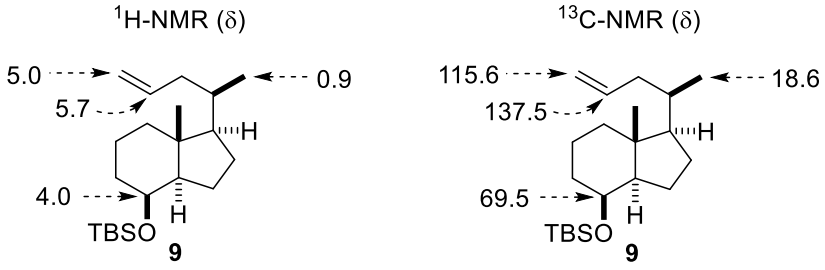

Figure 18. Characteristic NMR signals for compound **9**.

Desilylation of **9** with hydrogen fluoride in a mixture of dichloromethane/acetonitrile, provided alcohol **10** in 98% yield.

3.2. Preliminary experiments for the synthetic approach

3.2.1. Preliminary experiments for the cross metathesis of compound **E4**

Instead of continuing with the synthesis of boronate **1**, it was decided to face the introduction of the boronate functionality at the side chain of **10**.

The intent of these experiments was to find reaction conditions to produce the boronic ester **E4**. Given the foreseeable difficulty in the synthesis, several conditions were tested using the **CD** bicycle of the vitamin as a simplified version of the full vitamin (Scheme 6, Table 1).

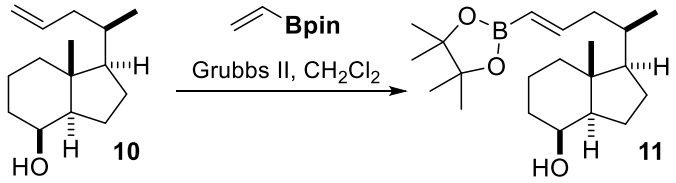

Scheme 6. Preparation of boronic ester **11**.

In the first attempt to produce boronate **11** by cross metathesis, 2 equivalents of alkene **10** were used, together with 1 eq. of vinyl boronic pinacol ester (pinBCH=CH_2) in dichloromethane at room temperature, for 6 hours. The results were unsatisfactory, as only 40% of the desired product was obtained (Table 1, entry 1). In this reaction it was also observed the formation of vinyl boronic pinacol ester dimers, as well as the recovery of some initial substance **10**.

The use of pinBCH=CH_2 in excess (2 eq) with the same reaction conditions gave boronate 11 in 95% yield (entry 2).[55] In this experiment, another modification made to the protocol was the addition of the Grubbs catalyst before adding the reactants. These modifications led to an increased yield and reduced the formation of by-products.

Table 1. Tested conditions for olefin cross metathesis reaction.

Entry	Equivalents		Solvent	Temperature (ºC)	Time (h)	**11** (Yield)
	10	Bpin				
1	2	1	CH_2Cl_2	20	6	40%
2	1	2	CH_2Cl_2			95%

The *trans* configuration of the side chain double bond is proposed on the basis of a coupling constant J_H = 17.9 between CH23-CH24.

3.2.2. Attempts to deprotect the pinacol ester group

Once demonstrated the feasibility of the cross-metathesis reaction to introduce the trans-alkenyl boronate functionality, the transformation of the boronate functionality into the boronic acid group was also examined.

The previously synthesized boronic ester **11** was protected by addition of TBSCl, to give compound **12** (Scheme 7).

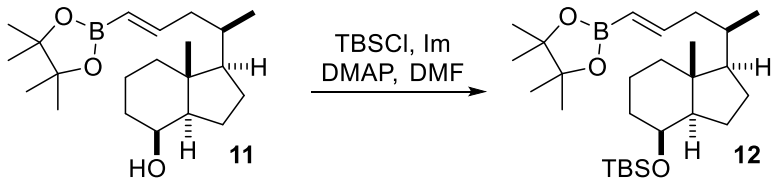

Scheme 7. Protection of the alcohol functional group of compound **11**.

The protected compound **12** was used to test the hypothesis that, with the use of deprotecting conditions, it was possible to obtain both, free OH groups as well as the boronic acid in the side chain.

The tested conditions for the attempts to deprotect compound **12** are shown in Scheme 8 below.

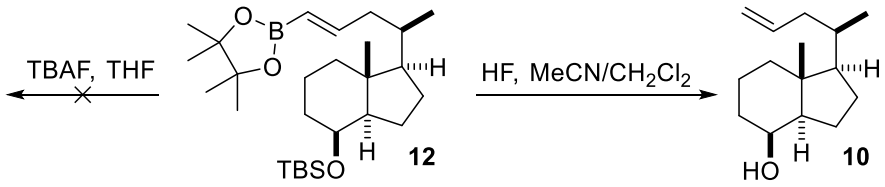

Scheme 8. Attempts to deprotect compound **12**.

Unfortunately, the attempts to deprotect the pin-moiety with TBAF or HF were unsuccessful. Treatment of **12** with TBAF in THF at room temperature for two days resulted in the recovery of the initial boronate **12**. Removal of the TBS group under these reaction conditions is difficult due to its axial localization. Treatment of **12** with hydrogen fluoride in a mixture of MeCN and CH_2Cl_2, led to the obtention of the previously described alkene **10,** as a result of protonation.

As this point, it was decided to continue with the synthesis of analog **E4**, through boronate **1.**

3.3. Synthesis of (*E*)-vinyl bromide **14**

Oxidation of alcohol **10** with Dess-Martin Periodinane (DMP).in dichloromethane produced ketone **13** in 98% yield.

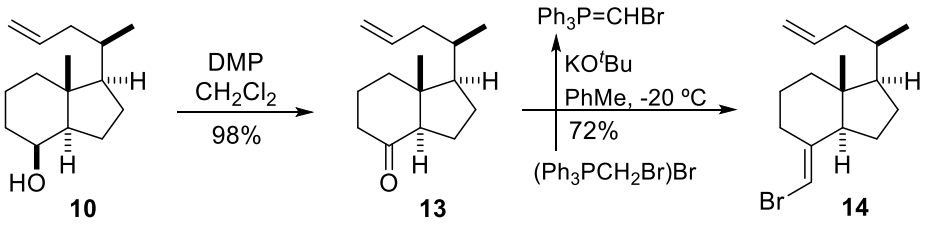

Scheme 9. Preparation of vinyl bromide **14** from alkene **10**.

The resulting ketone was submitted to Wittig chemistry using the ylide $Ph_3P=CHBr$, prepared by reaction of phosphonium salt $(Ph_3PCH_2Br)Br$ with potassium *tert*-butoxide, to give vinyl bromide **14** in 72% yield.

The main ^{1}H-NMR and ^{13}C-NMR signals for compounds **13** and **14** are indicated in Figure 19 and Figure 20, respectively.

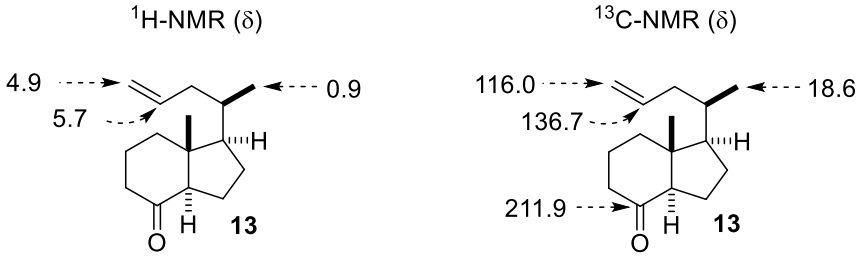

Figure 19. Key NMR signals for compound **13**.

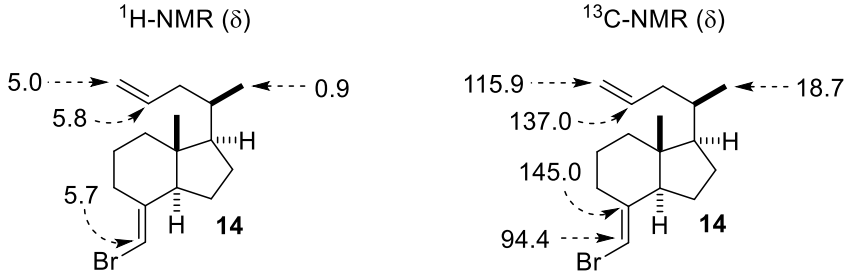

Figure 20. Key NMR signals for compound **14**.

The main problem in this olefination is the geometric selectivity, since the (*E*)-vinyl bromide **14** is required. Curiously, there is a noticeable *E* geometric selectivity in this reaction, contrary to the expected *Z* configuration. This observation can be explained in the light of two different theories, as shown by Trost.[56] On the one hand, dipole-dipole

interactions favour the *E* configuration and, on the other hand, a mechanism involving nucleophilic addition to a betaine may also be taken into account here. The result is an intermediate state that minimizes both dipole and eclipsing geometry, illustrated in Figure 21, below.[56]

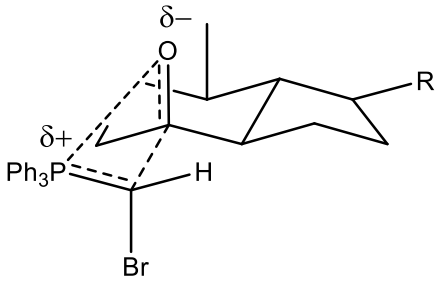

Figure 21. Proposed transition-state compound that leads to the (*E*)-vinyl bromide **14**.

3.4. Synthesis of boronate **1**

We next employed a Miyaura borylation reaction for the bromo-boron interchange. Thus, treatment of bromide **14** with bispinacolate diboron in the presence of [1,1′-Bis(diphenylphosphino)ferrocene]dichloropalladium(II) complexed with dichloromethane as the catalyst and triciclohexylphosphine in DMSO gave the desired boronate **1** in 84% yield.

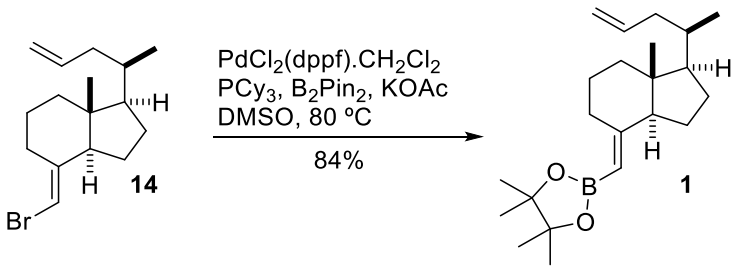

Scheme 10. Preparation of boronic ester **1** from vinyl bromide **14**.

The mechanism of Miyaura borylation comprises three steps. The first step is the oxidative addition of the $Pd^{(0)}$-complex into the C-Br of the vinyl bromide **14**. Next, trasmetallation allows the interchange of Br by a Bpin moiety into the palladium complex. In the last step, the reductive elimination affords the boronate **1** and the regeneration of the palladium(0) catalyst.

Figure 22 shows the most relevant NMR signals for compound **1**.

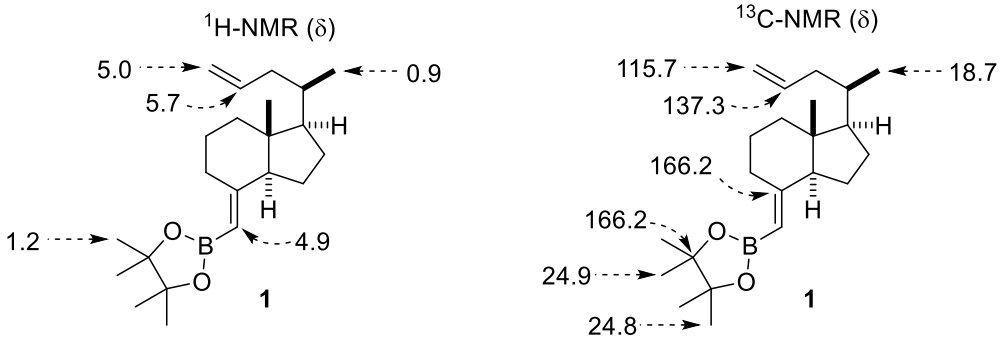

Figure 22. Key NMR signals for compound **1**.

4. Synthesis of enol-triflate **2** (bottom fragment)

The next step in the synthesis of the desired analog **E4** was the preparation of enol-triflate **2** (Scheme 11).

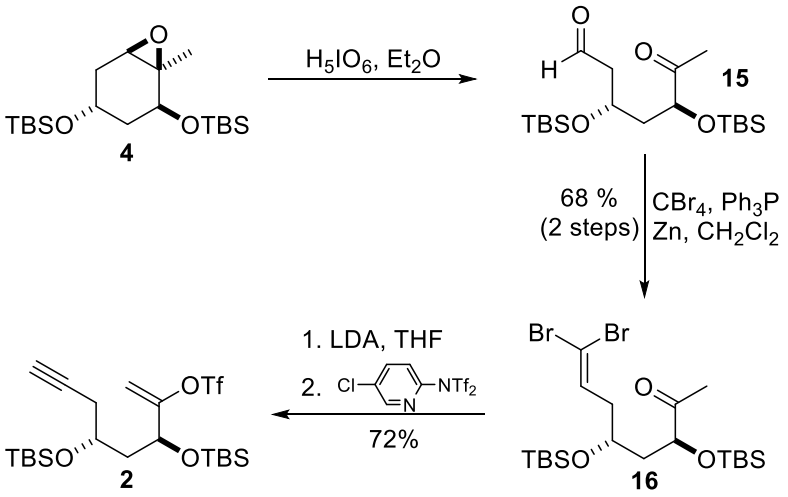

Scheme 11. Preparation of enol-triflate **16** from epoxide **4**.

Treatment of epoxide **4** with periodic acid in ether afforded the dicarbonilic compound **15**, which was converted into dibromide **16** by treatment with carbon tetrabromide in the presence of PPh_3 and zinc.[57] Finally, dibromide **16** was treated with LDA to form the triple bond and the enolate, which was trapped with Comins' reagent [N-(5-Chloro-2-pyridyl)bis(trifluoromethanesulfonimide)][58] to produce the desired enol-triflate **2**.

Figure 23 shows the characteristic NMR signals for enol-triflate **2**.

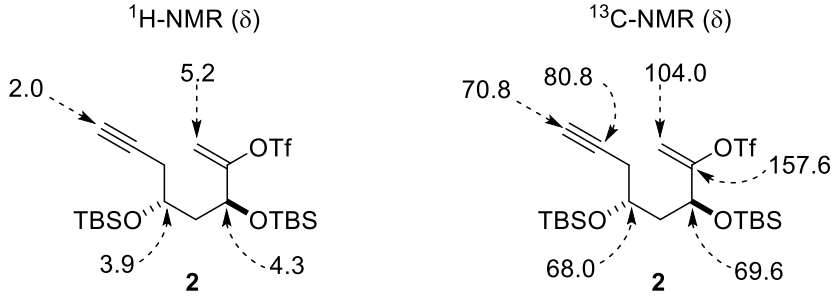

Figure 23. Key NMR signals for compound **2**.

5. Synthesis of 17

With boronic ester **1** and enol-triflate **2** in hands, the preparation of compound **17** was faced. Pd-catalyzed ring closure of enol-triflate **2** and subsequent Suzuki−Miyaura coupling with boronate **1**, in the presence of aqueous K_3PO_4, afforded, after desilylation with TBAF, the desired vitamin D analog **17** in 89% yield (Scheme 12).

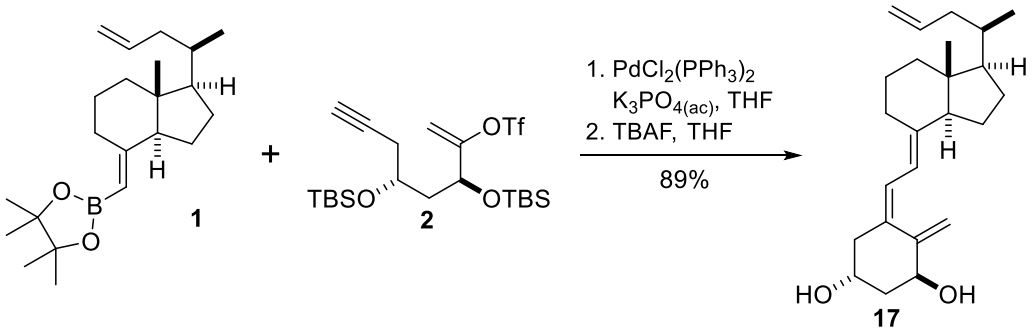

Scheme 12. Preparation of compound **17** from boronic ester **1** and enol-triflate **2**.

Scheme 13 illustrates the proposed mechanism for this Pd(0)-catalysed convergent tandem cyclization Suzuki cross-coupling between enol-triflate **2** and boronate **1**. The use of K_3PO_4 activates boronate **1**, favouring the transmetallation step.

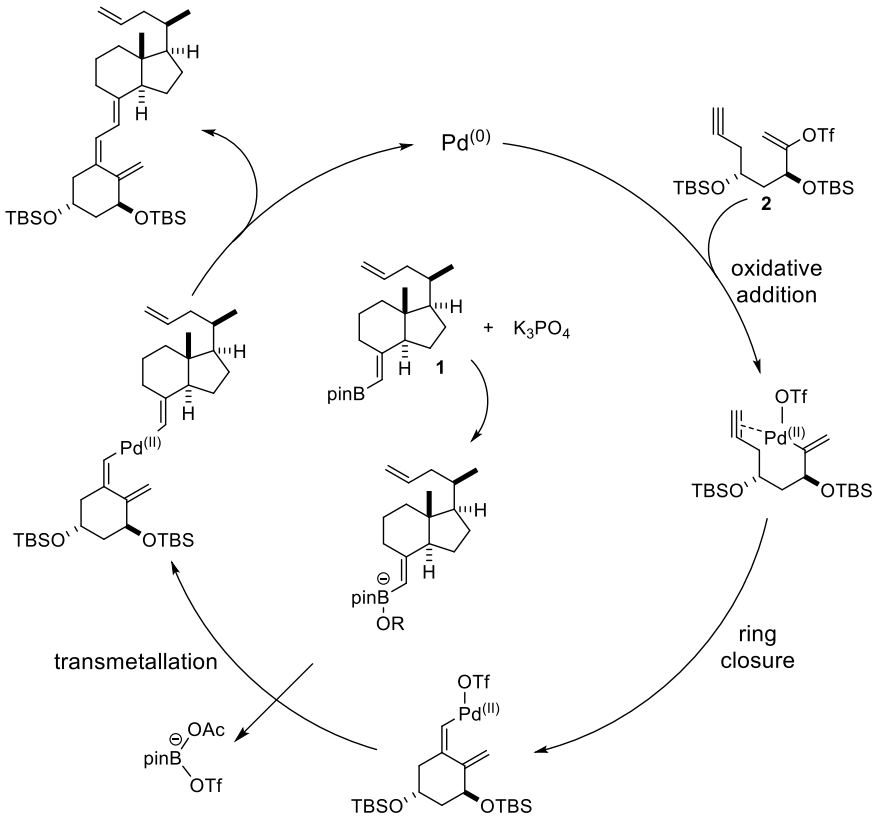

Scheme 13. Proposed mechanism for the Suzuki cross-coupling reaction between enol-triflate **2** and boronic ester **1**.

6. Synthesis of boronic ester **E4**

In the last step, the synthesis of the target analog **E4** was accomplished using the cross metathesis reaction previously described in this work (Scheme 14).

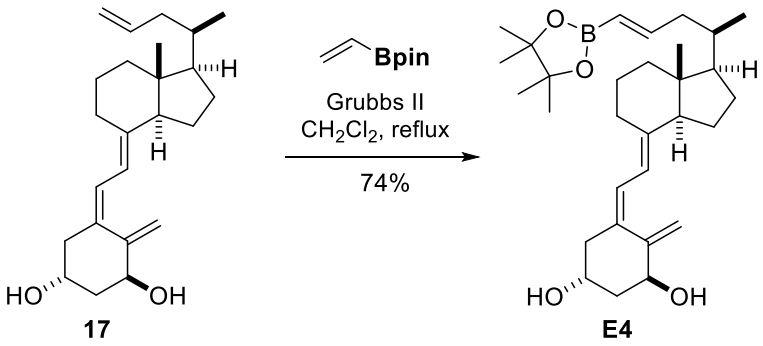

Scheme 14. Preparation of analog **E4** from alkene **17**.

Treatment of alkene **17** (1 equiv) with vinyl boronic pinacol ester (pinBCH=CH_2) in the presence of the second generation Grubbs catalyst (2 equiv) gave the target analog **E4** in 74% yield.

Scheme 15 shows the proposed reaction mechanism for this reaction.

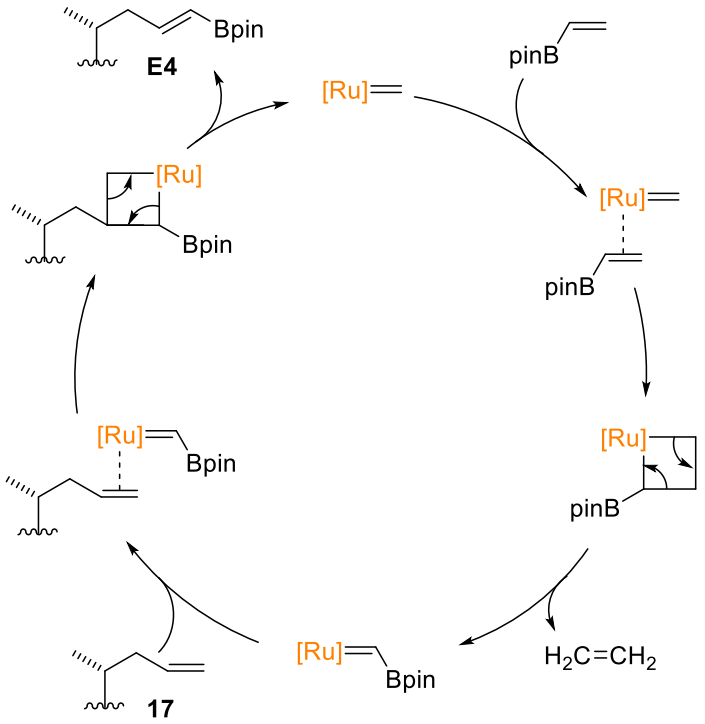

Scheme 15. Proposed mechanism for the olefin cross metathesis reaction.

Figure 24 shows the ^{1}H-NMR spectrum of analog **E4**.

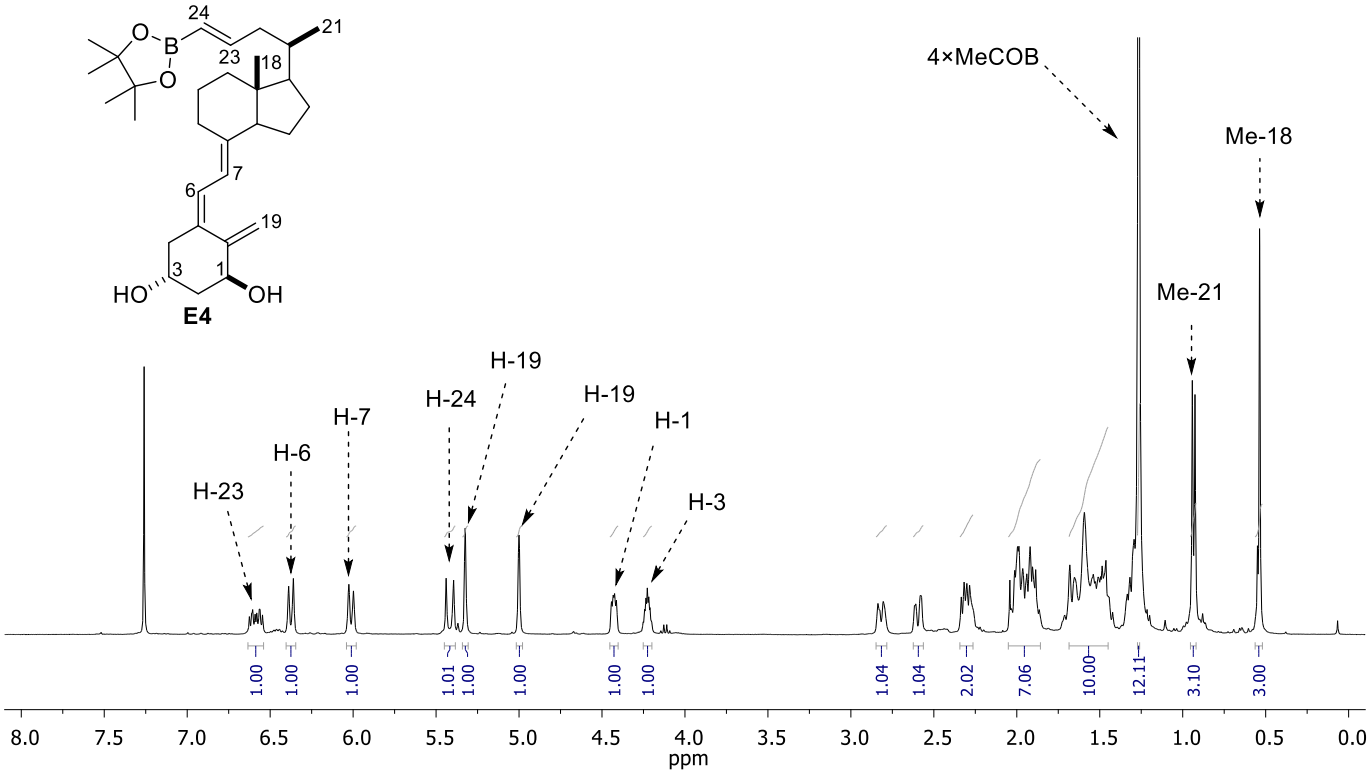

Figure 24. ^{1}H-NMR spectrum (400 MHz, $CDCl_3$) of analog **E4** and most relevant signals

The characteristic signals belonging to the **A** ring and triene system are observed. A singlet peak for the methyl groups of the Bpin moiety at 1.27 ppm is also identified. The *trans* configuration of the side chain double bond is confirmed by a coupling constant of $J_{H\text{-}H}$ = 17.9 Hz.

Conclusions

Conclusions

Through docking calculations, it was possible to test eight vitamin D analogs (**A1, A2, A3, A4, E1, E2, E3, E4**) in terms of their affinity to the VRD(LBD). These *in silico* studies indicated that analogs **A4** and **E4** adopted a similar conformation to the natural hormone 1,25D in the binding pocket. Both analogs showed similar or even higher affinities to VDR in comparison with the native hormone 1,25D and, therefore, should behave as agonists of the VDR.

Although the plan was to synthesize both analogs **A4** and **E4**, it was only possible to obtain the target compound **E4**.

The synthesis started from the individual formation of both the upper and bottom fragments of the vitamin D. These fragments were put together through a Suzuki Miyaura Pd-catalyzed tandem carbocyclization process. In a last step and by an olefin metathesis, it was possible to obtain the target compound **E4** with a global yield of 14% in twelve steps.

Analog **E4** is about to undergo both *in vitro* and *in vivo* biological assays, to test the biological effects of this analog in different cell lines, as well as its role in the regulation of serum calcium levels in mice.

This work allowed the development of a new methodology for the preparation of vitamin D analogs containing a boronate group that could have interesting biological properties and promising applications in drug research.

Experimental Procedures

Experimental Procedures

1. General Procedures

All reactions including oxygen or moisture-sensitive compounds or mixtures were carried out under dry argon atmosphere (Alphagaz-1 Argon). The used glassware was dried in a 150 ºC oven and heat or flame-dried and cooled under argon pressure immediately before use. Standard syringe/septa techniques were employed.

In low-temperature experiments, water/ice baths were used in reactions carried out at 0 ºC. Methanol baths cooled with a CRYOCOOL immersion cooler, provided with a temperature regulator were employed in experiments at negative temperatures.

In high-temperature experiments, silicon baths were used, provided with a contact thermometer directly in the bath. All indicated temperatures refer to the external bath temperatures employed, unless stated otherwise.

All dry solvents were distilled under argon pressure immediately prior to use. Et_2O, THF and toluene were distilled from Na/benzophenone and CH_2Cl_2 was distilled from P_2O_5. DMSO was distilled from CaH_2 under vacuum and then stored on molecular sieves of 4 Å. DMF was dried with 4 Å molecular sieves.

Commercial solutions of ^{n}BuLi (in hexanes) were titrated with *N*-benzylbenzamide before use.

The progress of the reactions was followed by thin layer chromatography (TLC) using aluminum plates with a silca gel layer Merck 60 (0.2 mm thickness). In the revealing process, the chromatograms, were visualized under UV light (254 nm) and then immersed in solutions of ceric ammonium molybdate or *p*-anisaldehyde.

Reactions that made use of ultrasounds were carried out in a JP Selecta Ultrasons.

Organic extracts were dried over anhydrous Na_2SO_4, filtered and concentrated using a rotary evaporator at reduced pressure (20-30 mmHg).

During flash column chromatography, Merck silica gel 60 (230-400 mesh) was used. Solvents used in the mobile phase such as hexanes, EtOAc or CH_2Cl_2 were distilled prior to their use.

Compound's HPLC purifications were performed in a Shimadzu liquid preparative chromatograph model LC-8A with an absorbance detector TSP-UV1. The column used with this equipment was a HPLC column Phenomenex® Luna® 5 µm with a Silica (2) stationary phase (5 µm particle size, 100 Å pore size, 250 mm length, 10 mm internal

diameter). Yields refer to chromatographically purified compounds unless otherwise specified.

The NMR spectra were registered in Brucker DPX-250 (250 MHz for ^{1}H, 63 MHz for ^{13}C) and Varian Inova-400 (400 MHz for ^{1}H) spectrometers, from RMN services at Universidad de Santiago de Compostela. The spectra were performed using $CDCl_3$ as a solvent. Chemical shifts are reported on the δ scale (ppm) downfield from tetramethylsilane (δ = 0.0 ppm) using the residual solvent signal at δ = 7.26 ppm (^{1}H, s, CDCl3) or δ = 77.0 ppm (^{13}C, t, $CDCl_3$). Coupling constants (*J*) are reported in the Hz scale.

High resolution mass spectra (HRMS) were performed in a Micromass Instruments Autospec (EI^+, CI^+), a Thermo Finningan MAT95XP (EI^+) and an Applied Biosystems QSTAR Elite spectrometers (ESI^+). IR spectra were recorded in a silicon disc on Bruker IFS 66V and VECTOR 22 FT-IR spectrometers.

The references and respective distributor for each of the reactants used in this work are presented below.

B_2Pin_2: Aldrich, Ref. 47,329-4

CBr_4: Aldrich, Ref. C11081

DIBAL-H: Aldrich, Ref. 214973

DMAP: Fluka, Ref. 29224

Grubbs Catalyst™ 2nd Generation: Aldrich, Ref. 569747

H_5IO_6: Fluka, Ref. 77310

HF, Acros: Ref.423805000

I_2: Fluka, Ref. 56750

Imidazole: Fluka, Ref. 56750

$K_3PO_4 \cdot 3H_2O$: Aldrich, Ref. P5629

KOAc: Merck, Ref. 104820

KO^tBu: Fluka, Ref. 60100

$Na_2S_2O_3$: Quimipur, w/o Ref.

Na_2SO_4: Quimipur, w/o Ref.

$NaHCO_3$: Quimipur, w/o Ref.

^{n}BuLi: Acros, 18127

NH_4Cl: Quimipur, w/o Ref.

PCy_3: Aldrich, Ref. 261971

$PdCl_2(dppf) \cdot CH_2Cl_2$: Aldrich, Ref. 379670

$PdCl_2(PPh_3)_2$: Fluka, Ref. 15253

PPh_3: Aldrich, Ref. T84409

Silica Gel (SiO_2): Merck, Ref. 1.09385.2500

TBAF: Aldrich, Ref. 216143

TBSCl: ABCR, Ref. AB110655

Vinylboronic acid pinacol ester: Acros, Ref. 395530

The compounds were named and numbered following the systematic nomenclature proposed by IUPAC using Chemdraw® computer software. In all the synthesized molecules, steroidal nomenclature and numbering was employed for the RMN analysis.

(1*R*,3a*R*,4*S*,7a*R*)-1-((*S*)-1-Iodopropan-2-yl)-7a-methyloctahydro-1*H*-inden-4-ol

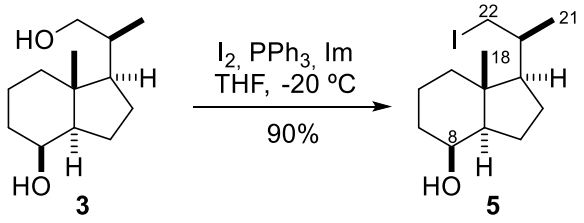

Triphenylphosphine (679 mg, 2.59 mmol, 1.1 equiv) and Imidazole (480 mg, 7.05 mmol, 3 equiv) were successively added to a solution of **3** (500 mg, 2.35 mmol, 1 equiv) in dry THF (20 mL). After cooling at -20 ºC, I_2 was added. The mixture was stirred at *rt* for 2h. The reaction was quenched with a saturated solution of $NaHCO_3$ (20 mL) and $Na_2S_2O_3$ (20 mL). The mixture was extracted with CH_2Cl_2 (3×15 mL). The combined organic extracts were dried, filtered and concentrated *in vacuo*. The residue was purified by flash column chromatography (SiO_2, 2.5×5 cm, 20% EtOAc/hexanes) to give **5** [722 mg, 90%, R_f = 0.54 (30% EtOAc-hexanes), white solid].

^{1}H NMR (250 MHz, $CDCl_3$) δ 4.06 (s, 1H, H-8), 3.30 (dd, *J* = 9.5, 1.9 Hz, 1H, H-22), 3.16 (dd, *J* = 9.4, 4.5 Hz, 1H, H-22), 1.98 – 1.73 (m, 4H), 1.61 – 1.29 (m, 5H), 1.25 – 1.08 (m, 4H), 1.00 – 0.94 (m, 6H, Me-18, Me-21). **^{13}C NMR** (63 MHz, CDCl3) δ 69.06 (CH, C8), 55.79 (CH), 52.23 (CH), 41.74 (C, C-13), 40.01 (CH2), 36.25 (CH), 33.46 (CH2), 26.45 (CH2), 22.31 (CH2), 21.24 (CH2), 20.59 (CH3, C-21), 17.30 (CH2), 14.30 (CH3, C-18).

(*R*)-3-((1*R*,3a*R*,4*S*,7a*R*)-4-Hydroxy-7a-methyloctahydro-1*H*-inden-1-yl)butanenitrile

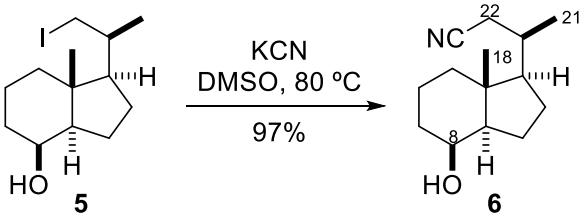

Potassium cyanide (365 mg, 5.60 mmol, 2.5 equiv) was added to a solution of **5** (722 mg, 2.24 mmol, 1 equiv) in DMSO (20 mL). The mixture was stirred at 85 ºC for 2 h, and then cooled to *rt*. The reaction was quenched with H_2O (40 mL). Saturated NaCl (10 mL) was added and the mixture was extracted with 10% EtOAc/hexanes (4×10 mL). The combined organic phases were dried with Na_2SO_4, filtered and concentrated *in vacuo*. The residue was purified by flash column chromatography (SiO_2, 3×5 cm, 20% EtOAc/hexanes) to give **6** [483 mg, 97%, R_f = 0.37 (30% EtOAc-hexanes), white solid].

^{1}H NMR (250 MHz, $CDCl_3$) δ 4.06 (s, 1H, H-8), 2.36 – 2.19 (m, 2H, H-22), 1.97 – 1.75 (m, 5H), 1.57 – 1.36 (m, 6H), 1.28 – 1.17 (m, 3H), 1.12 (d, *J* = 6.6 Hz, 3H, Me -21), 0.93 (s, 3H, Me-18). **^{13}C NMR** (63 MHz, $CDCl_3$) δ 118.84 (C, C≡N), 68.81 (CH, C-8), 55.09 (CH), 52.29 (CH), 41.82 (C, C-13), 39.93 (CH_2), 33.42 (CH_2), 32.94 (CH), 26.95 (CH_2), 24.56 (CH_2), 22.30 (CH_2), 19.08 (CH_3, C-21), 17.22 (CH_2), 13.54 (CH_3, C-18).

(*R*)-3-((1*R*,3a*R*,4*S*,7a*R*)-4-((*tert*-Butyldimethylsilyl)oxy)-7a-methyloctahydro-1*H*-inden-1-yl)butanenitrile

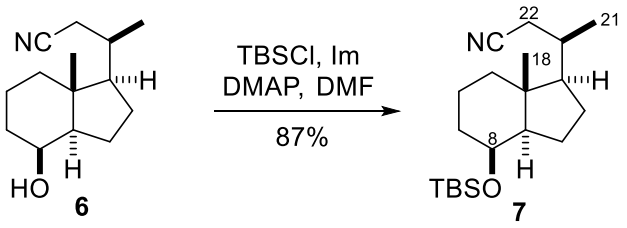

Imidazole (365 mg, 5.36 mmol, 2.1 equiv), DMAP (94 mg, 0.77 mmol, 0.3 equiv) and TBSCl (498 mg, 3.32 mmol, 1.3 equiv) were successively added to a solution of **6** (565 mg, 2.55 mmol, 1 equiv) in DMF (20 mL). The mixture was stirred at *rt* for 10 h. The reaction was quenched with a saturated solution of NaCl (20 mL). The mixture was extracted with hexanes (3×15 mL). The combined organic extracts were dried, filtered and concentrated *in vacuo*. The residue was purified by flash column chromatography (SiO_2, 3×5 cm, 5% EtOAc/hexanes) to yield **7** [746 mg, 87%, R_f = 0.85 (30% EtOAc/hexanes), white solid].

^{1}H NMR (250 MHz, $CDCl_3$) δ 3.96 (s, 1H, H-8), 2.29 (dd, *J* = 16.6, 3.9 Hz, 1H, H-22), 2.16 (dd, *J* = 16.7, 6.8 Hz, 1H, H-22), 1.90 – 1.51 (m, 6H), 1.41 – 1.12 (m, 7H), 1.08 (d, *J* = 6.6 Hz, 3H, Me-21), 0.88 (s, 3H, Me-18), 0.83 (d, *J* = 0.9 Hz, 9H, ^{t}Bu-Si), -0.05 (d, *J* = 4.1 Hz, 6H, 2×Me-Si). **^{13}C NMR** (63 MHz, $CDCl_3$) δ 118.8 (C, C≡N), 69.1 (CH, C-8), 55.2 (CH), 52.7 (CH), 42.0 (C, C-13), 40.2 (CH_2), 34.1 (CH_2), 33.0 (CH), 27.1 (CH_2), 25.7 (3×CH_3, ^{t}Bu-Si), 24.5 (CH_2), 22.8 (CH_2), 19.1 (CH_3, C-21), 17.9 (C, Si), 17.40 (CH2), 13.7 (CH_3, C-18), -5.0 (CH_3, Me-Si), -5.3 (CH_3, Me-Si). **HRMS** (ESI-TOF)$^{+}$: $[M+Na]^{+}$ calcd for $C_{14}H_{23}NONa$ 244.1671, found 244.1679.

(*R*)-3-((1*R*,3a*R*,4*S*,7a*R*)-4-((*tert*-Butyldimethylsilyl)oxy)-7a-methyloctahydro-1*H*-inden-1-yl)butanal

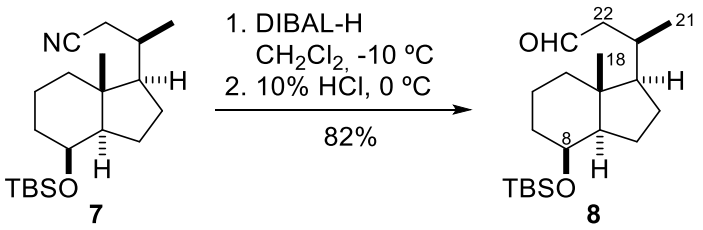

7 **8**

DIBAL-H (1.0 M in hexanes, 4.41 mL, 4.41 mmol) was added dropwise to a solution of **7** (740 mg, 2.20 mmol, 1 equiv) in CH_2Cl_2 (20 mL) cooled at -10 ºC and stirred for 1h. The reaction was quenched by pouring the mixture into an aqueous solution of HCl (10%, 50 mL) and CH_2Cl_2 (50 mL) and then the mixture was stirred at 0 ºC for 2 h. The mixture was extracted with CH_2Cl_2 (3×20 mL). The organic phase was washed with saturated solutions of $NaHCO_3$ (30 mL) and NaCl (30 mL). The combined organic extracts were dried, filtered, and concentrated *in vacuo*. The crude product was purified by flash chromatography (SiO_2, 3×5 cm, 5% EtOAc/hexanes) to yield **8** [613 mg, 82%, R_f = 0.48 (5% EtOAc/hexanes), yellow oil].

^{1}H NMR (250 MHz, $CDCl_3$) δ 9.70 (dd, *J* = 3.4, 1.4 Hz, 1H, CHO), 3.96 (s, 1H, H-8), 2.41 (d, *J* = 14.0 Hz, 1H), 2.16 – 1.85 (m, 3H), 1.79 – 1.51 (m, 4H), 1.39 – 1.09 (m, 7H), 0.95 (d, *J* = 6.4 Hz, 3H, Me-21), 0.92 (s, 3H, Me-18), 0.85 (s, 9H, ^{t}Bu-Si), -0.04 (d, *J* = 3.6 Hz, 6H, 2×Me-Si). **^{13}C NMR** (63 MHz, $CDCl_3$) δ 203.5 (CH, CHO), 69.3 (CH, C-8), 56.5 (CH), 53.0 (CH), 50.8 (CH_2), 42.3 (C, C-13), 40.5 (CH_2), 34.31 (CH_2), 31.24 (CH), 27.54 (CH_2), 25.78 (3×CH_3, ^{t}Bu-Si), 23.0 (CH_2), 20.0 (CH_3, C-21), 18.0 (C, Si), 17.6 (CH_2), 13.7 (CH_3, C-18), -4.8 (CH_3, Me-Si), -5.2 (CH_3, Me-Si).

***tert*-Butyldimethyl(((1*R*,3a*R*,4*S*,7a*R*)-7a-methyl-1-((*R*)-pent-4-en-2-yl)octahydro-1*H*-inden-4-yl)oxy)silane**

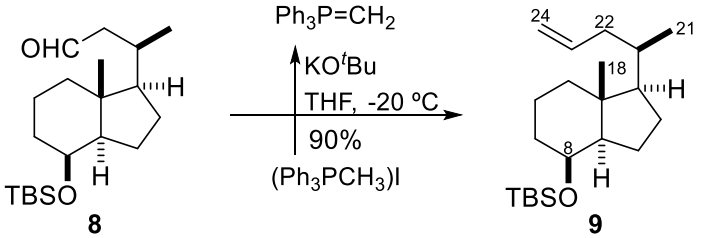

8 **9**

A suspension of $(Ph_3PCH_3)I$ (2.00 g, 4.95 mmol, 5 equiv) in dry THF (15 mL) was sonicated for 30 min. After cooling the suspension at 0 ºC, an aqueous solution of KO^{t}Bu (8.87 mL, 4.85 mmol, 1 M, 4.9 equiv) was added, dropwise.

After 1.5 h of stirring at 0 ºC, the mixture was warmed to *rt* and a solution of **8** (335 mg, 0,99 mmol, 1 equiv) in THF (5 mL) was added. The resulting mixture was stirred at *rt* for 2 h. The reaction was quenched with a saturated NH_4Cl solution (2 mL) and filtered through a layer of silica gel. The silica was washed with hexanes (40 mL) and the filtrate was concentrated *in vacuo*. The residue was purified by flash chromatography (SiO_2, 2.5×5 cm, hexanes) to give **9** [299 mg, 90%, R_f = 0.96 (5% EtOAc/hexanes), $[\alpha]_D^{20}$ = 38.2 (c = 1, $CHCl_3$), yellow oil].

^{1}H NMR (250 MHz, $CDCl_3$) δ 5.84 – 5.62 (m, 1H, H-23), 4.95 (d, *J* = 13.3 Hz, 2H, H-24), 3.97 (s, 1H, H-8), 2.15 (d, *J* = 12.5 Hz, 1H), 1.99 – 1.44 (m, 7H), 1.40 – 1.19 (m, 5H), 1.12 – 0.95 (m, 2H), 0.88 (d, *J* = 7.2 Hz, 15H, Me-21, Me-18, ^{t}Bu-Si), -0.02 (d, *J* = 2.8 Hz, 6H, 2×Me-Si). **^{13}C NMR** (63 MHz, $CDCl_3$) δ 137.5 (CH, C-23), 115.57 (CH_2, C-24), 69.47 (CH, C-8), 56.4 (CH), 53.0 (CH), 42.1 (C, C-13), 40.6 (CH_2), 40.5 (CH_2), 35.3 (CH), 34.5 (CH_2), 27.3 (CH_2), 25.8 (3×CH_3, ^{t}Bu-Si), 23.1 (CH_2), 18.6 (CH_3, C-21), 18.0 (C, C-Si), 17.7 (CH_2), 13.8 (CH_3, C-18), -4.8 (CH_3, Me-Si), -5.2 (CH_3, Me-Si). **HRMS** (EI): $[M]^+$ calcd for $C_{21}H_{40}OSi$ 336.2843, found 336.2847.

(1*R*,3a*R*,4*S*,7a*R*)-7a-Methyl-1-((*R*)-pent-4-en-2-yl)octahydro-1*H*-inden-4-ol

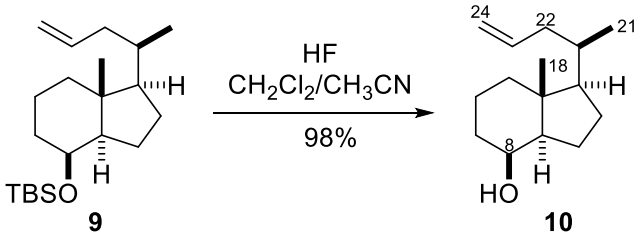

9 **10**

HF (15 drops, 48%) was added to a solution of **9** (460 mg, 1.37 mmol) in CH_2Cl_2 (6 mL) and CH_3CN (12 mL). The reaction mixture was stirred at *rt* during 4 h. The reaction was quenched by slowly pouring the mixture into a saturated solution of $NaHCO_3$ (50 mL). The mixture was extracted with CH_2Cl_2 (3×20 mL). The combined organic extracts were dried, filtered and concentrated *in vacuo*. The resulting residue was purified by flash chromatography (SiO_2, 2.5×5 cm, 5-10 % EtOAc/hexanes) to give **10** [298 mg, 98%, Rf = 0.22 (10% EtOAc/hexanes), $[\alpha]_D^{20}$ = 29.8 (c = 0.5, $CHCl_3$), yellow oil].

^{1}H NMR (250 MHz, $CDCl_3$) δ 5.81 – 5.62 (m, 1H, H-23), 4.93 (d, *J* = 12.6 Hz, 2H, H-24), 4.02 (s, 1H, H-8), 2.19 – 2.06 (m, 1H), 2.00 – 1.89 (m, 1H), 1.86 – 1.65 (m, 4H), 1.52 – 1.22 (m, 8H), 1.16 – 1.00 (m, 2H), 0.89 (s, 3H, Me-18), 0.86 (d, *J* = 8.0 Hz, 3H, Me-21). **^{13}C NMR** (63 MHz, $CDCl_3$) δ 137.2 (CH, C-23), 115.7 (CH_2, C-24), 69.2 (CH, C8), 56.1 (CH), 52.5 (CH), 41.8 (C, C13), 40.4 (CH_2), 40.2 (CH_2) 35.2 (CH), 33.52 (CH_2), 27.0 (CH_2), 22.5 (CH_2), 18.4 (CH_3, Me-21), 17.4 (CH_2), 13.5 (CH_3, Me-18).

(1*R*,3a*R*,7a*R*)-7a-Methyl-1-((*R*)-pent-4-en-2-yl)octahydro-4*H*-inden-4-one

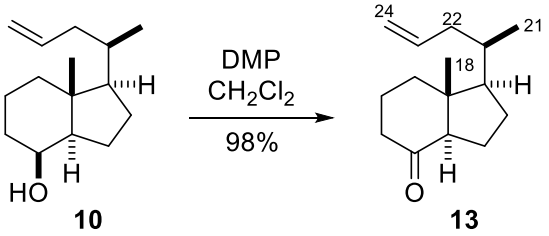

10 **13**

Dess-Martin Periodinane (626 mg, 1.47 mmol, 1.1 equiv) was added to a solution of **10** (298 mg, 1.34 mmol, 1 equiv) in dry CH_2Cl_2 (10 mL). After stirring at *rt* for 2 h, the mixture was concentrated *in vacuo* to remove excess CH_2Cl_2. The residue was then purified by flash chromatography (SiO_2, 3×4 cm, hexanes) to give **13** [290 mg, 98%, R_f = 0.65 (20% EtOAc/hexanes), $[\alpha]_D^{20}$ = -19.8 (c = 1, $CHCl_3$), yellow oil].

^{1}H NMR (250 MHz, $CDCl_3$) δ 5.80 – 5.56 (m, 1H, H-23), 4.95 (d, *J* = 12.6 Hz, 2H, H-24), 2.40 (dd, *J* = 11.5, 7.5 Hz, 1H), 2.27 – 1.98 (m, 4H), 1.97 – 1.62 (m, 5H), 1.57 – 1.24 (m, 5H), 0.91 (d, *J* = 6.1 Hz, 3H, Me-21), 0.59 (s, 3H, Me-18). **^{13}C NMR** (63 MHz, $CDCl_3$) δ 211.9 (C, C-8), 136.7 (CH, C-23), 116.0 (CH_2, C-24), 61.8 (CH), 56.1 (CH), 49.8 (C, C-13), 40.9 (CH_2), 40.3 (CH_2), 38.8 (CH_2), 35.4 (CH), 27.4 (CH_2), 24.0 (CH_2), 19.0 (CH_2), 18.6 (CH_3, Me-21), 12.4 (CH_3, Me-18).

(1*R*,3a*R*,7a*R*,*E*)-4-(Bromomethylene)-7a-methyl-1-((*R*)-pent-4-en-2-yl)octahydro-1*H*-indene

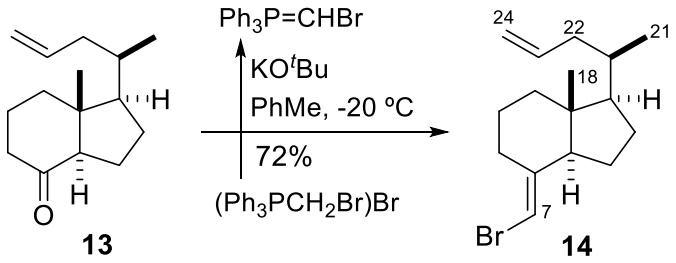

13 **14**

A suspension of $(Ph_3PCH_2Br)Br$ (4.018 g, 9.21 mmol, 7 equiv) in toluene (20 mL) was sonicated for 30 min. The suspension was cooled to -20 ºC and a solution of KO^{t}Bu (9.08 mL, 9.08 mmol, 1M, 6.9 equiv) was added. After 2 h, an aqueous solution of **13** (290 mg, 1.32 mmol, 1 equiv) in toluene (10 mL) was added. The resulting mixture was stirred during 2 h at -20 ºC. The reaction was quenched with NH_4Cl (2 mL) and filtered through a layer of silica gel. The silica was washed with MTBE (40 mL) and the combined filtrate was concentrated.

The residue was then purified by flash chromatography (SiO_2, 3×5 cm, hexanes) to give **14** [246 mg, 72%, R_f = 0.91 (5% EtOAc/hexanes), $[\alpha]_D^{20}$ = 84.0 (c = 1, $CHCl_3$), yellow oil].

^{1}H NMR (250 MHz, $CDCl_3$) δ 5.89 – 5.67 (m, 1H, H-23), 5.65 (s, 1H, H-7), 4.99 (d, *J* = 13.6 Hz, 2H, H-24), 2.87 (dd, *J* = 11.0, 2.5 Hz, 1H), 2.24 – 2.13 (m, 1H), 2.03 – 1.80 (m, 4H), 1.69 – 1.44 (m, 6H), 1.36 – 1.23 (m, 3H), 0.94 (d, *J* = 6.5 Hz, 3H, Me-21), 0.57 (s, 3H, Me-18). **^{13}C NMR** (63 MHz, $CDCl_3$) δ 145.0 (C-8), 137.0 (CH, C-23), 115.9 (CH_2, C24), 97.4 (CH, C-7), 55.8 (CH), 55.3 (CH), 45.4 (C, C-13), 40.5 (CH), 39.7 (CH), 35.9 (CH), 31.0 (CH_2), 27.5 (CH_2), 22.5 (CH_2), 22.0 (CH_2), 18.7 (CH_3, Me-21), 11.8 (CH_3, Me-18). **HRMS** (EI): $[M]^+$ calcd for $C_{16}H_{25}Br$ 296.1134, found 296.1135.

4,4,5,5-Tetramethyl-2-(((1*R*,3a*S*,7a*R*,*E*)-7a-methyl-1-((*R*)-pent-4-en-2-yl)octahydro-4*H*-inden-4-ylidene)methyl)-1,3,2-dioxaborolane

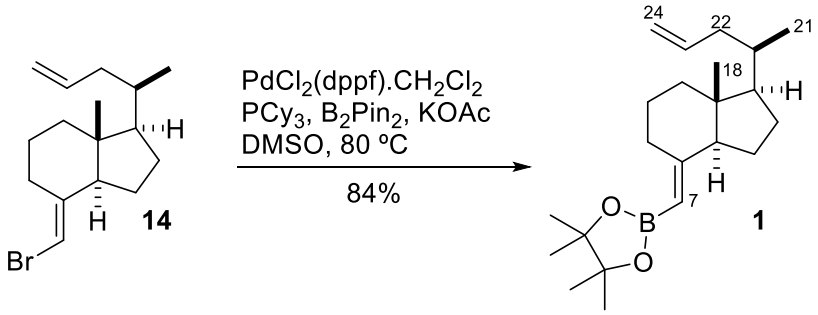

$PdCl_2(dppf).CH_2Cl_2$ (8 mg, 0.01 mmol, 0.03 equiv) and PCy_3 (6 mg, 0.02 mmol, 0.03 equiv) were dissolved in dry DMSO (1 mL). The solution was stirred for 30 min. A solution of **14** (102 mg, 0.34 mmol, 1 equiv) in DMSO (2 mL) was then added through cannula. B_2pin_2 (173 mg, 0.68 mmol, 2 equiv) and KOAc (100 mg, 1.02 mmol, 3 equiv) were added to the reaction. The reaction mixture was stirred at 80 ºC for 2 h. The reaction was quenched with H_2O (20 mL) and the mixture was extracted with MTBE (4×15 mL). The combined organic extracts were dried, filtered and concentrated. The residue was purified by flash chromatography (SiO_2, 2×5.5 cm, 0-5% EtOAc-hexanes) to give **1** [93 mg, 68%, R_f = 0.54 (5% EtOAc-hexanes), $[\alpha]_D^{20}$ = 66.7 (c = 1, $CHCl_3$), yellow oil].

^{1}H NMR (400 MHz, $CDCl_3$) δ 5.73 (s, 1H, H-23), 4.95 (d, *J* = 13.4 Hz, 2H, H-24), 4.88 (s, 1H, H-7), 3.14 (d, *J* = 12.9 Hz, 1H), 2.15 (d, *J* = 11.0 Hz, 1H), 2.04 – 1.41 (m, 13H), 1.23 (s, 12H, 4×CH_3COB), 0.90 (s, 3H, Me-21), 0.53 (s, 3H, Me-18). **^{13}C NMR** (63 MHz, $CDCl_3$) δ 166.2 (C, C-8), 137.3 (CH, C-23), 115.7 (CH_2, C-24), 82.5 (C, 2×COB), 57.9 (CH), 56.3 (CH), 46.2 (C, C-13), 40.5 (CH_2), 40.3 (CH_2), 36.0 (CH), 33.2 (CH_2), 27.4

(CH_2), 24.9 (CH_3, 2×COB), 24.8 (CH_3, 2×COB), 24.3 (CH_2), 22.3 (CH_2), 18.7 (CH_3, Me-21), 12.1 (CH_3, Me-18). **HRMS** (ESI-TOF)$^+$: $[M+Na]^+$ calcd for $C_{22}H_{37}BO_2Na$ 367.2778, found 367.2771.

(1*R*,3*S*,*Z*)-5-(2-((1*R*,3a*S*,7a*R*,*E*)-7a-Methyl-1-((*R*)-pent-4-en-2-yl)octahydro-4*H*-inden-4-ylidene)ethylidene)-4-methylenecyclohexane-1,3-diol

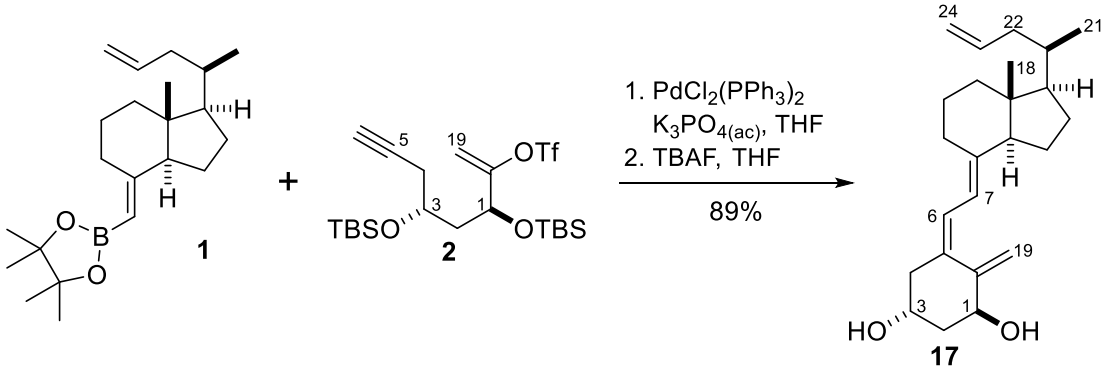

An aqueous solution of K_3PO_4 (2.0 mL, 2M) was added to a solution of **1** (93 mg, 0.27 mmol, 1 equiv) and **2** (167 mg, 0.32 mmol, 1.2 equiv) in dry THF (2 mL). Then, $PdCl_2(PPh_3)_2$ (9.2 mg, 0.01 mmol, 0.05 equiv) was added. The mixture was vigorously stirred at *rt* for 4 h and protected from light. The reaction was quenched with H_2O (20 mL) and the mixture was extracted with MTBE (4×15 mL). The resulting combined organic extracts were dried, filtered and concentrated. The residue was then dissolved in THF and a solution of TBAF in THF (1.54 mL, 1.54 mmol, 1M, 5 equiv) was added. After 20 h of stirring at *rt*, the reaction was quenched with H_2O (20 mL). The mixture was extracted with EtOAc (3×15 mL). The combined organic extracts were dried, filtered and concentrated *in vacuo*. The residue was purified by flash column chromatography (SiO_2, 1.5×6 cm, 50% EtOAc/hexanes) to yield **17** [86 mg, 89%, R_f = 0.2 (40 % EtOAc/hexanes), $[\alpha]_D^{20}$ = 27.6 (c = 0.5, $CHCl_3$), yellow oil].

^{1}H NMR (400 MHz, $CDCl_3$) δ 6.38 (d, *J* = 11.2 Hz, 1H, H-6), 6.02 (d, *J* = 11.3 Hz, 1H, H-7), 5.83 – 5.71 (m, 1H, H-23), 5.33 (s, 1H, H-19), 4.99 (d, *J* = 11.8 Hz, 3H, H-19, H-24), 4.43 (dd, *J* = 7.4, 4.3 Hz, 1H, H-1), 4.26 – 4.20 (m, 1H, H-3), 2.82 (dd, *J* = 11.9, 3.6 Hz, 1H), 2.59 (dd, *J* = 13.3, 2.9 Hz, 1H), 2.31 (dd, *J* = 13.4, 6.5 Hz, 1H), 2.18 (d, *J* = 13.5 Hz, 1H), 2.03 – 1.85 (m, 6H), 1.67 (d, *J* = 10.8 Hz, 5H), 1.53 – 1.44 (m, 4H), 1.34 – 1.25 (m, 4H), 0.93 (d, *J* = 6.6 Hz, 3H, Me-21), 0.55 (s, 3H, Me-18). **^{13}C NMR** (63 MHz, $CDCl_3$) δ 147.6 (C, C-10), 143.2 (C, C-8), 137.3 (CH, C-23), 132.9 (C, C-5), 125.0 (CH, C-6), 117,0 (CH, C-7), 115,8 (CH_2, C-24) 111.8 (CH_2, C-19), 70.8 (CH, C-OH), 66.8 (CH, C-OH), 56.3 (CH), 56.0 (CH), 45.9 (C, C-13), 45.2 (CH_2), 42.8 (CH_2), 40.5 (CH_2), 40.3 (CH_2), 36.1 (CH), 29.1 (CH_2), 27.6 (CH_2), 23.6 (CH_2),

22.3 (CH_2), 18.7 (CH_3, Me-21), 12.0 (CH_3, Me-18). **HRMS** (ESI-TOF)$^+$: $[M+Na]^+$ calcd for $C_{24}H_{36}O_2Na$ 379.2608, found 379.2616.

(1*R*,3*S*,*Z*)-5-(2-((1*R*,3a*S*,7a*R*,*E*)-7a-methyl-1-((*R*,*E*)-5-(4,4,5,5-tetramethyl-1,3,2-dioxaborolan-2-yl)pent-4-en-2-yl)octahydro-4*H*-inden-4-ylidene)ethylidene)-4-methylenecyclohexane-1,3-diol

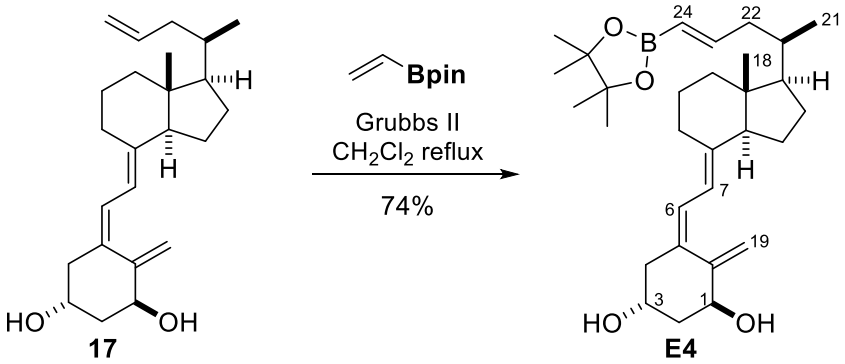

Vinylboronic acid pinacol ester (22 mg, 0.14 mmol, 2 equiv) was added to a mixture of compound **17** (25 mg, 0.07 mmol, 1 equiv) and 2nd generation Grubbs Catalyst™ (2.97 mg, 0.0035 mmol, 0.05 equiv) in dry CH_2Cl_2 (2 mL). The resulting mixture was then heated at 46 ºC and stirred for 6 h. The mixture was cooled to *rt* and then concentrated *in vacuo* to remove excess CH_2Cl_2. The residue was purified by flash chromatography (SiO_2, 2×4 cm, 70% EtOAc-hexanes) to give **E4** [25 mg, 74%, R_f = 0.97 (70% EtOAc-hexanes), $[\alpha]_D^{20}$ = 14.8 (c = 0.7, $CHCl_3$), yellow oil].

^{1}H NMR (400 MHz, $CDCl_3$) δ 6.59 (ddd, *J* = 17.8, 7.9, 5.9 Hz, 1H, H-23), 6.37 (d, *J* = 11.2 Hz, 1H, H-6), 6.01 (d, *J* = 11.2 Hz, 1H, H-7), 5.42 (d, *J* = 17.9 Hz, 1H, H-24), 5.32 (s, 1H, H-19), 5.00 (s, 1H, H-19), 4.43 (dd, *J* = 7.6, 4.3 Hz, 1H, H-1), 4.22 (dt, *J* = 9.9, 3.3 Hz, 1H, H-3), 2.82 (d, *J* = 12.7 Hz, 1H), 2.60 (d, *J* = 10.5 Hz, 1H), 2.31 (dd, *J* = 13.4, 6.7 Hz, 2H), 2.05 – 1.86 (m, 7H), 1.68 – 1.45 (m, 10H), 1.27 (s, 12H, 4×CH_3COB), 0.93 (d, *J* = 6.5 Hz, 3H, Me-21), 0.54 (s, 3H, Me-18). **^{13}C NMR** (63 MHz, $CDCl_3$) δ 153.3 (CH, C-23), 147.6 (C, C-10), 143.1 (C, C-8), 132.8 (C, C-5), 124.9 (CH, C-6), 117.0 (CH, C-7), 111.8 (CH_2, C-19), 83.0 (C, COB), 70.8 (CH), 66.8 (CH), 56.2 (CH), 56.1 (CH), 45.9 (C, C-13), 45.2 (CH_2) 42.8 (CH_2), 40.3 (CH_2), 35.9 (CH), 29.0 (CH_2), 27.6 (CH_2), 24.8 (CH_3, 4×COB), 23.5 (CH_2), 22.2 (CH_2), 19.1 (CH_3, C-21), 12.0 (CH_3, C-18). **HRMS** (ESI-TOF)$^+$: $[M+H]^+$ calcd for $C_{30}H_{48}BO_4$ 483.3640, found 483.3638.

References

References

1. Mellanby, E., *An experimental investigation on rickets.* Nutrition reviews, 1976. **34**(11): p. 338-340.
2. DeLuca, H.F., *History of the discovery of vitamin D and its active metabolites.* BoneKEy reports, 2014. **3**.
3. McCollum, E.V., et al., *Studies on experimental rickets XXI. An experimental demonstration of the existence of a vitamin which promotes calcium deposition.* Journal of Biological Chemistry, 1922. **53**(2): p. 293-312.
4. Wolf, G., *The discovery of vitamin D: the contribution of Adolf Windaus.* The Journal of nutrition, 2004. **134**(6): p. 1299-1302.
5. Feldman, D., J.W. Pike, and F.H. Glorieux, *Vitamin D*. 2005: Elsevier Science.
6. Bouillon, R., W.H. Okamura, and A.W. Norman, *Structure-function relationships in the vitamin D endocrine system.* Endocrine reviews, 1995. **16**(2): p. 200-257.
7. Windaus, A. and F. Bock, *Über das Provitamin aus dem Sterin der Schweineschwarte.* Hoppe-Seyler´ s Zeitschrift für physiologische Chemie, 1936. **245**(3-4): p. 168-170.
8. AW, N. and L. GL, *Hormones*. 1979: Academic Press: New York.
9. Andersen, R., C. Brot, and L. Ovesen, *Towards a strategy for optimal vitamin D fortification (OPTIFORD).* Nutrition, metabolism, and cardiovascular diseases: NMCD, 2001. **11**(4 Suppl): p. 74-77.
10. Holick, M.F., *McCollum Award Lecture, 1994: vitamin D—new horizons for the 21st century*. 1994, Oxford University Press.
11. DeLuca, H.F., *The vitamin D story: a collaborative effort of basic science and clinical medicine.* The FASEB Journal, 1988. **2**(3): p. 224-236.
12. Cheng, J.B., et al., *De-orphanization of Cytochrome P450 2R1 a microsomal vitamin D 25-hydroxylase.* Journal of Biological Chemistry, 2003. **278**(39): p. 38084-38093.
13. Cheng, J.B., et al., *Genetic evidence that the human CYP2R1 enzyme is a key vitamin D 25-hydroxylase.* Proceedings of the National Academy of Sciences of the United States of America, 2004. **101**(20): p. 7711-7715.
14. Holick, M., H. Schnoes, and H. DeLuca, *Identification of 1, 25-dihydroxycholecalciferol, a form of vitamin D3 metabolically active in the intestine.* Proceedings of the National Academy of Sciences, 1971. **68**(4): p. 803-804.
15. Omdahl, J.L., H.A. Morris, and B.K. May, *Hydroxylase enzymes of the vitamin D pathway: expression, function, and regulation.* Annual review of nutrition, 2002. **22**(1): p. 139-166.
16. Jones, G., D.E. Prosser, and M. Kaufmann, *Cytochrome P450-mediated metabolism of vitamin D.* Journal of lipid research, 2014. **55**(1): p. 13-31.
17. St-Arnaud, R., *Targeted inactivation of vitamin D hydroxylases in mice.* Bone, 1999. **25**(1): p. 127-129.
18. Norman, A.W., *From vitamin D to hormone D: fundamentals of the vitamin D endocrine system essential for good health–.* The American journal of clinical nutrition, 2008. **88**(2): p. 491S-499S.
19. Masuyama, H., et al., *Evidence for ligand-dependent intramolecular folding of the AF-2 domain in vitamin D receptor-activated transcription and coactivator interaction.* Molecular Endocrinology, 1997. **11**(10): p. 1507-1517.
20. Kimmel-Jehan, C., F. Jehan, and H.F. DeLuca, *Salt Concentration Determines 1, 25-Dihydroxyvitamin D3Dependency of Vitamin D Receptor–Retinoid X Receptor–Vitamin D-Responsive Element Complex Formation.* Archives of biochemistry and biophysics, 1997. **341**(1): p. 75-80.
21. Bouillon, R., et al., *Vitamin D and human health: lessons from vitamin D receptor null mice.* Endocrine reviews, 2008. **29**(6): p. 726-776.

22. Freedman, L.P., et al., *The function and structure of the metal coordination sites within the glucocorticoid receptor DNA binding domain.* Nature, 1988. **334**(6182): p. 543.
23. Khorasanizadeh, S. and F. Rastinejad, *Nuclear-receptor interactions on DNA-response elements.* Trends in biochemical sciences, 2001. **26**(6): p. 384-390.
24. Zhao, Q., et al., *Structural basis of RXR-DNA interactions1.* Journal of molecular biology, 2000. **296**(2): p. 509-520.
25. Rochel, N., et al., *The crystal structure of the nuclear receptor for vitamin D bound to its natural ligand.* Molecular cell, 2000. **5**(1): p. 173-179.
26. Zamir, I., et al., *A nuclear hormone receptor corepressor mediates transcriptional silencing by receptors with distinct repression domains.* Molecular and cellular biology, 1996. **16**(10): p. 5458-5465.
27. Moras, D. and H. Gronemeyer, *The nuclear receptor ligand-binding domain: structure and function.* Current opinion in cell biology, 1998. **10**(3): p. 384-391.
28. Rochel, N. and D. Moras, *Ligand binding domain of vitamin D receptors.* Current topics in medicinal chemistry, 2006. **6**(12): p. 1229-1241.
29. Yamamoto, K., et al., *Vitamin D receptor: ligand recognition and allosteric network.* Journal of medicinal chemistry, 2006. **49**(4): p. 1313-1324.
30. Lips, P., *Vitamin D physiology.* Progress in biophysics and molecular biology, 2006. **92**(1): p. 4-8.
31. Nemere, I., et al., *Identification of a specific binding protein for 1 alpha, 25-dihydroxyvitamin D3 in basal-lateral membranes of chick intestinal epithelium and relationship to transcaltachia.* Journal of Biological Chemistry, 1994. **269**(38): p. 23750-23756.
32. Demay, M.B., et al., *Sequences in the human parathyroid hormone gene that bind the 1, 25-dihydroxyvitamin D3 receptor and mediate transcriptional repression in response to 1, 25-dihydroxyvitamin D3.* Proceedings of the National Academy of Sciences, 1992. **89**(17): p. 8097-8101.
33. Canaff, L. and G.N. Hendy, *Human calcium-sensing receptor gene Vitamin D response elements in promoters P1 and P2 confer transcriptional responsiveness to 1, 25-dihydroxyvitamin D.* Journal of Biological Chemistry, 2002. **277**(33): p. 30337-30350.
34. Martin, K.J. and E.A. González. *Vitamin D analogs: actions and role in the treatment of secondary hyperparathyroidism*. in *Seminars in nephrology*. 2004. Elsevier.
35. Van Cromphaut, S.J., et al., *Duodenal calcium absorption in vitamin D receptor–knockout mice: functional and molecular aspects.* Proceedings of the National Academy of Sciences, 2001. **98**(23): p. 13324-13329.
36. Li, Y.C., et al., *Normalization of mineral ion homeostasis by dietary means prevents hyperparathyroidism, rickets, and osteomalacia, but not alopecia in vitamin D receptor-ablated mice.* Endocrinology, 1998. **139**(10): p. 4391-4396.
37. Boros, S., R.J. Bindels, and J.G. Hoenderop, *Active Ca2+ reabsorption in the connecting tubule.* Pflügers Archiv-European Journal of Physiology, 2009. **458**(1): p. 99-109.
38. Furuya, M., et al., *Direct cell–cell contact between mature osteoblasts and osteoclasts dynamically controls their functions in vivo.* Nature communications, 2018. **9**(1): p. 300.
39. Panda, D.K., et al., *Inactivation of the 25-hydroxyvitamin D 1α-hydroxylase and vitamin D receptor demonstrates independent and interdependent effects of calcium and vitamin D on skeletal and mineral homeostasis.* Journal of Biological Chemistry, 2004. **279**(16): p. 16754-16766.
40. Leyssens, C., L. Verlinden, and A. Verstuyf, *The future of vitamin D analogs.* Frontiers in physiology, 2014. **5**: p. 122.
41. Carlberg, C., *Molecular basis of the selective activity of vitamin D analogues.* Journal of cellular biochemistry, 2003. **88**(2): p. 274-281.

42. Carlberg, C. and F. Molnár, *Current status of vitamin D signaling and its therapeutic applications.* Current topics in medicinal chemistry, 2012. **12**(6): p. 528-547.
43. Coyne, D., et al., *Paricalcitol capsule for the treatment of secondary hyperparathyroidism in stages 3 and 4 CKD.* American Journal of Kidney Diseases, 2006. **47**(2): p. 263-276.
44. Hagino, H., et al., *Eldecalcitol reduces the risk of severe vertebral fractures and improves the health-related quality of life in patients with osteoporosis.* Journal of bone and mineral metabolism, 2013. **31**(2): p. 183-189.
45. Uchiyama, Y., et al., *ED-71, a vitamin D analog, is a more potent inhibitor of bone resorption than alfacalcidol in an estrogen-deficient rat model of osteoporosis.* Bone, 2002. **30**(4): p. 582-588.
46. Hunter, P., *Not boring at all: Boron is the new carbon in the quest for novel drug candidates.* EMBO reports, 2009. **10**(2): p. 125-128.
47. Kane, R.C., et al., *Velcade®: US FDA approval for the treatment of multiple myeloma progressing on prior therapy.* The oncologist, 2003. **8**(6): p. 508-513.
48. Locher, G.L., *Biological effects and therapeutic possibilities of neutrons.* Am J Roentgenol, 1936. **36**: p. 1-13.
49. Soloway, A.H., et al., *The Chemistry of Neutron Capture Therapy.(Chem. Rev. 1998, 98, 1515. Published on the Web May 20, 1998).* Chemical reviews, 1998. **98**(6): p. 2389-2390.
50. Altieri, S., et al., *Neutron autoradiography imaging of selective boron uptake in human metastatic tumours.* Applied Radiation and Isotopes, 2008. **66**(12): p. 1850-1855.
51. Matteson, D.S., *Stereodirected synthesis with organoboranes*. Vol. 32. 2012: Springer Science & Business Media.
52. Wiskur, S.L., et al., *p K a Values and Geometries of Secondary and Tertiary Amines Complexed to Boronic Acids Implications for Sensor Design.* Organic letters, 2001. **3**(9): p. 1311-1314.
53. Yang, W., X. Gao, and B. Wang, *Boronic acid compounds as potential pharmaceutical agents.* Medicinal Research Reviews, 2003. **23**(3): p. 346-368.
54. Lythgoe, B., D.A. Roberts, and I. Waterhouse, *Calciferol and its relatives. Part 20. A synthesis of Windaus and Grundmann's C 19 ketone.* Journal of the Chemical Society, Perkin Transactions 1, 1977(23): p. 2608-2612.
55. Yamamoto, Y., M. Takahashi, and N. Miyaura, *Synthesis of pinacol allylic boronic esters via olefin cross-metathesis between pinacol allylboronate and terminal or internal alkenes.* Synlett, 2002(1): p. 128-130.
56. Trost, B.M., J. Dumas, and M. Villa, *New strategies for the synthesis of vitamin D metabolites via palladium-catalyzed reactions.* Journal of the American Chemical Society, 1992. **114**(25): p. 9836-9845.
57. Corey, E. and P. Fuchs, *Synthetic method for conversion of formyl groups into ethynyl groups (RCHO. far. RC. idn. CH or RC. idn. CR1).* Tetrahedron Lett, 1972: p. 3769-3772.
58. Comins, D.L. and A. Dehghani, *Pyridine-derived triflating reagents: An improved preparation of vinyl triflates from metallo enolates.* Tetrahedron letters, 1992. **33**(42): p. 6299-6302.

Supplementary Information

Supplementary Information

1. NMR Spectra

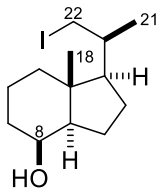

5

^{1}H NMR (250 MHz, $CDCl_3$) δ 4.06 (s, 1H, H-8), 3.30 (dd, *J* = 9.5, 1.9 Hz, 1H, H-22), 3.16 (dd, *J* = 9.4, 4.5 Hz, 1H, H-22), 1.98 – 1.73 (m, 4H), 1.61 – 1.29 (m, 5H), 1.25 – 1.08 (m, 4H), 1.00 – 0.94 (m, 6H, Me-18, Me-21).

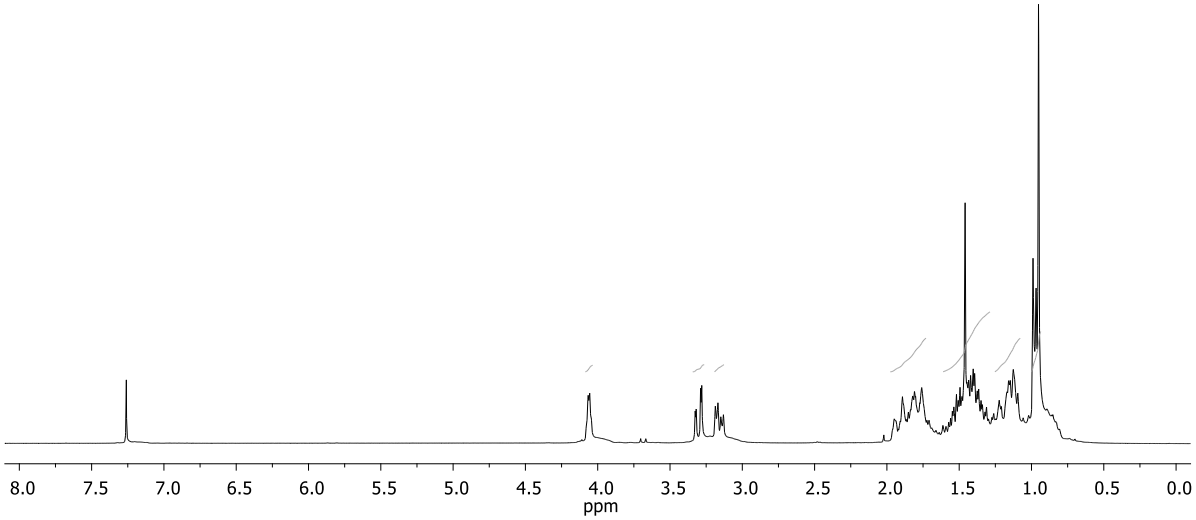

^{13}C NMR (63 MHz, $CDCl_3$) δ 69.06 (CH, C8), 55.79 (CH), 52.23 (CH), 41.74 (C, C-13), 40.01 (CH_2), 36.25 (CH), 33.46 (CH_2), 26.45 (CH_2), 22.31 (CH_2), 21.24 (CH_2), 20.59 (CH_3, C-21), 17.30 (CH_2), 14.30 (CH_3, C-18).

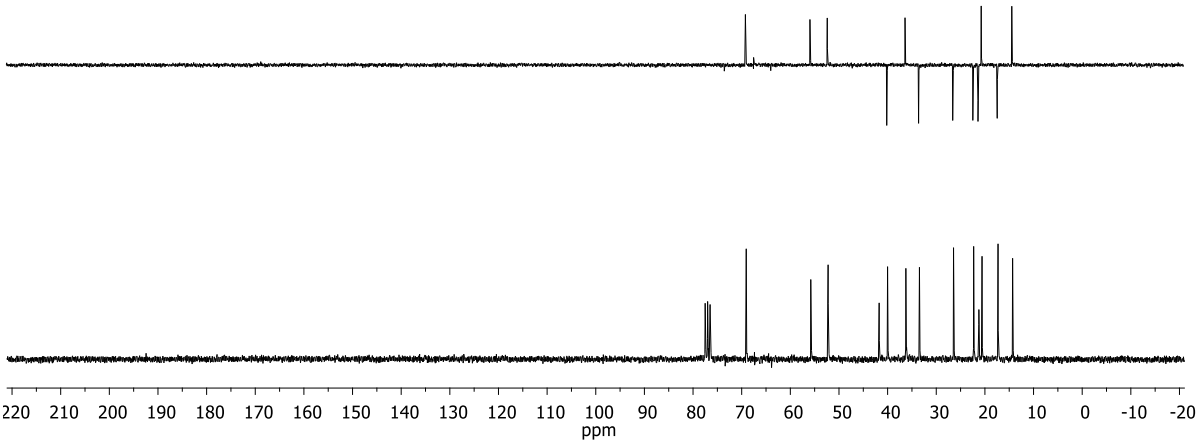

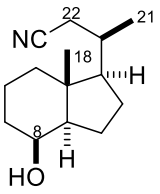

6

^{1}H NMR (250 MHz, $CDCl_3$) δ 4.06 (s, 1H, H-8), 2.36 – 2.19 (m, 2H, H-22), 1.97 – 1.75 (m, 5H), 1.57 – 1.36 (m, 6H), 1.28 – 1.17 (m, 3H), 1.12 (d, *J* = 6.6 Hz, 3H, Me -21), 0.93 (s, 3H, Me-18).

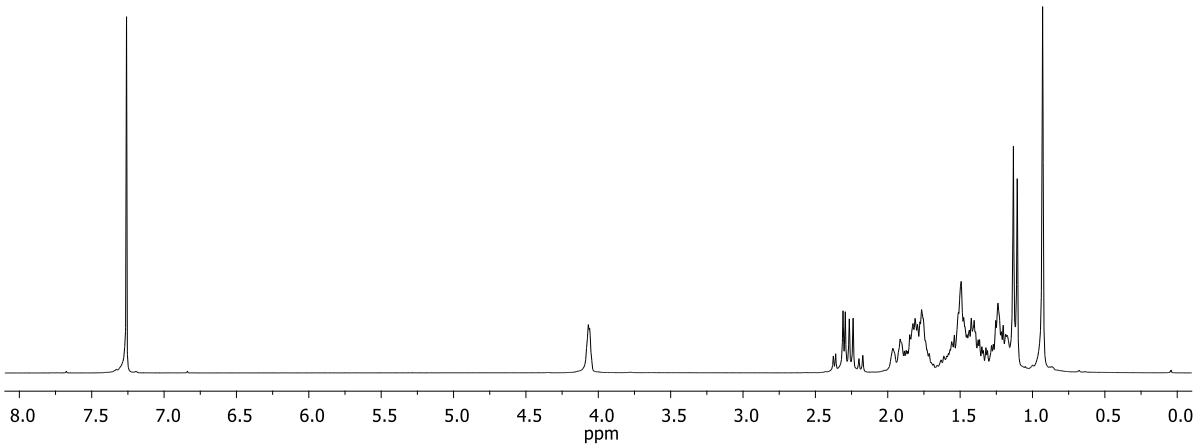

^{13}C NMR (63 MHz, $CDCl_3$) δ 118.84 (C, C≡N), 68.81 (CH, C-8), 55.09 (CH), 52.29 (CH), 41.82 (C, C-13), 39.93 (CH_2), 33.42 (CH_2), 32.94 (CH), 26.95 (CH_2), 24.56 (CH_2), 22.30 (CH_2), 19.08 (CH_3, C-21), 17.22 (CH_2), 13.54 (CH_3, C-18).

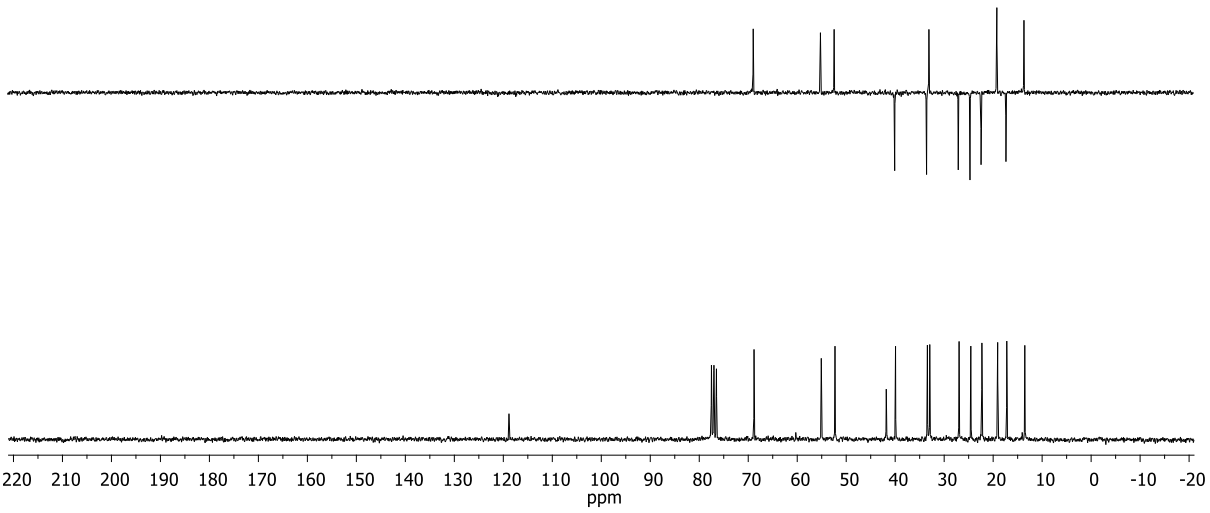

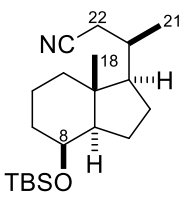

7

^{1}H NMR (250 MHz, $CDCl_3$) δ 3.96 (s, 1H, H-8), 2.29 (dd, *J* = 16.6, 3.9 Hz, 1H, H-22), 2.16 (dd, *J* = 16.7, 6.8 Hz, 1H, H-22), 1.90 – 1.51 (m, 6H), 1.41 – 1.12 (m, 7H), 1.08 (d, *J* = 6.6 Hz, 3H, Me-21), 0.88 (s, 3H, Me-18), 0.83 (d, *J* = 0.9 Hz, 9H, ^{t}Bu-Si), -0.05 (d, *J* = 4.1 Hz, 6H, 2×Me-Si).

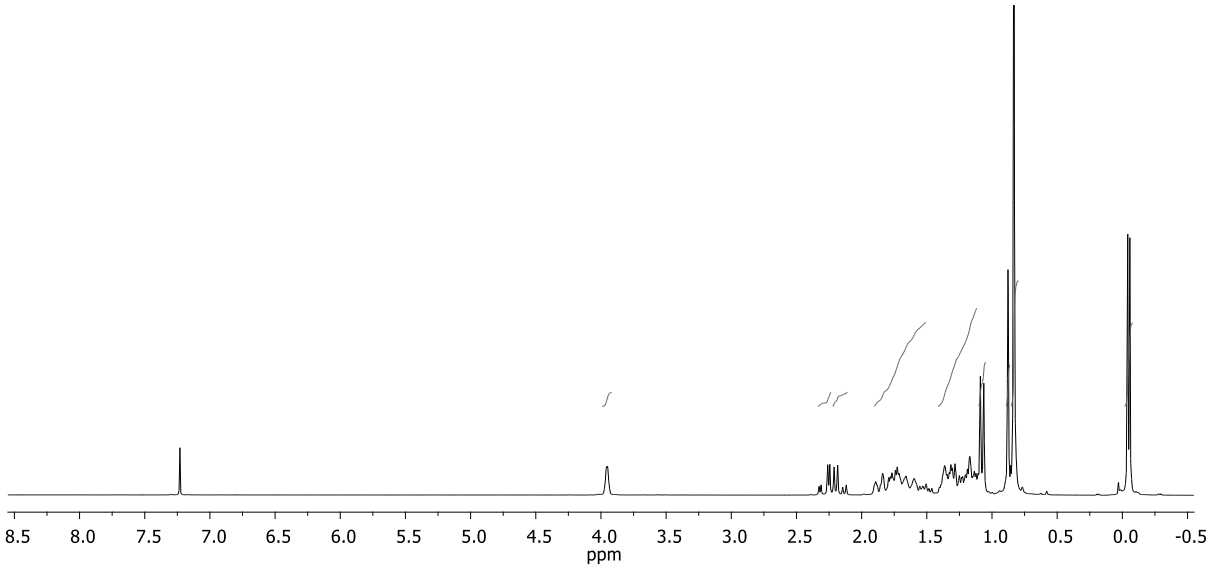

^{13}C NMR (63 MHz, $CDCl_3$) δ 118.8 (C, C≡N), 69.1 (CH, C-8), 55.2 (CH), 52.7 (CH), 42.0 (C, C-13), 40.2 (CH_2), 34.1 (CH_2), 33.0 (CH), 27.1 (CH_2), 25.7 (3×CH_3, ^{t}Bu-Si), 24.5 (CH_2), 22.8 (CH_2), 19.1 (CH_3, C-21), 17.9 (C, Si), 17.40 (CH2), 13.7 (CH_3, C-18), -5.0 (CH_3, Me-Si), -5.3 (CH_3, Me-Si).

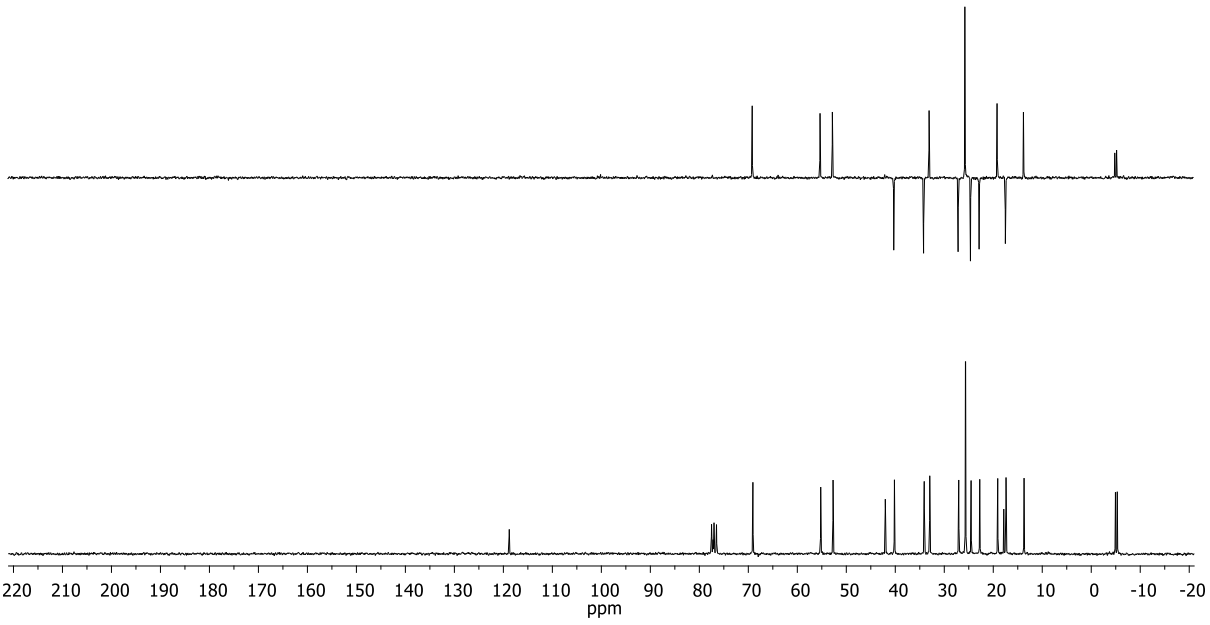

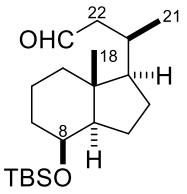

8

^{1}H NMR (250 MHz, $CDCl_3$) δ 9.70 (dd, *J* = 3.4, 1.4 Hz, 1H, CHO), 3.96 (s, 1H, H-8), 2.41 (d, *J* = 14.0 Hz, 1H), 2.16 – 1.85 (m, 3H), 1.79 – 1.51 (m, 4H), 1.39 – 1.09 (m, 7H), 0.95 (d, *J* = 6.4 Hz, 3H, Me-21), 0.92 (s, 3H, Me-18), 0.85 (s, 9H, ^{t}Bu-Si), -0.04 (d, *J* = 3.6 Hz, 6H, 2×Me-Si).

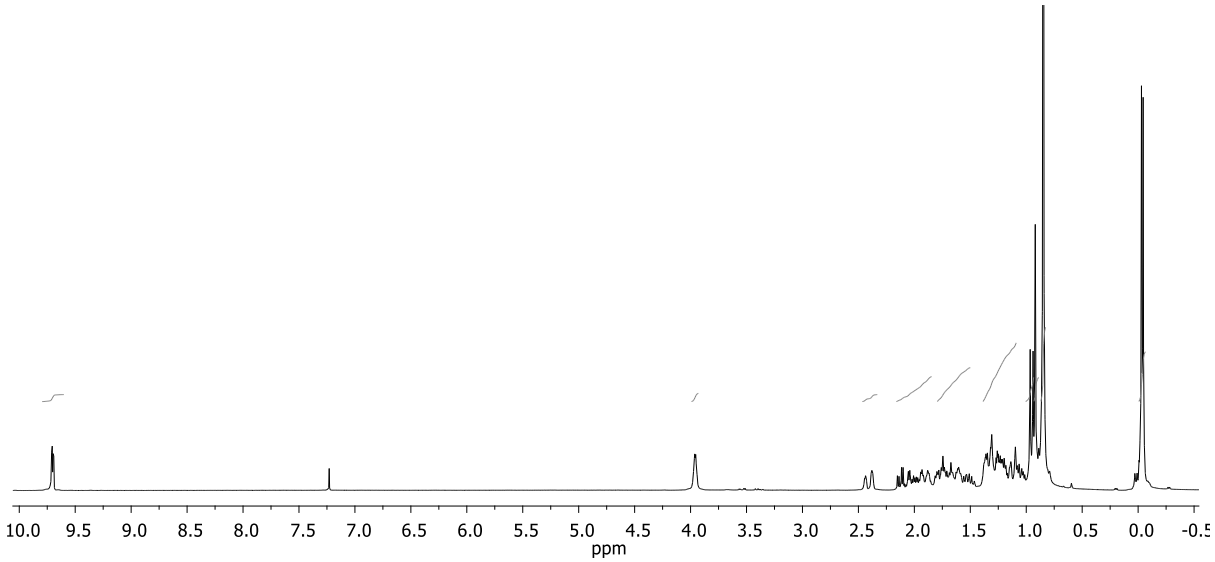

^{13}C NMR (63 MHz, $CDCl_3$) δ 203.5 (CH, CHO), 69.3 (CH, C-8), 56.5 (CH), 53.0 (CH), 50.8 (CH_2), 42.3 (C, C-13), 40.5 (CH_2), 34.31 (CH_2), 31.24 (CH), 27.54 (CH_2), 25.78 (3×CH_3, ^{t}Bu-Si), 23.0 (CH_2), 20.0 (CH_3, C-21), 18.0 (C, Si), 17.6 (CH_2), 13.7 (CH_3, C-18), -4.8 (CH_3, Me-Si), -5.2 (CH_3, Me-Si)

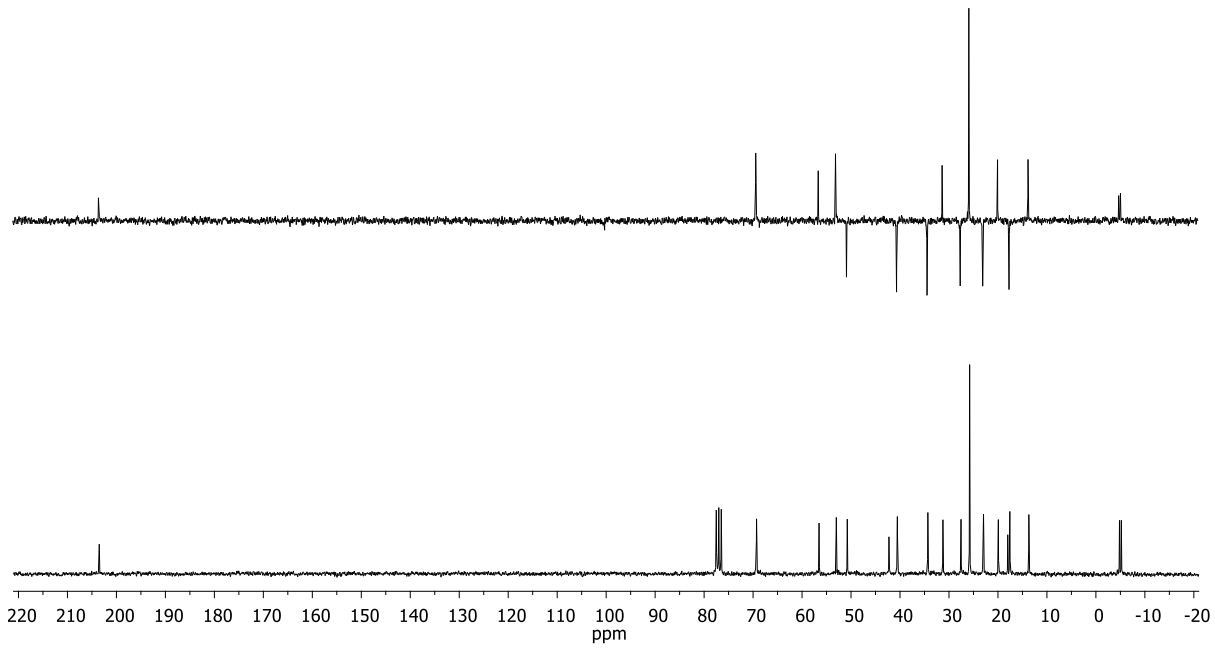

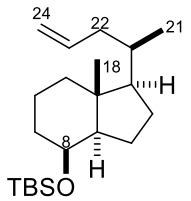

9

^{1}H NMR (250 MHz, $CDCl_3$) δ 5.84 – 5.62 (m, 1H, H-23), 4.95 (d, *J* = 13.3 Hz, 2H, H-24), 3.97 (s, 1H, H-8), 2.15 (d, *J* = 12.5 Hz, 1H), 1.99 – 1.44 (m, 7H), 1.40 – 1.19 (m, 5H), 1.12 – 0.95 (m, 2H), 0.88 (d, *J* = 7.2 Hz, 15H, Me-21, Me-18, ^{t}Bu-Si), -0.02 (d, *J* = 2.8 Hz, 6H, 2×Me-Si).

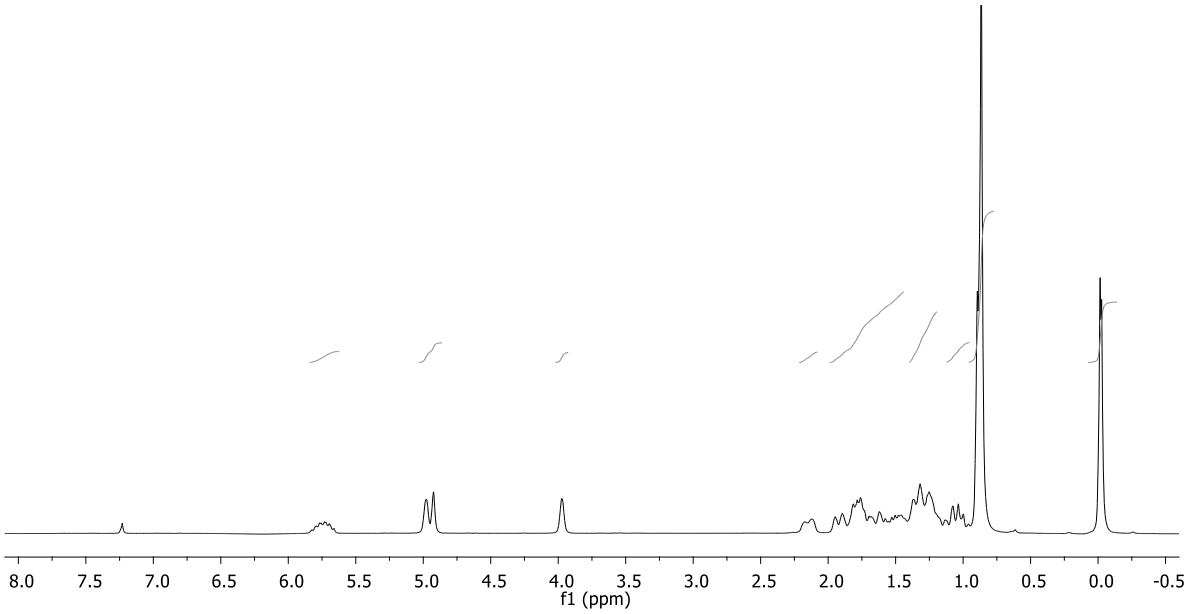

^{13}C NMR (63 MHz, $CDCl_3$) δ 137.5 (CH, C-23), 115.57 (CH_2, C-24), 69.47 (CH, C-8), 56.4 (CH), 53.0 (CH), 42.1 (C, C-13), 40.6 (CH_2), 40.5 (CH_2), 35.3 (CH), 34.5 (CH_2), 27.3 (CH_2), 25.8 (3×CH_3, ^{t}Bu-Si), 23.1 (CH_2), 18.6 (CH_3, C-21), 18.0 (C, C-Si), 17.7 (CH_2), 13.8 (CH_3, C-18), -4.8 (CH_3, Me-Si), -5.2 (CH_3, Me-Si).

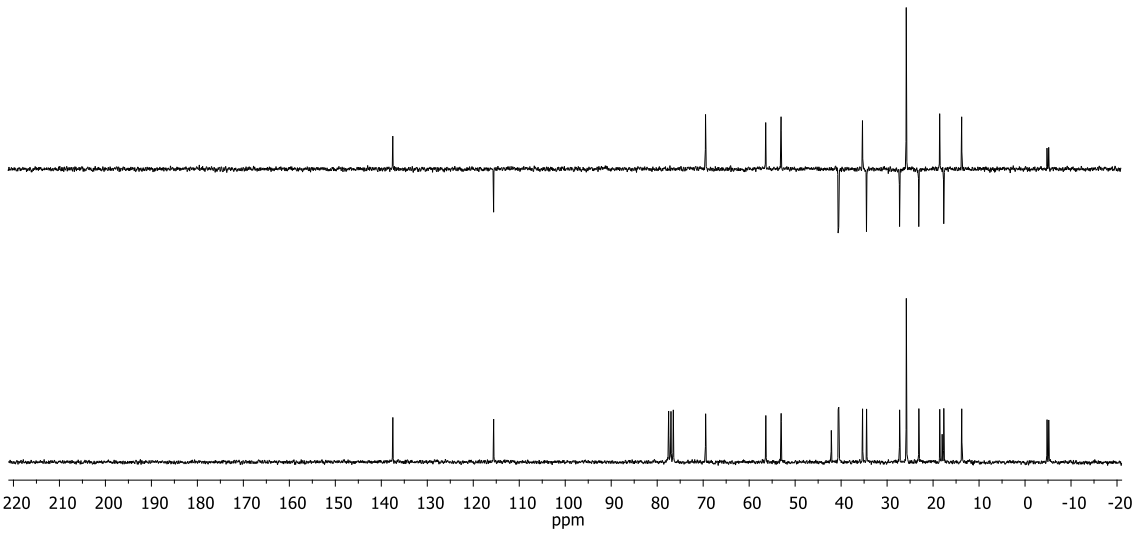

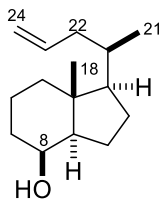

10

^{1}H NMR (250 MHz, $CDCl_3$) δ 5.81 – 5.62 (m, 1H, H-23), 4.93 (d, *J* = 12.6 Hz, 2H, H-24), 4.02 (s, 1H, H-8), 2.19 – 2.06 (m, 1H), 2.00 – 1.89 (m, 1H), 1.86 – 1.65 (m, 4H), 1.52 – 1.22 (m, 8H), 1.16 – 1.00 (m, 2H), 0.89 (s, 3H, Me-18), 0.86 (d, *J* = 8.0 Hz, 3H, Me-21).

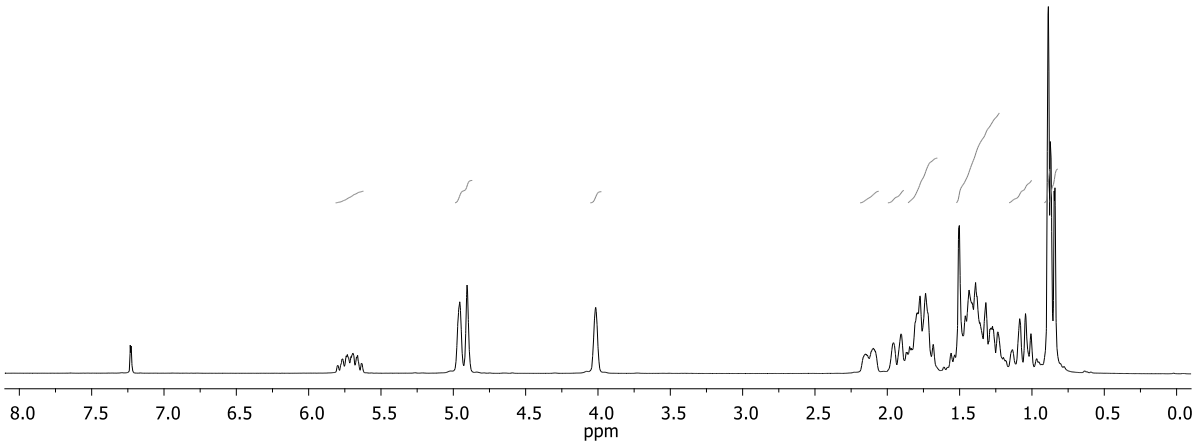

^{13}C NMR (63 MHz, $CDCl_3$) δ 137.2 (CH, C-23), 115.7 (CH_2, C-24), 69.2 (CH, C8), 56.1 (CH), 52.5 (CH), 41.8 (C, C13), 40.4 (CH_2), 40.2 (CH_2) 35.2 (CH), 33.52 (CH_2), 27.0 (CH_2), 22.5 (CH_2), 18.4 (CH_3, Me-21), 17.4 (CH_2), 13.5 (CH_3, Me-18).

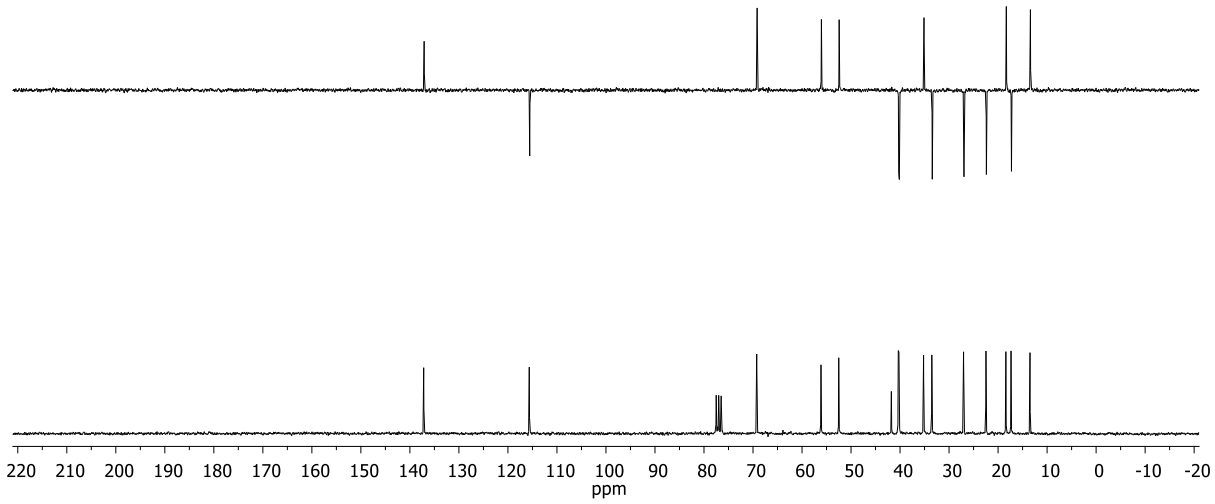

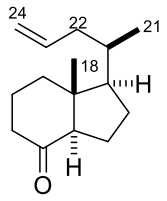

13

^{1}H NMR (250 MHz, $CDCl_3$) δ 5.80 – 5.56 (m, 1H, H-23), 4.95 (d, *J* = 12.6 Hz, 2H, H-24), 2.40 (dd, *J* = 11.5, 7.5 Hz, 1H), 2.27 – 1.98 (m, 4H), 1.97 – 1.62 (m, 5H), 1.57 – 1.24 (m, 5H), 0.91 (d, *J* = 6.1 Hz, 3H, Me-21), 0.59 (s, 3H, Me-18).

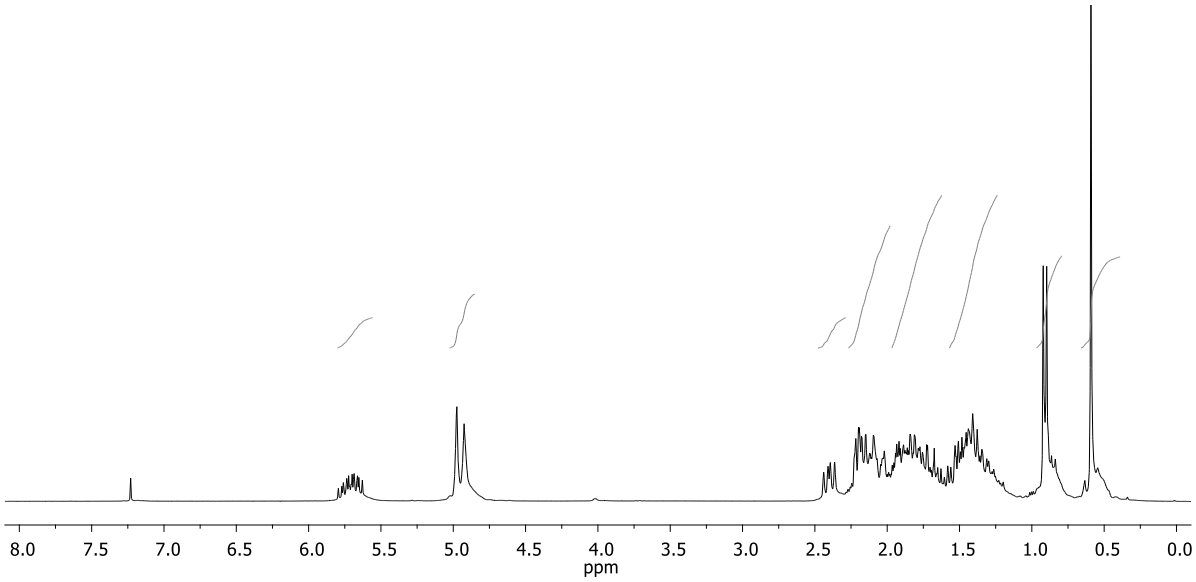

^{13}C NMR (63 MHz, $CDCl_3$) δ 211.9 (C, C-8), 136.7 (CH, C-23), 116.0 (CH_2, C-24), 61.8 (CH), 56.1 (CH), 49.8 (C, C-13), 40.9 (CH_2), 40.3 (CH_2), 38.8 (CH_2), 35.4 (CH), 27.4 (CH_2), 24.0 (CH_2), 19.0 (CH_2), 18.6 (CH_3, Me-21), 12.4 (CH_3, Me-18).

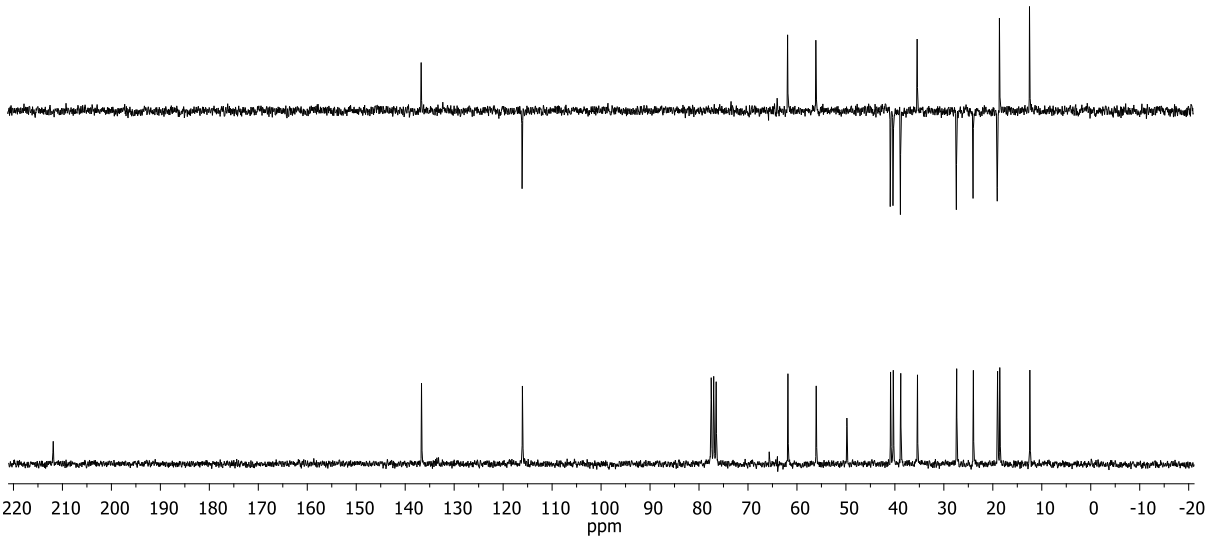

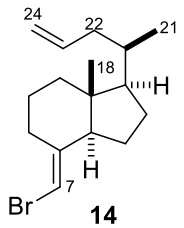

14

^{1}H NMR (250 MHz, $CDCl_3$) δ 5.89 – 5.67 (m, 1H, H-23), 5.65 (s, 1H, H-7), 4.99 (d, *J* = 13.6 Hz, 2H, H-24), 2.87 (dd, *J* = 11.0, 2.5 Hz, 1H), 2.24 – 2.13 (m, 1H), 2.03 – 1.80 (m, 4H), 1.69 – 1.44 (m, 6H), 1.36 – 1.23 (m, 3H), 0.94 (d, *J* = 6.5 Hz, 3H, Me-21), 0.57 (s, 3H, Me-18).

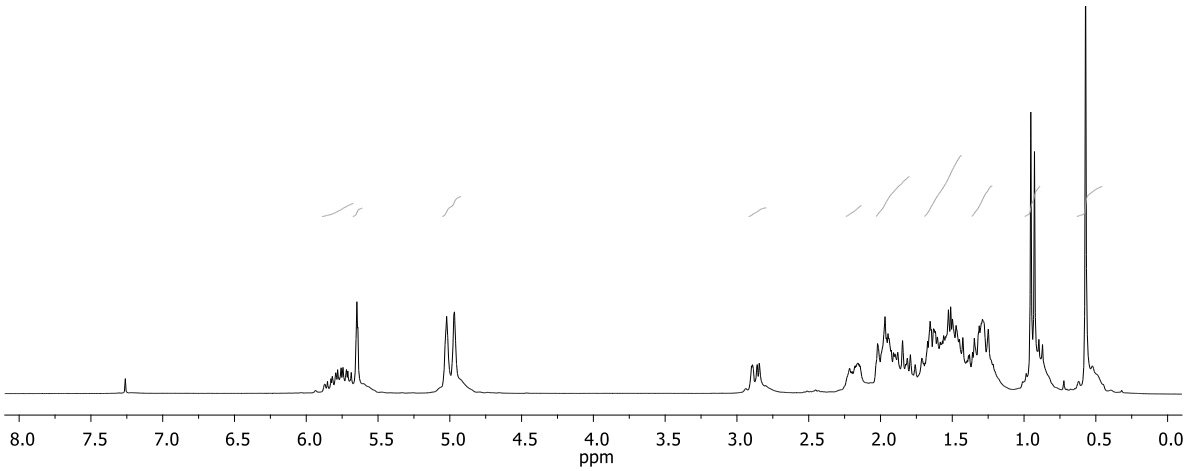

^{13}C NMR (63 MHz, $CDCl_3$) δ 145.0 (C-8), 137.0 (CH, C-23), 115.9 (CH_2, C24), 97.4 (CH, C-7), 55.8 (CH), 55.3 (CH), 45.4 (C, C-13), 40.5 (CH), 39.7 (CH), 35.9 (CH), 31.0 (CH_2), 27.5 (CH_2), 22.5 (CH_2), 22.0 (CH_2), 18.7 (CH_3, Me-21), 11.8 (CH_3, Me-18).

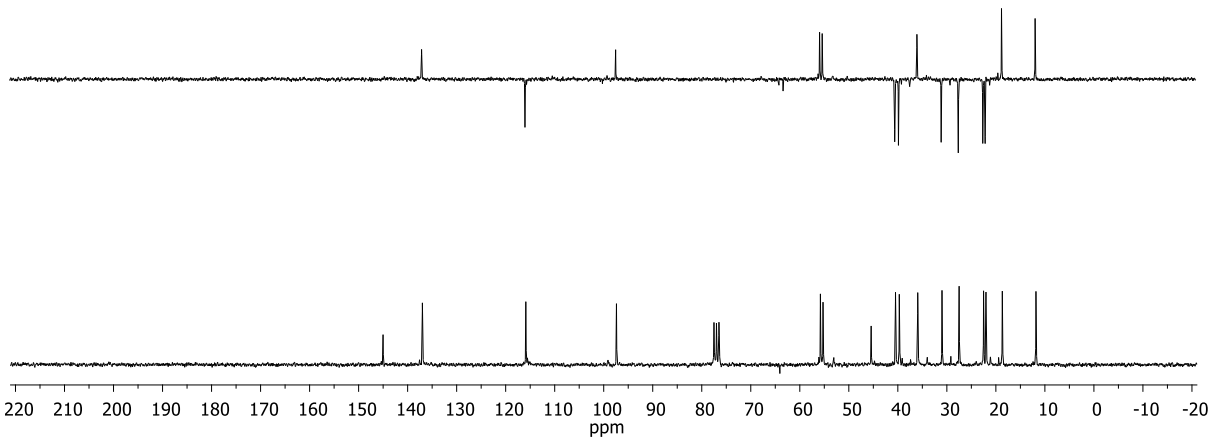

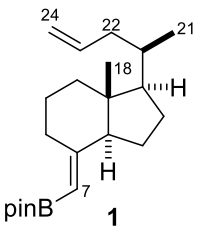

1

^{1}H NMR (400 MHz, cdcl$_3$) δ 5.73 (s, 1H, H-23), 4.95 (d, *J* = 13.4 Hz, 2H, H-24), 4.88 (s, 1H, H-7), 3.14 (d, *J* = 12.9 Hz, 1H), 2.15 (d, *J* = 11.0 Hz, 1H), 2.04 – 1.41 (m, 13H), 1.23 (s, 12H, 4×CH_3COB), 0.90 (s, 3H, Me-21), 0.53 (s, 3H, Me-18).

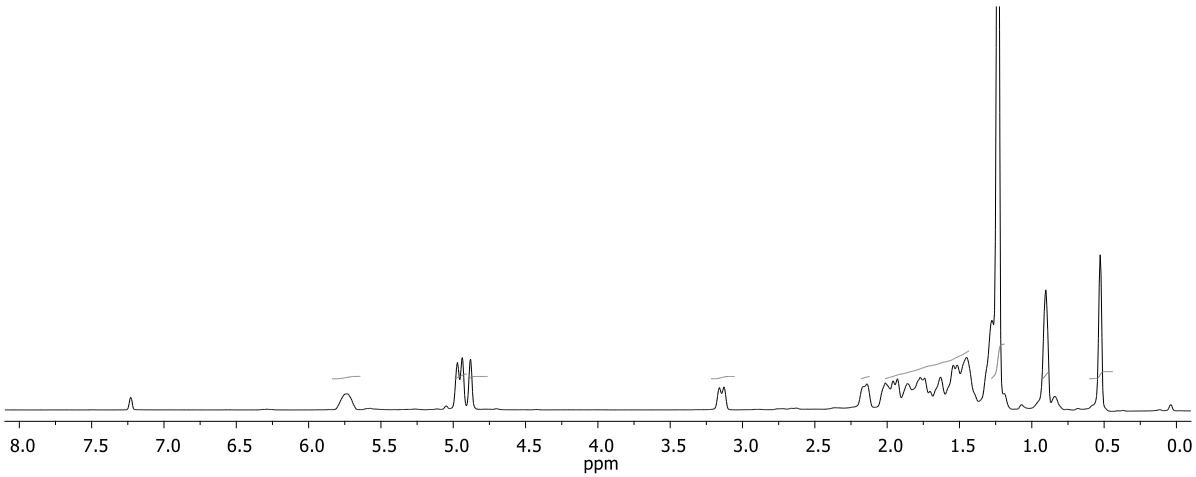

^{13}C NMR (63 MHz, $CDCl_3$) δ 166.2 (C, C-8), 137.3 (CH, C-23), 115.7 (CH_2, C-24), 82.5 (C, 2×COB), 57.9 (CH), 56.3 (CH), 46.2 (C, C-13), 40.5 (CH_2), 40.3 (CH_2), 36.0 (CH), 33.2 (CH_2), 27.4 (CH_2), 24.9 (CH_3, 2×COB), 24.8 (CH_3, 2×COB), 24.3 (CH_2), 22.3 (CH_2), 18.7 (CH_3, Me-21), 12.1 (CH_3, Me-18).

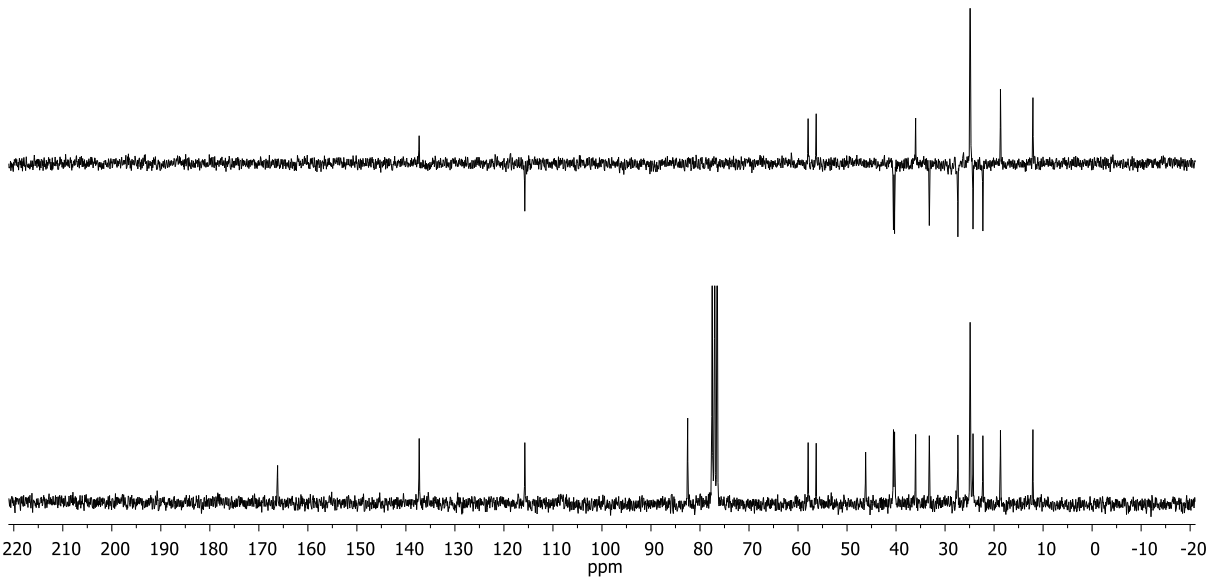

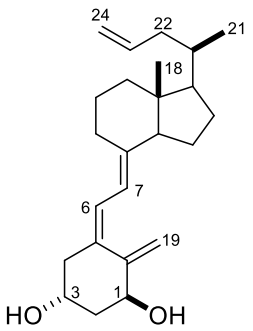

17

^{1}H NMR (400 MHz, $CDCl_3$) δ 6.38 (d, *J* = 11.2 Hz, 1H, H-6), 6.02 (d, *J* = 11.3 Hz, 1H, H-7), 5.83 – 5.71 (m, 1H, H-23), 5.33 (s, 1H, H-19), 4.99 (d, *J* = 11.8 Hz, 3H, H-19, H-24), 4.43 (dd, *J* = 7.4, 4.3 Hz, 1H, H-1), 4.26 – 4.20 (m, 1H, H-3), 2.82 (dd, *J* = 11.9, 3.6 Hz, 1H), 2.59 (dd, *J* = 13.3, 2.9 Hz, 1H), 2.31 (dd, *J* = 13.4, 6.5 Hz, 1H), 2.18 (d, *J* = 13.5 Hz, 1H), 2.03 – 1.85 (m, 6H), 1.67 (d, *J* = 10.8 Hz, 5H), 1.53 – 1.44 (m, 4H), 1.34 – 1.25 (m, 4H), 0.93 (d, *J* = 6.6 Hz, 3H, Me-21), 0.55 (s, 3H, Me-18).

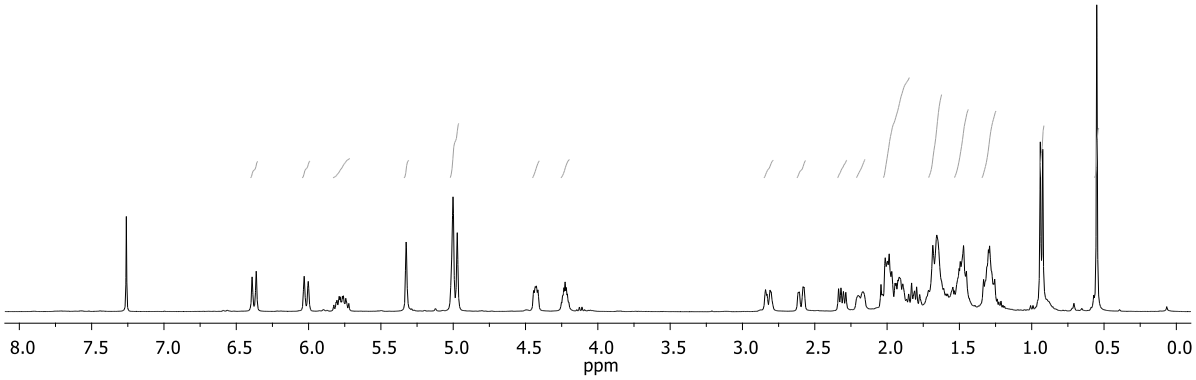

^{13}C NMR (63 MHz, $CDCl_3$) δ 147.6 (C, C-10), 143.2 (C, C-8), 137.3 (CH, C-23), 132.9 (C, C-5), 125.0 (CH,C-6), 117,0 (CH, C-7), 115,8 (CH_2, C-24) 111.8 (CH_2, C-19), 70.8 (CH, C-OH), 66.8 (CH, C-OH), 56.3 (CH), 56.0 (CH), 45.9 (C, C-13), 45.2 (CH_2), 42.8 (CH_2), 40.5 (CH_2), 40.3 (CH_2), 36.1 (CH), 29.1 (CH_2), 27.6 (CH_2), 23.6 (CH_2), 22.3 (CH_2), 18.7 (CH_3, Me-21), 12.0 (CH_3, Me-18).

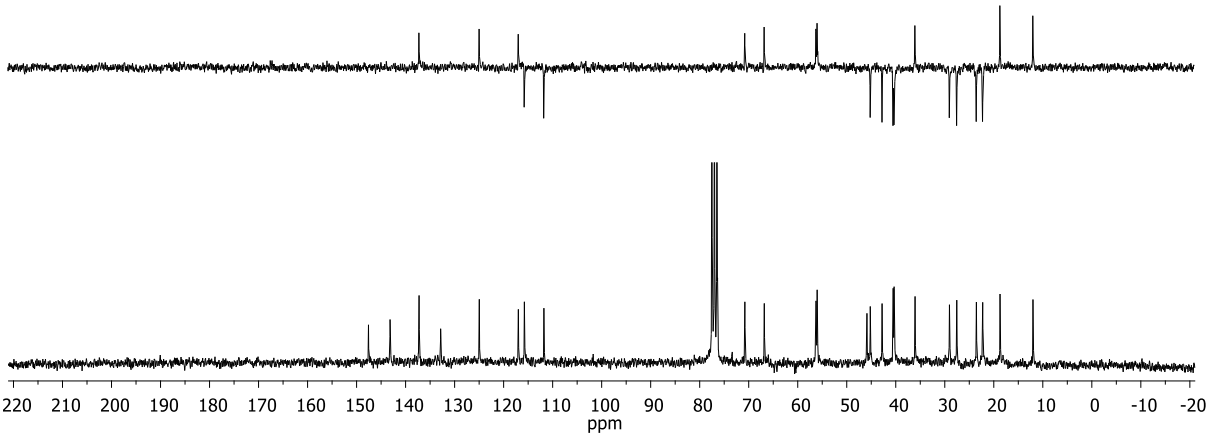

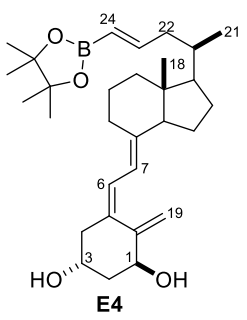

E4

^{1}H NMR (400 MHz, cdcl$_3$) δ 6.59 (ddd, *J* = 17.8, 7.9, 5.9 Hz, 1H, H-23), 6.37 (d, *J* = 11.2 Hz, 1H, H-6), 6.01 (d, *J* = 11.2 Hz, 1H, H-7), 5.42 (d, *J* = 17.9 Hz, 1H, H-24), 5.32 (s, 1H, H-19), 5.00 (s, 1H, H-19), 4.43 (dd, *J* = 7.6, 4.3 Hz, 1H, H-1), 4.22 (dt, *J* = 9.9, 3.3 Hz, 1H, H-3), 2.82 (d, *J* = 12.7 Hz, 1H), 2.60 (d, *J* = 10.5 Hz, 1H), 2.31 (dd, *J* = 13.4, 6.7 Hz, 2H), 2.05 – 1.86 (m, 7H), 1.68 – 1.45 (m, 10H), 1.27 (s, 12H, 4×CH$_3$COB), 0.93 (d, *J* = 6.5 Hz, 3H, Me-21), 0.54 (s, 3H, Me-18).

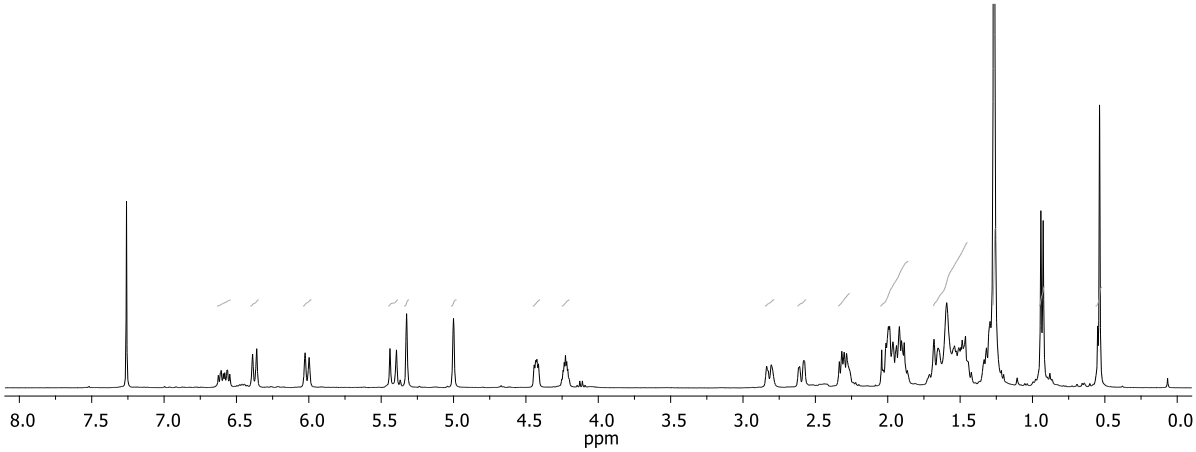

^{13}C NMR (63 MHz, CDCl$_3$) δ 153.3 (CH, C-23), 147.6 (C, C-10), 143.1 (C, C-8), 132.8 (C, C-5), 124.9 (CH, C-6), 117.0 (CH, C-7), 111.8 (CH$_2$, C-19), 83.0 (C, COB), 70.8 (CH), 66.8 (CH), 56.2 (CH), 56.1 (CH), 45.9 (C, C-13), 45.2 (CH$_2$) 42.8 (CH$_2$), 40.3 (CH$_2$), 35.9 (CH), 29.0 (CH$_2$), 27.6 (CH$_2$), 24.8 (CH$_3$, 4×COB), 23.5 (CH$_2$), 22.2 (CH$_2$), 19.1 (CH$_3$, C-21), 12.0 (CH$_3$, C-18).

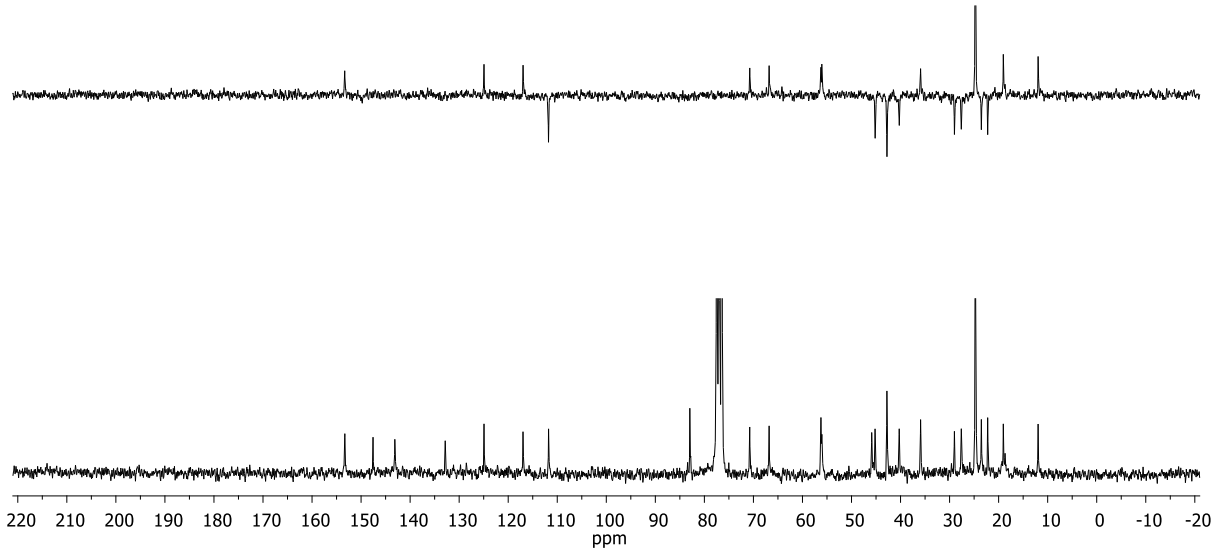

7. Index of Structures

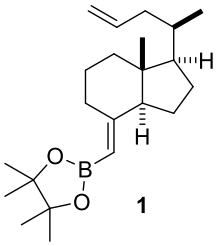

1

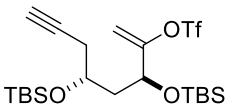

2

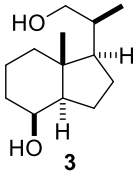

3

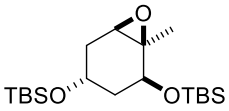

4

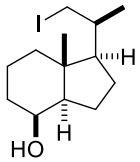

5

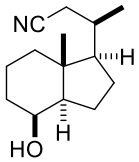

6

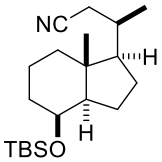

7

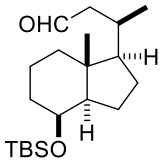

8

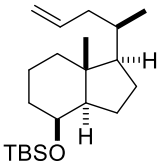

9

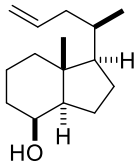

10

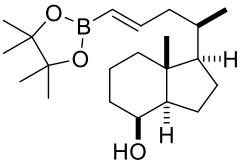

11

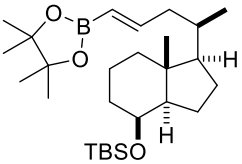

12

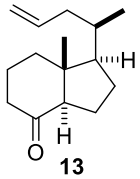

13

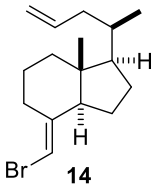

14

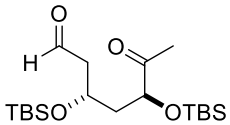

15

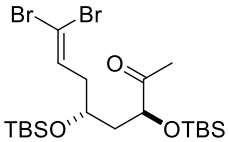

16

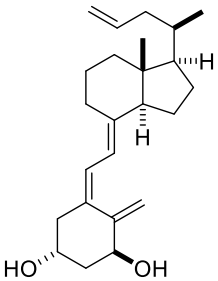

17

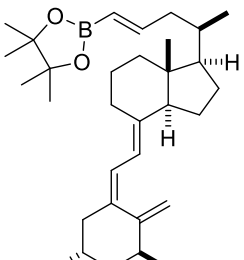

E4

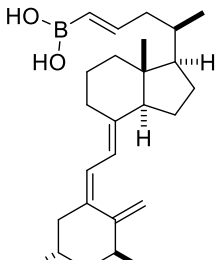

A4